Efferent Effects on Auditory-Nerve Responses to Tones: Substantial Inhibition Even at High Sound Levels and Tail Frequencies

by

Konstantina Marka Stanković

B.S. Physics
Massachusetts Institute of Technology (June 1992)
B.S. Biology
Massachusetts Institute of Technology (June 1992)

Submitted to the Division of Health Sciences and Technology
in partial fulfillment of the requirements for the degree of

Doctor of Philosophy

at the

MASSACHUSETTS INSTITUTE OF TECHNOLOGY

February 1998

Author .....
Division of Health Sciences and Technology
December 31, 1997

Certified by .....
John J. Guinan, Jr.
Associate Professor of Otology and Laryngology, Harvard Medical School
Thesis Supervisor

Accepted by .....
Martha L. Gray
Co-director, Division of Health Sciences and Technology

Efferent Effects on Auditory-Nerve Responses to Tones: Substantial Inhibition Even at High Sound Levels and Tail Frequencies

by

Konstantina Marka Stanković

Submitted to the Division of Health Sciences and Technology
on December 31, 1997, in partial fulfillment of the
requirements for the degree of
Doctor of Philosophy

ABSTRACT

The central nervous system modulates auditory sensory transduction in the mammalian cochlea via medial olivocohlear neurons. These efferents project from the brainstem to the cochlea, synapse on outer hair cells, and inhibit responses from auditory-nerve fibers that synapse on inner hair cells. It is now believed that the major mechanism producing this inhibition is an efferent-induced reduction in motion of the basilar membrane, a tuned structure that extends along the length of the cochlea. The experimental data of this thesis indicate that this mechanism is stronger than previously thought, but that it is not the only mechanism. Specifically, by using improved methodological techniques, and by systematically exploring conditions that were little explored in earlier work, we obtained new data on efferent effects on responses of cat auditory-nerve fibers to various sound levels and frequencies. We focused on frequencies to which auditory-nerve fibers are sharply tuned, and on frequencies from the broadly-tuned low-frequency "tail" region of tuning curves.

A summary of highlights from the thesis that challenge the previous "common wisdom" follows. First, we show that efferents produce the largest equivalent attenuation at moderate to high sound levels (45-75 dB SPL), not low sound levels as previously thought. In addition, large attenuations, some over 50 dB SPL, and the presence of inhibition even at 100 dB SPL, indicate that medial efferent inhibition is more potent than previously reported. Second, we show that efferent stimulation can inhibit auditory-nerve-fiber responses even to tail-frequency tones. The inhibition can be as large as 20 dB SPL in individual fibers, although it typically averages 5 dB SPL. Third, we show that efferent stimulation can substantially shift the response phase of auditory-nerve fibers to tail-frequency tones with little effect on the phase of the cochlear microphonic. The tail-frequency phase data suggest that efferents can affect cochlear micromechanics without changing basilar-membrane motion. Our results are consistent with previous views that efferents extend the dynamic range of hearing, reduce masking by background noise, and protect the ear from damage due to intense sounds.

Thesis Supervisor: John J. Guinan, Jr.
Title: Associate Professor of Otology and Laryngology, Harvard Medical School

Acknowledgments

I would like to express my sincere gratitude to many individuals who have helped me through my studies by providing guidance, support or example.

Foremost on this list is my mentor and research supervisor, Dr. John Guinan. I have benefited repeatedly from his vast technical expertise, patient teaching, and gentle guidance. I feel fortunate to have been introduced to auditory physiology by John, as his probing questions, constructive criticism, and attention to detail have set towering standards for my future conceptual and experimental explorations in the area.

I thank my four thesis committee members, Drs. Don Eddington, David Mountain, Joe Nadol, and Bill Sewell for their many useful suggestions, support, and criticism (and willingness to read my thesis in installments). In particular, I am indebted to Don for his insistence to quantitatively describe classification criteria used in the thesis; to Dr. Mountain for his experimental insight and attention to detail, both of which have significantly improved the work carried in this thesis; to Bill for ensuring that I not lose sight of a coherent big picture; and to Dr. Nadol for providing physician's perspective and reminding me to think about clinical ramifications of basic research.

I owe special gratitude to Dr. Christopher Shera – the unofficial, but invaluable member of my thesis committee, my officemate, and friend. I have repeatedly benefited from Chris' scientific knowledge, computer wizardry, and exquisite sense of humor. Chris' genuine pursuit of crispness and beauty in nature and the world around him, and his generous readiness to offer help (in matters ranging from Matlab and Latex to music and poetry) have been inspirational.

I am indebted to Professor Nelson Kiang whose infectious enthusiasm about auditory physiology has stimulated me to pursue research in hearing. Nelson's relentless quest for truth in scientific endeavors, his boundless energy, and passionate love of intellectual adventures will continue to be an inspiration for my professional career. I am also thankful to Nelson for his continued interest in my work and in the well–being of my family.

From my undergraduate years, I fondly remember my physics advisors Drs. Lomon and Villars, who gently steered me toward the exciting interface of physics and biology. In graduate school, my registration advisor, Dr. Bill Peake, handled the myriad of issues along the way with friendly efficiency and keen wit.

I would like to thank all members of the Eaton–Peabody Laboratory (and other amiable people on the fourth floor of the Massachusetts Eye and Ear Infirmary) for their friendship and support. A special thanks goes to Dr. Joe Adams for his ready and much appreciated advice (especially at odd hours of a night when experiments did not work quite right). I also thank Dr. John Rosowski for introducing me to statistics packages, and to Dr. Bob Hall for lengthy discussions about the assumptions underlying statistical procedures. I am most grateful to Leslie Liberman, Dan O'Grady, Debbie Flandermeyer, and Melissa Duca for their skillful surgery. Barbara Kiang deserves a specially heartfelt thanks for her generous help over the years.

Working in the Eaton–Peabody Laboratory has been stimulative because of the atmosphere of creativity and high standards for research achievements set by EPL members, including Drs. Chris Brown, Peter Cariani, Bertrand Delgutte, Scott Dynes, Denny Free-

man, Barbara Fullerton, Bob Kimura, Jim Kobler, Bob Levine, Charlie Liberman, Jennifer Melcher, Saumil Merchant and Ed Mroz. I also appreciate the help provided by the able administrative staff members Dianna Sands and Robin Allen, and by the engineers – Frank Cardarelli, Charlie Gage, Mike Ravicz, Ish Stefanov-Wagner, and Dave Steffens.

Over the years, my student life has been enriched by my Chamber 3 officemates Mike McCue, Christopher Shera, and Tai Lin. Their working ethic, keen observations, valuable insights, and unique personalities made late nights at EPL a worthwhile experience. I will especially fondly remember when Chris, Tai and I turned Chamber 3 into a music studio by hooking CD players to loudspeakers normally used during experiments (listening to soothing choral music does prepare one for long nights of listening to neurons). I thank my SHS and BU classmates Susan Voss, Heidi Nakajima, John Iversen, P.K. Oberoi, Sridhar Kalluri, Jason Sroka, Paul Dimitri and Quinton Gopen for their comradery and support. Susan's and John's cordiality (and Susan's willingness to share her Latex files with me) is especially appreciated. I also thank all students in the Speech and Hearing Sciences Program for their warm friendship.

In the HST office, I am most grateful to Dr. Martha Gray for her support during the most critical parts of my graduate studies. Dr. Roger Marks' dedication to success of HST and his interest in the well-being of students serve as motivation to me as I contemplate my professional path. I also thank Drs. Joe Bonventre, Mike Rosenblatt, Lou Braida and Fred Bowman. I am indebted to the Harvard MD/PhD program, under the directorship of Drs. Denny Ausiello and Nancy Andrews, for supporting my medical education.

At Harvard Medical School, I am indebted to my three advisors – Drs. Martin Carey, Hallowell Churchill, and Mike McKenna for their guidance and timely support. I benefited greatly from being a teaching assistant for Dr. Carey for three years, as I was exposed both to the fascinating world of gastroenterology, and to his unparalleled wit and connoisseurship in classical music. I am indebted to Dr. Churchill for wholeheartedly welcoming me to the world of medicine, for making sure that all rules are followed in my course schedule, and for graciously allowing my thesis defense on the very day that I started my first clinical clerkship. I am grateful to Dr. McKenna for his unwavering support, enthusiasm about otolaryngology, and readiness to listen to an aspiring physician, despite his incredibly busy schedule.

An essential ingredient for this thesis has been the financial support provided in part by NIH grants awarded to Dr. John Guinan, by NIH Fellowship in Speech and Hearing Sciences, by the NIH Medical Scientist Training Program, and by the Marvin Asnes Scholarship in HST. I am grateful to Keiko Oh from the HST office who made possible (and smoothed) many of these transitions.

Outside the Lab, I thank my family – my husband whose boundless love, understanding, and dedication have been my strength and inspiration; my parents whose love surrounds me wherever I go despite the physical distance that separates us; my brothers Aleksandar and Siniša who have always encouraged me to follow my dreams; my mother- and father-in-law who have embraced me as their daughter. I also remember with deep gratitude my host family, the Roberts, who warmly welcomed me when I first came to this country as an exchange student in high school.

To my husband, Aleksandar,

and my parents, Marko and Danica Trbović.

... He who is in you is greater

than he who is in the world.

1 John 4:4

Contents

List of Figures

List of Tables

Chapter 1

Introduction

A. General overview

The auditory nerve is the main link between the auditory environment and the central nervous system. Therefore, understanding the processes that modulate auditory-nerve responses is important in establishing the connection between the auditory environment and perception by the central nervous system. One such process is activation of the olivocochlear efferent neurons whose cell bodies are located in the superior olivary complex of the brain stem and whose axons project to the cochlea (Rasmussen, 1946).

The discovery that olivocochlear neurons project to the cochlea (Rasmussen, 1946) suggested that the central nervous system is capable of modulating sensory input at the very first stage of auditory signal detection. Many investigators since then have attempted to decipher the functional role of such modulation (i.e., the "what does it do" question) and the mechanisms of its action (i.e., the "how does it do this" question). Despite a significant number of important discoveries, many aspects of the two broad categories of questions remain unanswered (reviewed by Guinan, 1996). This thesis provides measurements that put new constraints on the "how question," and thereby provides new insights into how the cochlea works.

From a mechanics point of view, the long-standing efferent puzzle has been: "How can medial olivocochlear efferents that synapse on outer hair cells influence responses from afferents that synapse on inner hair cells (Fig. 1-1)." This has been a puzzle because there

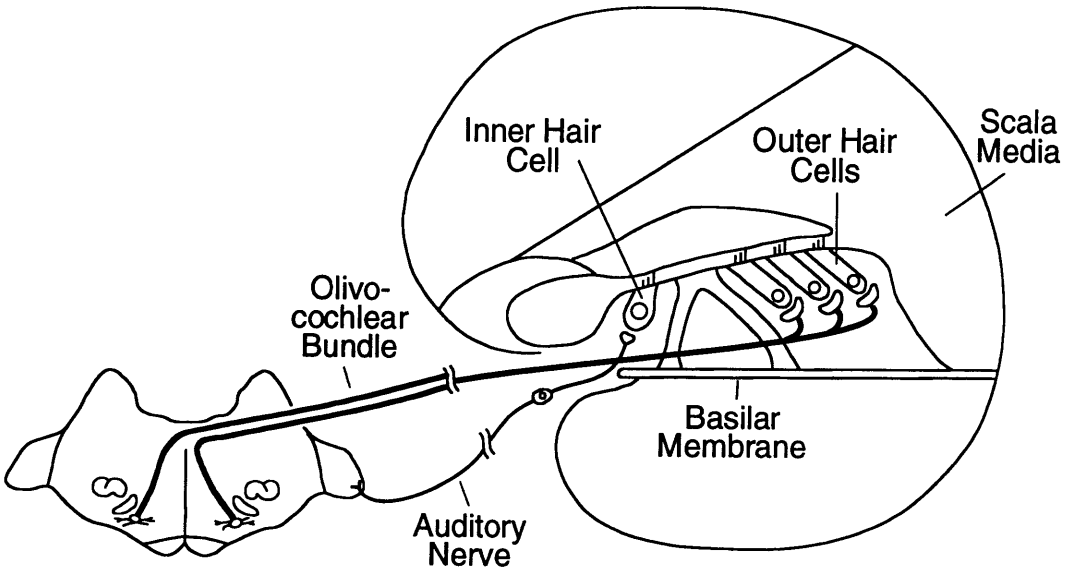

Figure 1-1: A simplified anatomical sketch of a cochlear cross-section illustrating afferent and efferent innervation by myelinated neurons.

are no known neuronal connections between afferent and efferent fibers, or between inner and outer hair cells. Note that we are using the term "afferent" synonymously with Type I myelinated afferent neurons that synapse on inner hair cells, and the term "efferent" synonymously with medial olivocochlear (MOC) efferents that synapse on outer hair cells. There are additional unmyelinated afferent neurons (Type II) that synapse on outer hair cells and unmyelinated efferent neurons (with cell bodies near the lateral superior olive) that synapse on Type I afferents. However, the physiology of the two latter types of unmyelinated neurons is unknown and they are though not to play a role in the phenomena discussed below (Kiang et al., 1986; Guinan, 1996).

Before the work described in this thesis was begun, the common wisdom about efferent effects could be summarized as follows:

1. Efferent effects are largest at low sound levels. Evidence for this came from measurements of efferent effects on: (a) the compound action potential of the auditory nerve (Galambos, 1956; Desmedt, 1962), (b) single auditory-nerve fibers (Weiderhold, 1970; Teas et al., 1972), (c) otoacoustic emissions (Mountain, 1980; Moulin et al., 1993),

and (d) basilar membrane motion (Dolan and Nuttall, 1994; Murugasu and Russell, 1996).

2. Efferents do not affect responses of ANFs from the broadly-tuned, insensitive, low-frequency "tail" region of tuning curves, even in fibers that show large inhibition at the characteristic frequency (CF) – the frequency to which the fiber is most sensitive (Kiang et al., 1970; Wiederhold, 1970; Guinan and Gifford, 1988a; but see also Guinan and Gifford, 1988c). This notion has also been supported by measurements from inner hair cells (Brown and Nuttall, 1984), and recent measurements of the basilar membrane (BM) motion (Murugasu and Russell, 1996).

3. Efferents that synapse on outer hair cells inhibit responses from afferents that synapse on inner hair cells only through a reduction of basilar membrane motion (Dolan and Nuttall, 1994; Murugasu and Russell, 1996). This reduction is though to reflect an efferent-induced reduction in the gain of the "cochlear amplifier", i.e., the "active" process that feeds mechanical energy into the traveling wave, and contributes to the exquisite sensitivity and frequency-selectivity of the cochlea (see Dallos, 1992, for a review of the cochlear amplifier).

The data presented in this thesis challenge all three parts of the "common wisdom" summarized above, and provide a distinctly different picture of efferent inhibition from that obtained from previous work. The two key components that allowed us to challenge the common wisdom are (1) improved methodological techniques, and (2) a systematic exploration of conditions that were not thoroughly explored in earlier work. The main methodological advance in this thesis is the use of "randomized", as opposed to "sequential" sound-level series. The randomized level series were obtained by simultaneously randomizing the presentation of sound level and efferent stimulation, while keeping duty cycles of sound stimulation and efferent stimulation low. In contrast, "sequential" level series used in earlier studies were obtained by sequentially increasing sound level, and at each level altering between the presence and absence of efferent stimulation. In such sequential level functions, adaptation increases as sound level increases, and can distort the shape of the level functions (Sachs and Abbas, 1974). Thus, randomized level series have several important advantages: (1)

adaptation of ANF responses is minimized, (2) adaptation of the efferent effect is minimized, and (3) potential contributions from the slow efferent effect (Sridhar et al., 1995) are evened-out across sound levels, thus allowing a focus on the fast efferent effect. Because of these advantages, randomized level series allow accurate comparisons of efferent effects across sound levels.

Besides using an improved methodological technique, this thesis provides measurements that are lacking in the literature. In particular, before this thesis was begun, a systematic exploration of efferent effects on responses to tail frequencies was lacking in the literature. All of the studies that reported on (the lack of) efferent effects at tail frequencies across sound levels – whether it be at the level of auditory nerve fibers (Wiederhold, 1970; Guinan and Gifford, 1988a), inner hair cells (Brown and Nuttall, 1984) or basilar membrane (Dolan and Nuttall, 1984; Murugasu and Russell, 1996) – were focused on other aspects of efferent inhibition. These earlier reports fit the common conceptual framework that tuning curve tails are determined by "passive" mechanics, without the involvement of the "active" cochlear amplifier. This conceptual framework has been supported by many studies of basilar membrane motion which show nonlinear growth with sound level, and vulnerability to insult near CF, but linear growth with sound level and no vulnerability to insult (i.e., "passive" responses) at frequencies one octave or more below CF. Perhaps the strong conceptual framework suggesting that efferents do nothing in the "passive" tail region has led to the lack of a study focused on this region. In any event, the finding that there are substantial efferent effects at tail frequencies indicates the need for a revision of common conceptions about both efferent effects and basic cochlear mechanisms.

B. Thesis organization

Given this overview, we proceed by providing a general organization of the thesis and then summarize the main findings from each chapter. Chapter two describes efferent effects on auditory-nerve fibers (ANFs) at the characteristic frequency, i.e., at the most sensitive part of the sharply-tuned "tip" region of tuning curves. These results have already been published (Guinan and Stanković, 1996). The results are included as a part of the thesis because they describe the experimental techniques used, and are a conceptual unit with the

work described in later chapters. In particular, the data from chapter two (Guinan and Stanković, 1996) provide benchmarks for my explorations of efferent effects on ANFs at tail frequencies; these studies are described in chapters three and four. Specifically, chapter three describes efferent effects on the *firing rate* of ANFs responding to tail-frequency tones. Chapter four complements chapter three by describing how efferents modulate the *response phase* of ANFs responding to tail-frequency tones.

The main finding in chapter two is that efferents produce the largest equivalent attenuation at moderate to high sound levels (45-75 dB SPL), contrary to the earlier reports that efferent inhibition is largest at low sound levels. In addition, large attenuations, some over 50 dB SPL, and the presence of some inhibition even at 100 dB SPL, indicate that medial efferent inhibition is more potent than previously reported. At the time when these results were published (Guinan and Stanković, 1996), it seemed that they could not be explained by efferent effects on the basilar membrane alone, because efferent effects on the BM motion were said to be the largest at low sound levels (Murugasu and Russell, 1996). However, our work stimulated Murugasu and Russell to reexamine their basilar membrane measurements. Most recently, these authors reported that, in response to tones at CF, efferents inhibit basilar membrane motion most at moderate to high sound levels (Russell and Murugasu, 1997). Therefore, it now appears that the sound-level dependence of the efferent effect on ANFs originates in the sound-level dependence of the efferent inhibition of basilar membrane motion. The detailed mechanisms by which efferents inhibit BM motion remain to be elucidated, but we now have a better idea of the net effect of these mechanisms over a wide range of sound levels.

In chapter three, we demonstrate that, contrary to the commonly held view, efferent stimulation can inhibit ANFs responses at tail frequencies. The inhibition can be as large as 20 dB SPL in individual fibers, although it typically averaged to about 5 dB SPL across fibers. The inhibition tended to be largest at sound levels near tail thresholds. Curiously, these are the same sound levels at which the efferent effect peaks at CF. The inhibition also depends on stimulus frequency relative to CF of the fiber, increasing with frequency over the three-octave range for which we have the most data.

The finding that efferents inhibit ANFs at tail frequencies, sometimes by substantial

amounts, suggests that – contrary to an earlier report (Murugasu and Russell, 1996) – efferents might inhibit BM motion at tail frequencies. Alternatively, ANF inhibition might be produced by efferents acting at stages of signal transformation beyond basilar membrane. If efferents indeed inhibit BM motion at tail frequencies, this would suggest that outer hair cells play an active role in BM mechanics even at frequencies at which BM responses are assumed to be "passive." Once again, our preliminary data (Stanković and Guinan, 1997) stimulated Murugasu and Russell to reevaluate their claims about the lack of an efferent effect on BM motion at tail frequencies. Most recently, these authors reported in a conference paper (Russell and Murugasu, 1997b) that efferent may indeed inhibit BM motion at tail frequencies. However, the authors warn that their data are from a single preparation and are "capricious." Therefore, it remains to be see what fraction, if any, of the ANF inhibition at tail frequencies is produced by efferent inhibition of BM motion.

In chapter four, we demonstrate that efferent stimulation can shift the response phase of ANFs at tail-frequencies. For fibers with CFs$\geq$ 10 kHz, the shift is usually in the direction opposite to what would be expected if the efferent effect were equivalent to an attenuation of sound. These results stand in contrast with the efferent-induced changes in rate and synchrony, both of which are consistent with an efferent effect that is equivalent to an attenuation of sound. The most parsimonious explanation of the results is that one process controls the efferent-induced changes in rate, synchrony and phase, and that this process is not equivalent to an attenuation of sound. The phase data also suggest that efferents might change cochlear micromechanics because they change the sound-level dependence of ANF phase - a dependence thought to arise from cochlear micromechanical processes (Ruggero et al., 1996)[1]. This idea is supported by our data that efferents have little effect on the phase of the cochlear microphonic (which is thought to indicate BM phase when CM is recorded at the round window in response to low-frequency tones), but that efferents can, at the same time, substantially change the ANF phase. Heretofore, efferents had not been thought to modify cochlear micromechanics.

[1]Micromechanics is defined as signal transformation taking place beyond the basilar membrane, but before changes in inner-hair-cell receptor potentials

C. Functional implications

Although the experiments were not designed to test specific hypotheses about the functional role of efferents, they can, nonetheless, be used to comment on the issue. Historically, the first functional role ascribed to the efferent system is the extension of the dynamic range of hearing (Galambos, 1956; Wiederhold, 1970). The data described in this thesis are certainly consistent with that view. The novel feature of the data is that they suggest that efferents extend the dynamic range more than has been previously thought – both in terms of extension to higher sound levels and in terms of extension to lower frequencies than was previously thought possible.

Another functional role attributed to the efferent system is a reduction of masking. In particular, efferents have been shown to have an antimasking effect on responses to transient sounds in a background of continuous noise (Kawase et al., 1993; also behavioral studies by e.g., Trachiotis and Elliott, 1970; Zeng et al., 1994), presumably by decreasing ANF adaptation to noise. Although data from this thesis indicate that the efferent inhibition of ANFs at tail frequencies is much smaller than at CF, this small inhibition may be functionally relevant in antimasking. Specifically, at high sound levels, responses to tail frequencies are much more robust upon addition of a background noise than responses at CF (Kiang and Moxon, 1974). Consequently, small efferent-induced changes at tail frequencies may be of similar importance as large efferent-induced changes at tip frequencies. This view is consistent with the finding that efferent activity similarly enhanced single-fiber detection of tail-frequency and tip-frequency transients in a broadband noise (Kawase et al., 1993).

Most recently, efferents have been shown to play an important role in preventing long-term damage due to acoustic trauma (Zheng et al., 1997; Liberman and Kujawa, 1998). Since the data presented in this thesis indicate that efferent inhibition persists at high sound levels, the data should help in understanding the mechanisms whereby efferents play a role in the prevention of acoustic trauma.

The functional significance of the efferent-induced changes in the response phase of ANFs is not clear. However, it is possible that these changes alter perception of direction and loudness. The idea that changes in phase across a population of fibers, in addition to

changes in firing rate, might alter the perception of loudness is consistent with the model of Carney (1994).

D. Summary

This thesis provides experimental data that put new constraints on common concepts of how the cochlea works. Contrary to the "common wisdom" before this thesis was begun, we have shown that efferent effects are biggest at moderate to high sound levels, and that efferents inhibit ANFs even at tail frequencies. Furthermore, our data on efferent effects on the response phase of ANFs suggest that efferents might change cochlear micromechanics. Preliminary data from this thesis have stimulated reexamination of the basilar membrane measurements by other authors, so that we now have a better idea of how efferents affect BM motion over a wide range of sound levels. Functional implications of the results from the thesis are speculative. However, the results are consistent with the views that efferents: extend the dynamic range of hearing, reduce masking by background noise, and protect the ear from damage due to intense sounds.

Chapter 2

Medial Efferent Inhibition Produces the Largest Equivalent Attenuations at Moderate to High Sound Levels in Cat Auditory-Nerve Fibers

I. Abstract

[1]

Previous work has shown that medial efferents can inhibit responses of auditory-nerve fibers to high-level sounds and that fibers with low spontaneous rates (SRs) are inhibited most. However, quantitative interpretation of these data is made difficult by effects of adaptation. To minimize systematic differences in adaptation, we measured efferent inhibition with a randomized presentation of both sound level and efferent stimulation. In

[1]Reprinted with permission from J. J. Guinan Jr. and K. M. Stanković, "Medial efferent inhibition produces the largest equivalent attenuations at moderate to high sound levels in cat auditory-nerve fibers", *Journal of the Acoustical Society of America*, 100: 1680-1690 (1996). Copyright 1996 Acoustical Society of America.

anesthetized cats, we stimulated efferents with 200/s shocks and recorded auditory-nerve-fiber responses to tone bursts (0-100 dB SPL, 5 dB steps) at their characteristic frequencies. Below 50 dB SPL, efferent inhibition (measured as equivalent attenuation) was similar for all fibers with similar CFs in the same cat. At 45-75 dB SPL, low-SR and medium-SR fibers often showed much larger inhibition, and substantial inhibition even at 100 dB SPL. Expressed as a fractional decrease in rate, at 90-100 dB SPL the inhibition was 0%, 6% and 13% for high-, medium- and low-SR fibers (differences statistically significant). Finding the largest equivalent attenuations at 45-75 dB SPL does not fit with the hypothesis that medial-efferent inhibition is due solely to a reduction of basilar-membrane motion. The large attenuations, some over 50 dB, indicate that medial efferent inhibition is more potent than previously reported.

II. Introduction

The earliest work on the effects of efferents left a lasting impression that efferent inhibition is large only at low sound levels (Galambos, 1956; Desmedt, 1962; Wiederhold, 1970; Teas et al. 1972). This impression has been reinforced by more recent work showing that efferent inhibition of evoked otoacoustic emissions (OAEs) and reduction of basilar-membrane motion is largest at low sound levels (Mountain 1980; Moulin et al., 1993; Dolan and Nuttall 1994). Furthermore, efferent inhibition being largest at low sound levels is consistent with the hypothesis that efferent inhibition is due to medial efferents acting on outer hair cells (OHCs) to reduce basilar-membrane motion.

However, medial efferents can produce substantial inhibition at high sound levels in responses of single auditory-nerve fibers (Guinan and Gifford 1988a; see also Gifford and Guinan 1983). This inhibition is largest for auditory-nerve fibers with low and medium spontaneous rates (SRs), the fibers which are probably most important in carrying information at high sound levels (Viemeister 1983; Young and Barta 1986).

Although this single-fiber work showed that efferent inhibition is present at high sound levels, the methods were not adequate for comparing the strength of efferent inhibition at low and high sound levels. Guinan and Gifford (1988a) used level functions run in sequence from

low to high sound levels with efferent stimulation alternating with no efferent stimulation at each level. In such sequential level functions, adaptation increases as sound level goes up and can distort the shape of the level function (Sachs and Abbas, 1974). In many low-SR and medium-SR auditory-nerve fibers, strong saturation of the firing rate (i.e. a"plateau") is seen at high sound levels in sequential level functions, but continued growth with a lower slope at high sound levels ("sloping saturation") is seen in randomized level functions (Sachs and Abbas, 1974). Thus, the efferent-induced reduction of plateau rate observed in sequential level functions by Guinan and Gifford (1988a) may actually be due to an efferent-induced attenuation of effective sound level, because adaptation turned a sloping saturation into a plateau. Such possibilities make it impossible to accurately compare efferent effects across sound levels using sequential level functions.

The primary goal of the present work is to measure efferent effects in a way that will allow valid comparisons across sound levels. To do this we have minimized the influence of adaptation by using randomized level functions. We simultaneously randomized sound level and the presence of efferent shocks to allow comparison of firing rates at different sound levels both with and without efferent stimulation.

A second goal of the present work is to compare efferent effects across auditory-nerve fibers grouped according to their spontaneous-rates. Guinan and Gifford (1988a, 1988c) reported that low-SR fibers showed substantially larger efferent inhibitions than high-SR fibers, both in threshold shift and plateau inhibition. Since differences in medial-efferent effects across SR groups would have important implications for the mechanisms involved (auditory-nerve fibers in each of the three SR classes can synapse with the same inner hair cell (IHC)), this issue is worthy of re-examination using data that are not strongly influenced by adaptation, i.e. with the randomized level functions.

Our results show that the largest efferent-induced effective attenuations occur in low-SR and medium-SR auditory-nerve fibers at moderate to high sound levels (45-75 dB SPL) with substantial efferent inhibition present even at 100 dB SPL[2]. These data do not fit with the hypothesis that medial-efferent inhibition is due solely to a reduction of basilar-membrane motion. The very large efferent-induced attenuations we have found, some over

[2]Preliminary results were previously presented (Guinan and Stankovic, 1996a).

50 dB, indicate that medial efferent inhibition is considerably more potent than previously reported.

III. Method

A. Surgical Preparation

Anesthesia was induced in adult cats by intraperitoneal injection of 0.15 ml/kg Dial in urethane (100 mg/ml diallyl barbiturate, 400 mg/ml monethyurea and 400 mg/ml urethane) and maintained with injections of 1/10 of the original dose, as needed. Treatment of experimental animals was in accordance with protocols approved by the Committees on Animal Care at the Massachusetts Institute of Technology and the Massachusetts Eye and Ear Infirmary.

Most aspects of the surgery, acoustic stimulation and recording from auditory-nerve fibers are similar to those used earlier (Gifford and Guinan, 1987; Guinan and Gifford, 1988a). Important points and differences are noted here. The ear canals were surgically exposed and the auditory bullae were opened. The bony septum between the bulla and middle ear was removed and the tendons of the middle-ear muscles were cut. After a posterior craniectomy, both the lateral and medial parts of the cerebellum were aspirated to expose the floor of the fourth ventricle and the exit of the auditory nerve.

Auditory-nerve compound action potentials (CAPs) were monitored with an electrode on, or near, the round window (RW). An automated tone-pip audiogram determined the sound level at 0.5, 1, 2, 4, 8, 16, 23 and 32 kHz which evoked CAPs of 5 μV (electrode near the RW) or 10 μV (electrode on the RW). Single fiber recordings began 10 or more hours after cutting the middle-ear-muscle tendons so that the CAP audiograms were within the normal range during the period over which the data reported here were obtained.

B. Stimulation and Recording

Efferents were stimulated with a multiprong electrode along the midline of the floor of the fourth ventricle (midline olivocochlear bundle (OCB) stimulation) (Gifford and Guinan, 1987). Shocks were delivered through the pair of adjacent prongs which yielded the greatest

inhibition of the CAP response without evoking movement. Shock pulses were 0.3 ms at 200/s and coupled by a transformer so that no net charge was delivered. The efferent inhibition of the CAP response was equivalent to decreasing the sound level by amounts ranging from 9 to 19 dB during the period over which the data reported here were obtained.

Single auditory-nerve fibers were recorded (as in Kiang 1965) using broad-band noise bursts as a search stimulus. Fibers of all SRs were studied but we were biased toward low-SR fibers to provide adequate numbers to contrast with the more numerous high-SR fibers. We were also biased toward studying fibers with characteristic frequencies (CFs) within a narrow range in the same cat, so that inhibition of high-SR and low-SR fibers of similar CFs could be examined. Because of this, comparison of the overall data set across frequency may be biased. After making contact with a fiber, the data gathering sequence was: (1) to obtain enough of a tuning curve to determine the CF of the fiber, (2) to record the spontaneous firing for 20 sec and calculate the SR of the fiber, (3) to run level functions. On most animals, we ran only randomized level functions, however in some cases (most fibers on cat 20) we ran both sequential and randomized level functions for comparison. Fibers were put into SR groups using the categories of Liberman (1978): low is SR $\leq$0.5, medium is 0.5 $<$ SR $<$ 18, high is SR $\geq$ 18 spikes/s.

We were careful to insure that each spike triggered a time marker. One important potential problem is spurious spike triggering caused by electronic artifacts at the recording electrode produced by the efferent shocks. For each data set, we examined peri-stimulus-time histograms locked to the shock times. We rejected those data which showed either extra time markers caused by the positive phase of the shock artifact triggering the spike detector , or a period of reduced time markers caused by the negative phase of the shock artifact reducing the number of triggers from the spikes. We also rejected data when spike interval histograms revealed that short-interval spikes were missed.

C. The Level-Function Paradigm

Level functions were simultaneously randomized across sound levels and the presence or absence of efferent stimulation. In the initial exploratory experiments, the range of sound levels was set separately for each fiber. In the final experimental series, all randomized

level functions went from 0-100 dB SPL in 5 dB steps. Thus, with 21 sound levels and 2 shock conditions, there were 42 randomized trials in a set. If the unit spikes remained high enough in amplitude, multiple sets of randomized level functions were obtained for a fiber, each randomized independently. The results were then combined by averaging the rates for each sound-level and shock condition.

All tone bursts were at the fiber CF, 50 ms on, 50 ms off, with 2.5 ms rise/fall times. At each level-function trial, the firing rates in response to 10 tone bursts were averaged. For each tone burst, the time window for counting spikes began 2 ms after the beginning of the rise of the tone burst and ended 3 ms after the end of the fall of the tone burst. If the trial was "with efferent shocks", the shocks began 100 ms before the beginning of the first tone burst and lasted 1.1 seconds (i.e. until the end of the 10th tone-burst period). Individual trials were every 3 seconds in the final animals (every 2.5 sec in some earlier animals). In some cases, 15 tone bursts were given in each trial (only the first 10 were averaged) so that there would be 5 tone bursts after the shocks for looking at the time course of efferent effects.

Sequential level series had the same timing within a trial as the randomized series. However, in the sequential level series, the sound levels increased monotonically from low to high, and at each level shocks/no-shocks trials were alternated. At every sound level, a fixed number (1 to 4, usually 2) of shocks/no-shocks trials were alternated with the same condition always presented first throughout the level function (arbitrarily chosen at the beginning of the series).

Randomized data were gathered on 8 cats. The data reported here are from 99 auditory-nerve fibers from the last 4 cats in which all of the runs were randomized over 0-100 dB SPL. The data from the earlier animals are consistent with these results.

IV. Results

A. Sequential versus Randomized Data

As expected from previous reports (Sachs and Abbas, 1974), randomization changed the shapes of many level functions. In particular, many medium-SR and low-SR auditory-

nerve fibers which showed plateaus in sequential level series showed sloping saturations in randomized level series (Fig. 2-1A, B). Some sequential level functions without efferent stimulation had their largest rate just above the rising phase (e.g. at * in Fig. 2-1C); the corresponding randomized level functions had plateaus or sloping saturations without this rate bulge (e.g. Fig. 2-1D)[3]. There were also many cases where randomization had little effect on the shapes of the level functions but increased the rates at high sound levels. This was the pattern for some very low SR auditory-nerve fibers (e.g. Fig. 2-1E, F) and for almost all high-SR auditory-nerve fibers (not illustrated).

Since a single randomized run usually produced a very "noisy" level function, multiple randomized runs had to be averaged to obtain a smooth level function. When multiple randomized runs were obtained from the same fiber, the overall shapes of the level functions, although noisy, were always similar (Figs. 2-2, 2-3, 2-4).

B. Level Shifts

The standard way to measure efferent effects has been the efferent-induced attenuation, or level shift, ΔL. This is the amount by which the sound level must be increased (i.e. shifted) with efferent stimulation to produce the same response as that obtained without efferent stimulation (see Fig. 2-2B). One advantage of measuring ΔL is that it is an equal response measure and is not changed by any nonlinear transformations which might occur functionally after the site of efferent action. Thus, if medial-efferent inhibition is produced solely by a reduction of basilar-membrane motion, then the ΔL measured from auditory-nerve responses would equal the ΔL measured from basilar-membrane motion.

Although the level shift, ΔL, is conceptually simple, calculating it from a pair of noisy level functions can be complicated. Furthermore, in some fibers, ΔL cannot be calculated at high sound levels because the firing rate without efferent stimulation is higher than

[3]This difference supports the hypothesis of Guinan and Gifford (1988a) that the bulge is due to adaptation interacting with the alternating shocks / no-shocks paradigm. At the sound level of the bulge, the fiber was alternating between a high firing rate when there was no efferent stimulation and a much lower rate when there was efferent stimulation. Presumably, the low rate during the efferent stimulation produced little adaptation and allowed subsequent no-efferent-stimulation responses to be large. At higher sound levels, the firing rate is high during efferent stimulation, presumably producing considerable adaptation and lowering subsequent no-efferent-stimulation responses.

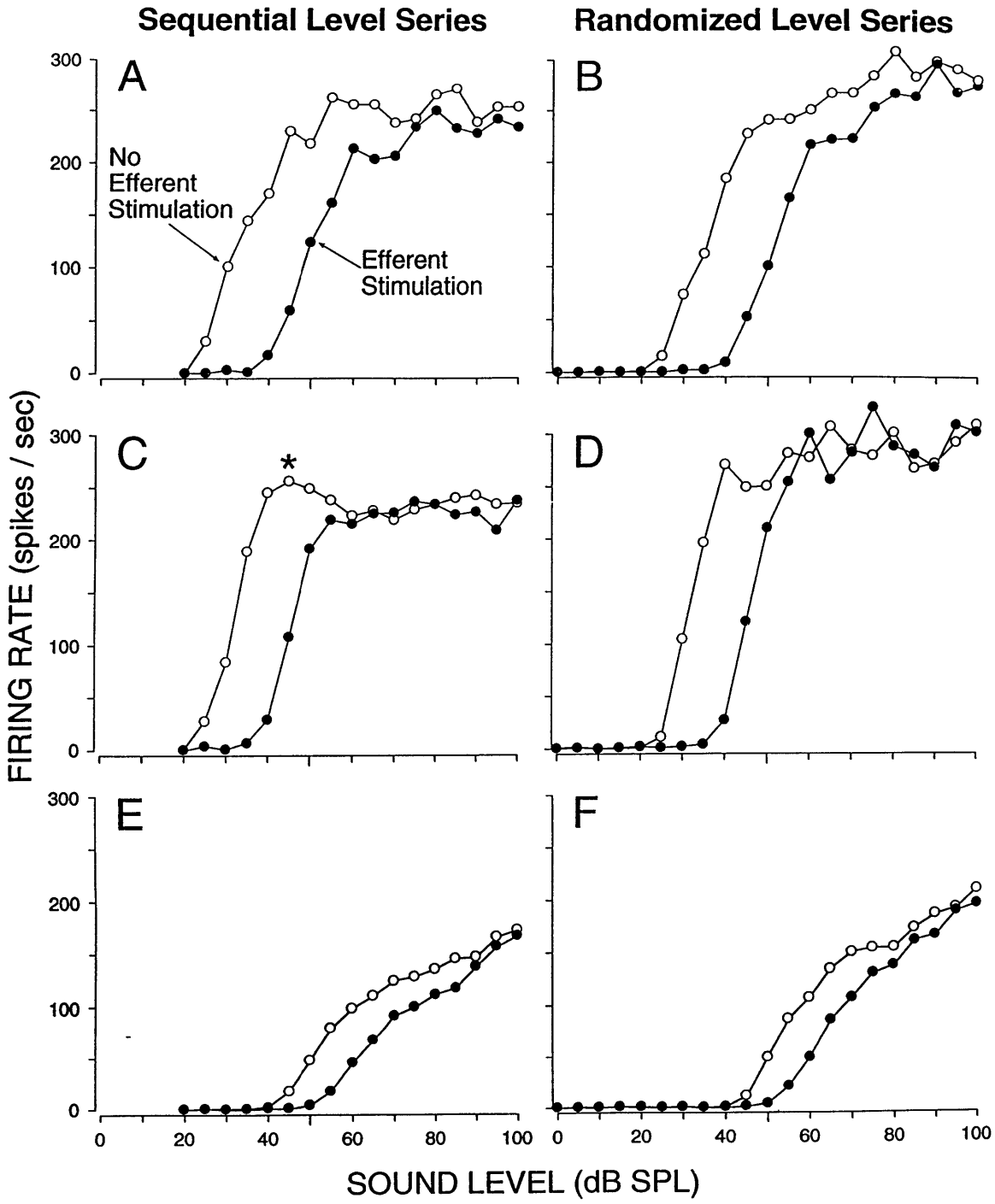

Figure 2-1: Examples of level series obtained sequentially (left) and randomized (right) from the same auditory-nerve fiber. Each row is from a different fiber. Top: Fiber: 20-65, characteristic frequency (CF) = 18.62 kHz, spontaneous rate (SR) = 0.1 sp/s. Middle: Fiber: 20-57, CF = 23.44 kHz, SR = 2.0 sp/s. Bottom: Fiber: 20-52, CF = 28.84 kHz, SR = 0.0 sp/s. The number of trials of each condition averaged for each panel, in sequence, are: 2, 2, 2, 2, 4, 4.

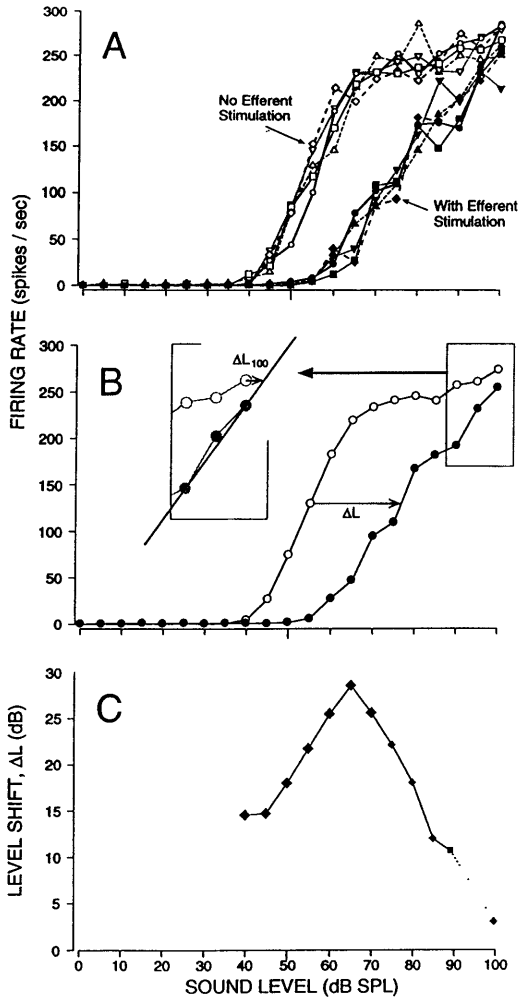

Figure 2-2: Randomized level series from a single auditory-nerve fiber. A: Five measurement sets (coded by different symbols) of the firing rate, each with a randomized presentation of sound level and efferent stimulation, illustrating the reproducibility of the randomized level functions. B: The level functions derived by averaging the rates obtained at each sound level and efferent stimulation condition. The inset shows the computation of the efferent-induced level shift, ΔL, at 100 dB SPL (see below). C: ΔL calculated from the data in panel B. For each no-shocks point, ΔL was the amount the sound level had to be raised to reach the same rate on the with-shocks level function (ΔL in panel B). ΔL was calculated for every no-shocks point clearly in the rising phase (i.e. no point at a higher sound level had a lower rate and no point at lower sound level had a higher rate) and is shown with large symbols. ΔL was also calculated, for low-SR and medium-SR fibers as follows: (1) for points at higher sound levels (small symbols) until their rates exceeded the maximum rate with efferent shocks, (2) from the no-shocks response curve to the with-shocks point at 100 dB SPL, whenever this point had the highest with-shocks rate (rotated small symbol), and (3) for 100 dB SPL, by extrapolating the with-shocks rates to sound levels above 100 dB SPL using a line through the 90 and 100 dB SPL points (see inset in panel B) (small symbol at 100 dB SPL). Since this last point is based on extrapolated data, it is connected by a dotted line. Fiber 20-47, CF = 3.55 kHz, SR = 0.05 sp/s.

the highest rate obtained with efferent stimulation (e.g. the no-efferent-stimulation points at, and above, 50 dB SPL in Fig. 2-3). Nonetheless, an automated procedure has been developed (see caption for Fig. 2-2C) which calculated ΔL in the fast rising phase of the level functions (large points in plots of ΔL), in noisy sloping regions (smaller points in plots of ΔL), and at 100 dB SPL by extrapolating the with-shocks data to sound levels above 100 dB SPL (points at 100 dB SPL, see Fig. 2-2B). This procedure provided calculations of ΔL over the range from threshold to 100 dB SPL for low-SR and medium-SR fibers and in the rising phase for high-SR auditory-nerve fibers.

The efferent induced level shift, ΔL, showed a variety of patterns across auditory-nerve fibers (Figs. 2-1, 2-2, 2-3, 2-4). In some fibers, ΔL was relatively constant in the fast rising phase (Fig. 2-1A, B). In many fibers with sloping saturations, the level function without efferent shocks had a sloping saturation but the level function with efferent shocks was relatively straight (Fig. 2-2). With this pattern, the resulting ΔL is greatest at sound levels near the bend in the sloping saturation (Fig. 2-2C). In a few cases, the level function with efferent stimulation appeared to plateau producing what might be called an efferent depression of plateau rate (Fig. 2-3).

High-SR auditory-nerve fibers often had level functions in which the fast rising phase with efferent stimulation had a higher slope than the fast rising phase without efferent stimulation (Fig. 2-4). This produced a ΔL which decreased as sound level increased (Fig. 2-4C). We hypothesized that this difference in slopes might be due to differences in adaptation caused by the efferent stimulation inhibiting the spontaneous activity which was present in the 50 ms between the tone bursts (somewhat like the process which produced the "bulge" in Fig. 2-1C). To test this hypothesis, on a sampling of fibers which showed large changes in ΔL with sound level, we reprocessed the spike-time data to include in the response window used to calculate the rate all spike times from both during the tone bursts and the time between the tone bursts. The resulting rate-level functions showed average rates of approximately half the previous values, but the ΔLs calculated from these (e.g. the open diamonds in Fig. 2-4C) were little different from those calculated just from the period during the tone bursts (e.g. the filled diamonds in Fig. 2-4C). Thus, the decrease in ΔL with sound level in high-SR fibers does not appear to be caused by efferent inhibition of

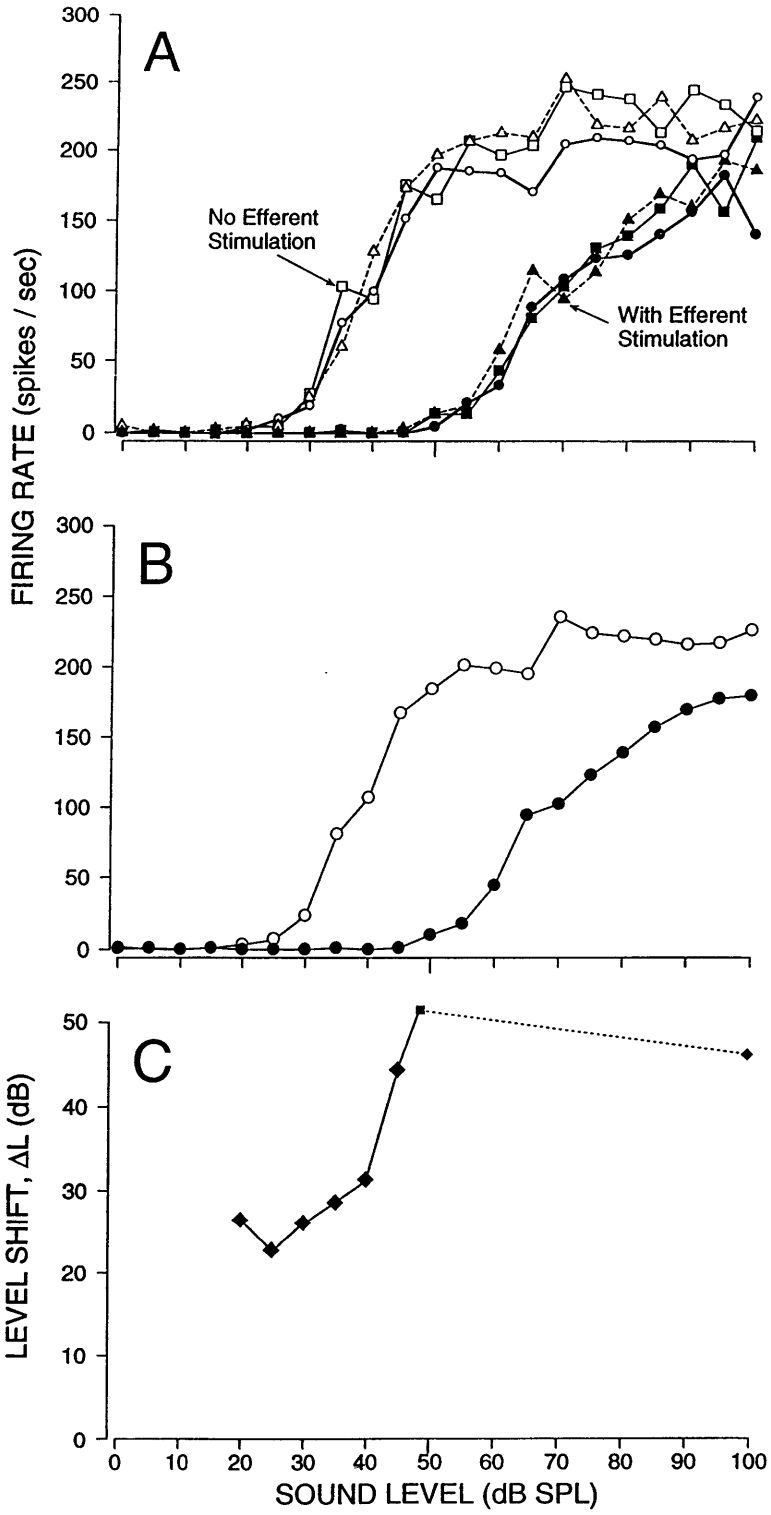

Figure 2-3: Randomized level series and the resulting level shifts from a single auditory-nerve fiber. Layout as in Fig. 2-2. Fiber 21-80, CF = 6.31 kHz, SR = 0.2 sp/s.

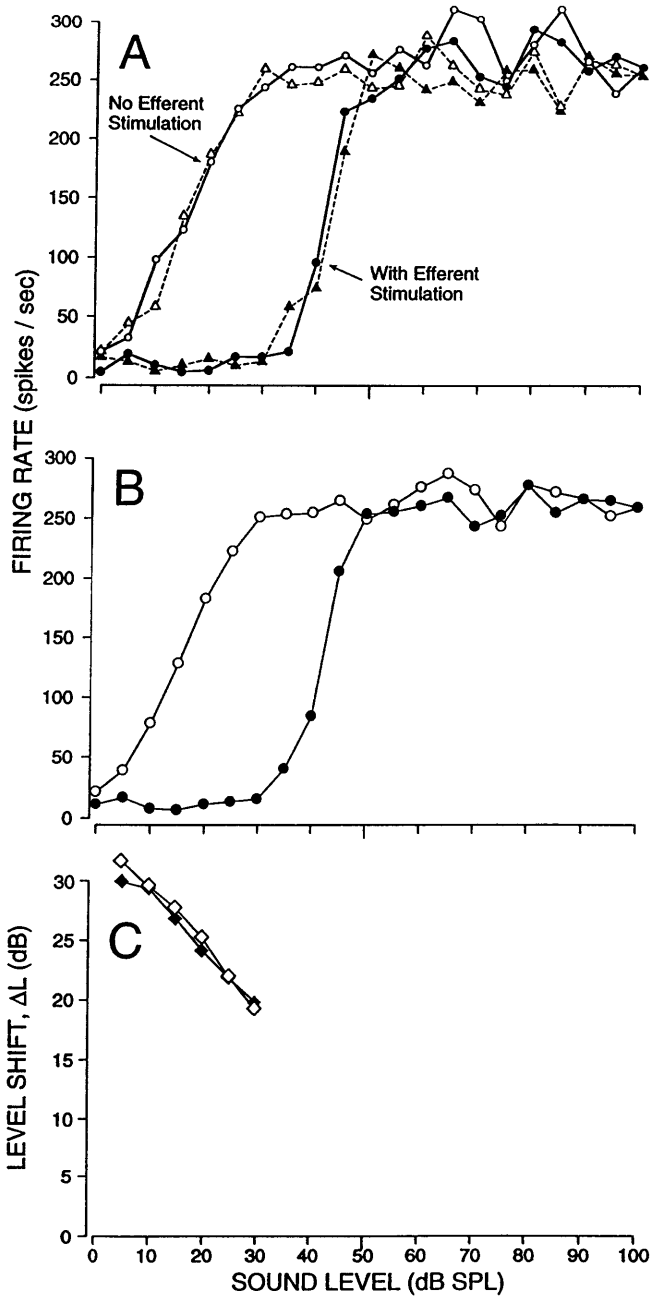

Figure 2-4: Randomized level series and the resulting level shifts from a single auditory-nerve fiber. Layout as in Fig. 2-2. In panel C, the closed symbols were obtained using a response window which just included the spikes during the tone bursts. The open symbols were obtained using a response window which included spikes both during the tone bursts and during the times between tone bursts (see text). Fiber 21-86, CF = 14.79 kHz, SR = 33.3 sp/s.

spontaneous activity changing the adaptation level.

C. Averaged Level Functions

In order to get an overall picture of the effects of efferent stimulation on the responses of auditory-nerve fibers, we averaged randomized level functions from many auditory-nerve fibers. For fibers in each SR class, we averaged the data from all fibers with CFs in octave bands centered at approximately 2, 4, 8, 16, and 32 kHz (Fig. 2-5). To make the curves smoother, we weighted data from each fiber by the number of runs done on that fiber. This is equivalent to averaging all of the runs from the fibers with CFs in the octave band. The resulting smoothness allows more accurate determinations of ΔL, particularly in regions of low slope. The ΔLs calculated from these average level functions are shown in Fig. 2-6.

Figure 2-5 shows that the shapes of the level functions and the pattern of efferent inhibition varied systematically with fiber SR and CF. The rates of high-SR fibers rise sharply with sound level and form clear plateaus with little efferent inhibition at high sound levels. In contrast, the medium-SR and low-SR fibers show less sharp plateaus and definite efferent inhibition at high sound levels. Across frequency, the pattern of efferent inhibition is similar to that found before (Wiederhold 1970, Guinan and Gifford 1988c). The greatest inhibition was in the 6-12 kHz band and there was less inhibition at higher and lower frequencies (Fig. 2-5, 2-6).

Despite averaging level functions from many fibers, the plots in Figs. 2-5 and Fig. 2-6 are still inadequate to accurately define ΔL for high-SR fibers at high sound levels. In an attempt to provide a better estimate of this ΔL, an overall average of the data for the frequency region in which efferent inhibition was large (6-24 kHz) is given in Fig. 2-7, along with the calculated ΔLs. It should be kept in mind that the plots in Fig. 2-7 average across frequency regions in which the strength of the efferent effect varied substantially.

Figures 2-6 and 2-7 show that within a given frequency band, the average ΔLs for high, medium, and low SR fibers are similar, usually within 5 dB for sounds below 50 dB SPL. At levels near 50 dB SPL, ΔL rises with sound level so that the highest ΔLs are at 45-75 dB SPL, at least for low-SR and medium-SR fibers. At sound levels above 75 dB SPL, ΔL decreases, but there are few ΔL points, principally because at these high levels the

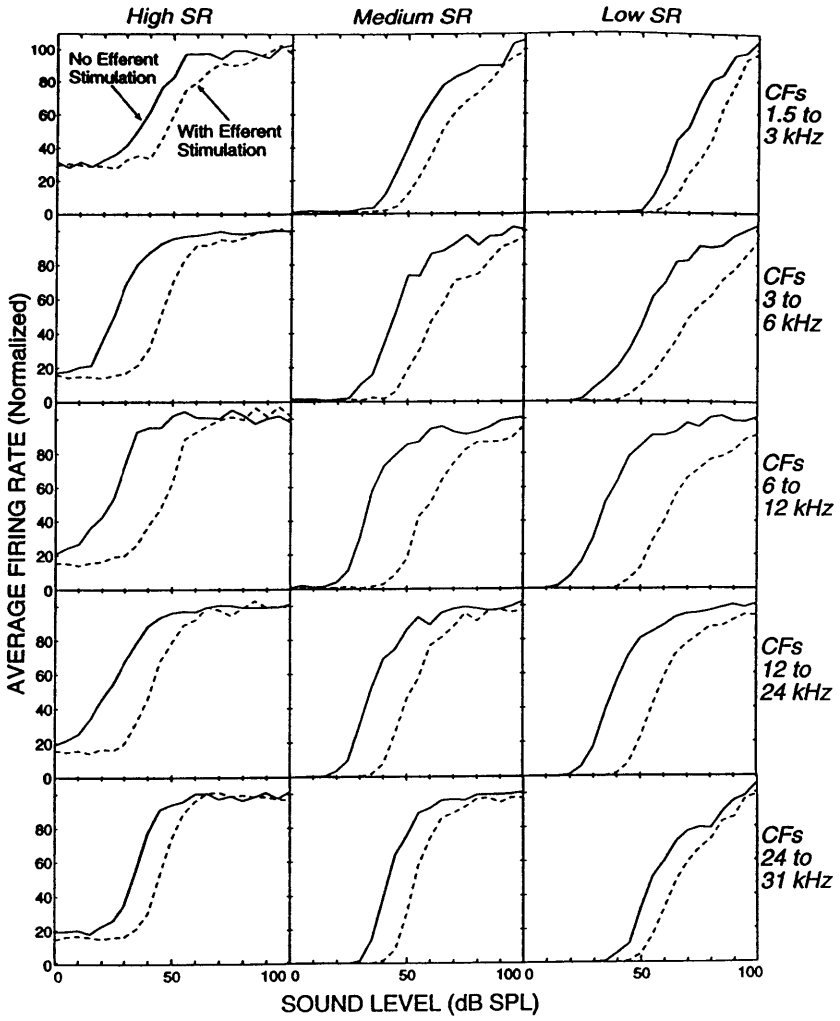

Figure 2-5: Average level functions from all of the auditory-nerve fibers in a SR category which have CFs in adjacent octave bands.Solid lines are level functions without efferent stimulation, dashed lines are level functions with efferent stimulation. The highest "octave" had no fiber CFs > 31 kHz. Averages were obtained by (1) normalizing the data from each fiber so that the rates equaled 100 averaged over the 90-100 dB SPL points with no efferent stimulation, and (2) at each level and efferent stimulation condition, averaging the normalized rates with the data from each fiber weighted by the number of randomized runs for that fiber. In each panel, the number of fibers and the total number of runs included are:

Range	High SR		Medium SR		Low SR	
(kHz)	fibers	runs	fibers	runs	fibers	runs
1.5–3	7	9	9	23	1	4
3–6	8	19	5	11	4	14
6–12	6	11	5	6	8	17
12–24	12	18	6	9	9	23
24–31	6	13	2	9	3	10

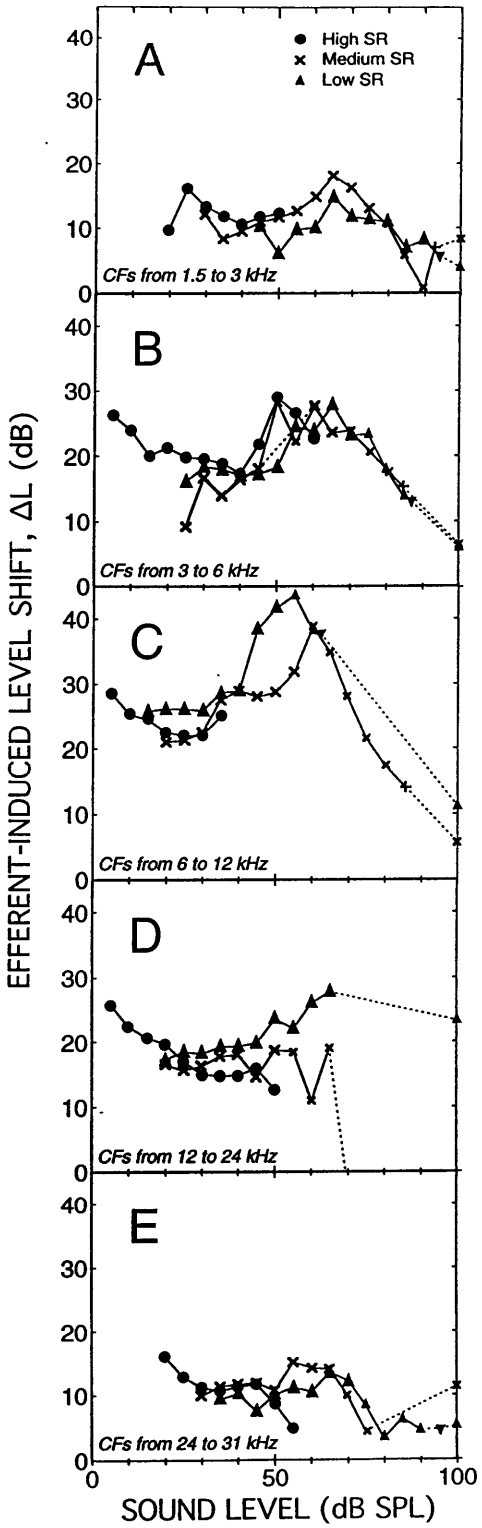

Figure 2-6: Level shifts of the high-SR (circles), medium-SR (X's) and low-SR (triangles) auditory-nerve fibers in octave bands, calculated from the data in Fig. 2-5. Symbol size and orientation indicate the method used to obtain the ΔL (see Fig. 2-2 caption).

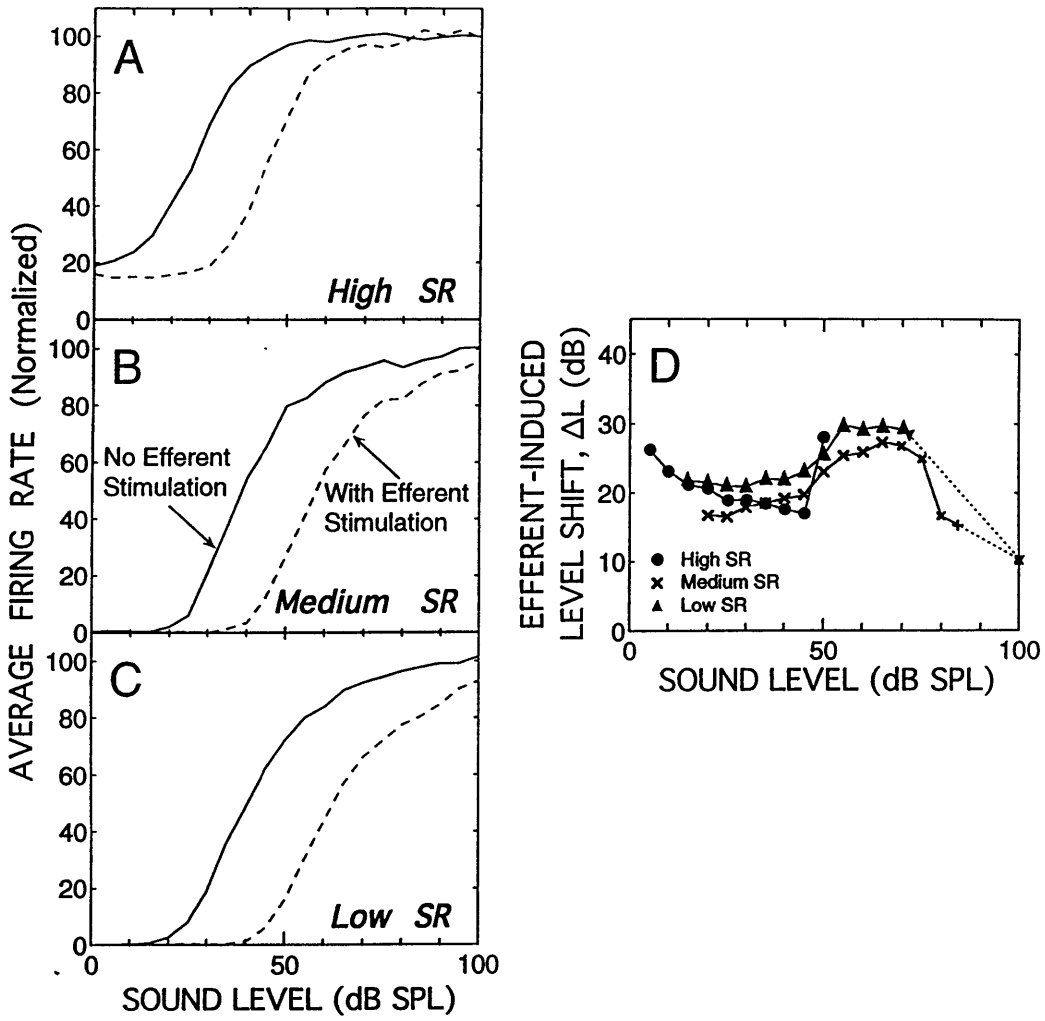

Figure 2-7: Level functions (left) and level shifts (right) averaged from all auditory-nerve fibers with CFs from 3-24 kHz. Fibers were separated into groups according to spontaneous rate: high-SR (circles), medium-SR (X's) and low-SR (triangles) . Symbol size and orientation indicate the method used to obtain the ΔL (see Fig. 2-2 caption).

rates without efferent stimulation often exceed the highest rate with efferent stimulation. Finally, extrapolation of the level functions with efferent stimulation past 100 dB SPL indicates that ΔL at 100 dB SPL is usually considerably below the peak ΔL. The data also show a relatively consistent pattern for the high-SR group at very low sound levels. In all frequency bands except one, ΔL was biggest at the lowest sound level and decreased as level increased up to about 40 dB SPL This is the pattern shown by the fiber in Fig. 2-4.

D. Comparison of Individual Level Functions in Narrow CF Bands

It is useful to look at level functions from fibers with a wide range of spontaneous rates but within a narrow range of CFs. The averaged level functions, and the ΔLs calculated from them, are useful for getting an overview of the data, but they may mask patterns which are present in some level functions but not in others. In addition, Gifford and Guinan (1988a, 1988c), using averaged data, reported that efferent-induced level shifts and threshold shifts were greater for low-SR fibers than for high-SR fibers. To help discern whether this is due to pooling data across cats and CFs, we wanted to compare ΔLs from fibers with similar CFs obtained in the same cat.

To compare fibers with similar CFs, we included each case in the four final cats for which there was at least one high-SR and one low-SR fiber in the same cat with CFs within 10%. We included all fibers with nearby CFs, as long as the frequency band was not made greater than 10%. All of the cases are from 2 cats because the CFs were too spread out on the other cats. The data obtained from earlier cats in which randomized level functions were done over ranges less than 0-100 dB SPL are similar to those shown here.

The efferent-induced shift, ΔL, as a function of sound level for fibers with CFs in narrow frequency bands are shown in Fig. 2-8. At low sound levels there was usually a tight distribution of ΔL values at each sound level, but at moderate to high sound levels there was sometimes considerable spread. The interpretation of these data is made difficult by the fact that noise in individual level functions can sometimes produce large differences, particularly at the end points of the fast rising phase and in sloping saturations. Within the level of accuracy of the data, Fig. 2-8 indicates that ΔL from high, medium and low SR fibers are about the same at low sound levels, although the data do not rule out small

differences. In particular, the largest difference reported by Guinan and Gifford (1988c) was that ΔL for low-SR fibers exceeded ΔL for high-SR fibers by more than a factor of two for the octave centered at 16 kHz. The data of Fig. 2-8 do not show any difference close to this for sounds less than 50 dB SPL. However, at the highest sound levels, some of the differences in Fig. 2-8 appear to be too large to attribute to random errors (e.g. Fig. 2-8F).

E. Efferent Inhibition at High Sound Levels

The efferent-induced level shift, ΔL, may not be the best way of looking at efferent inhibition at high sound levels, in part because the value of ΔL can be affected greatly by small changes in rate when the slope of the level function is very low. An alternate way of looking at this inhibition is the efferent-induced change in rate. The change in rate can be calculated for fibers which span the entire range of SRs and for any level-function shape.

We calculated the efferent-induced change in rate, ΔR, from the rates with and without efferent stimulation, each averaged over the responses from 90 to 100 dB SPL. The resulting ΔRs are plotted versus fiber spontaneous rate in Fig. 2-9. To include as many fibers as possible, but only fibers on which the efferent effect was large, we included only fibers with CFs from 3-24 kHz.

Figure 2-9 shows that the efferent inhibition of firing rate at high sound levels depends strongly on spontaneous rate. Efferent stimulation did not produce a significant change in rate for high-SR fibers (ave. $\Delta R = +0.4$ %). However, ΔR from the medium-SR fibers (ave. $\Delta R = -6.5$ %) was significantly less (t=4.34, $p = 0.00009$ by a Students t-test) than ΔR from the high-SR fibers, and ΔR from the low-SR fibers (ave. $\Delta R = -12.7$ %) was significantly less (t=2.29, $p = 0.028$) than ΔR from the medium SR fibers. If the one fiber with a very low ΔR is dropped from the low-SR group (see Fig. 2-8), the ΔR from low-SR fibers is still significantly less than the ΔR from medium-SR fibers ($t = 2.34$, $p = 0.025$). Although, these data show that at high sound levels efferent inhibition is significantly different across SR groups, they do not separate whether this inhibition is due to a level shift or a plateau depression.

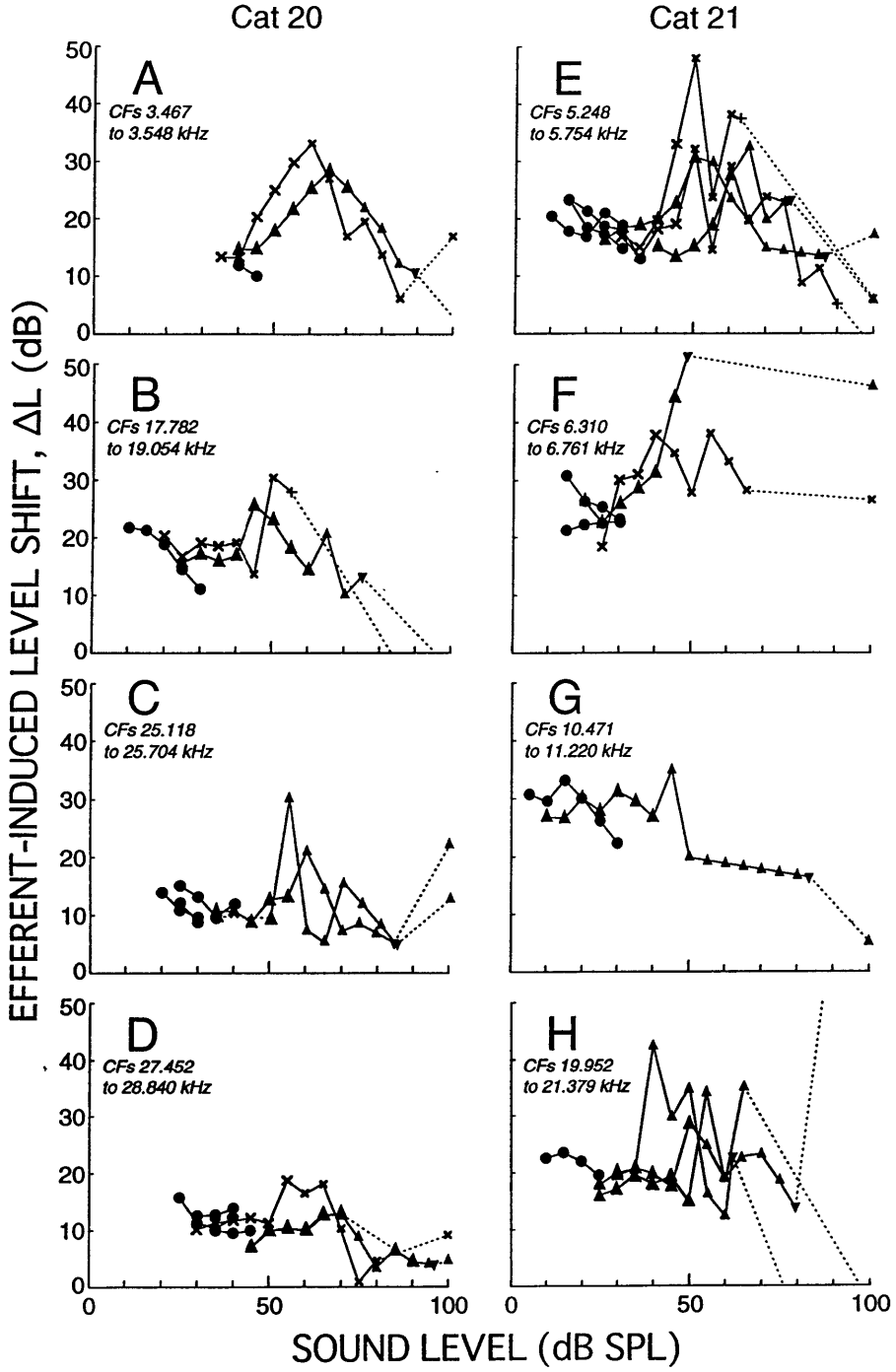

Figure 2-8: Level shifts of the high-SR (circles), medium-SR (X's) and low-SR (triangles) auditory-nerve fibers with CFs within a range of 10% or less. Symbol size and orientation indicate the method used to obtain the ΔL (see Fig. 2-2 caption). Left column: cat 20; right column: cat 21.

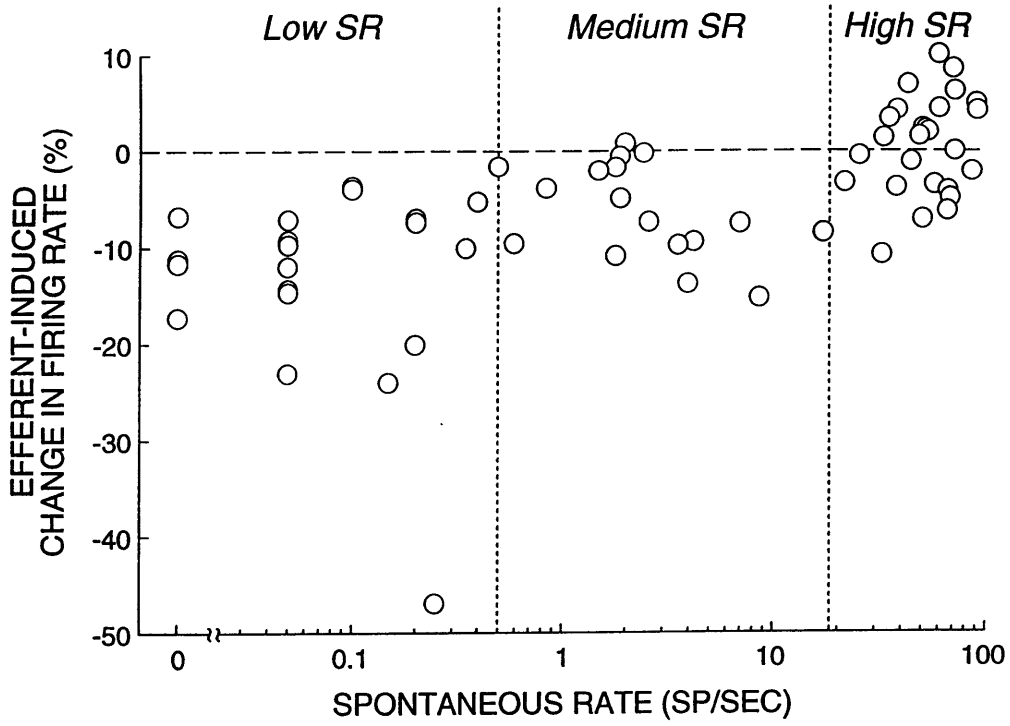

Figure 2-9: The efferent-induced change in firing rate as a function of fiber spontaneous rate. Each point is from a different single auditory nerve fiber. Included are all fibers with a CF in the range 3 to 24 kHz.

V. Discussion

A. Efferent Inhibition as a Function of Sound Level

Our data provide a distinctly different picture of efferent inhibition than that obtained from previous work. Although it had been thought that medial efferents produce the largest level shifts at low sound levels, our data show that the largest level shifts are actually at moderate to high sound levels (Figs. 2-2, 2-3, 2-6, 2-7, 2-8). Furthermore, we have found level shifts which are much greater than any previously reported. In the 6-12 kHz band, the average ΔL in low-SR fibers was over 40 dB, and in individual fibers ΔL was over 50 dB (Fig. 2-3). Thus, medial efferents can have a much more powerful influence on auditory-nerve responses than was indicated by previous evidence.

It seems worth noting, that even though high-SR fibers are the most common, medium-SR and especially low-SR fibers are probably more important carriers of information at high sound levels (Viemeister 1983; Young and Barta 1986). Thus, at high sound levels efferent effects on low-SR and medium-SR fibers are likely to be more important than efferent effects on high-SR auditory nerve fibers.

The impression that efferent inhibition is largest at low sound levels was due mostly to measurements which do not give a full picture of how efferents affect auditory-nerve fibers. The original reports were for efferent inhibition of CAP responses. CAPs are dominated by responses of high-SR fibers and are strongly influenced by responses from fibers responding to sound energy which is not at their CF (efferent inhibition is strongest at CF; Wiederhold 1970; Brown and Nuttall 1984; Guinan and Gifford 1988c). Thus, CAP responses do not reveal efferent effects on low-SR fibers, even though these may be the largest effects. Furthermore, reports of efferent inhibition of OAEs and basilar-membrane motion provide measures of efferent effects on cochlear mechanics (Mountain 1980; Moulin et al., 1993; Dolan and Nuttall 1994), but these do not reflect any influence of medial-efferents which takes place functionally after basilar-membrane motion. Finally, none of the previous reports of efferent effects on single auditory nerve fibers revealed the inhibitory ability of medial efferents at moderate to high sound levels because they did not randomize the presentation of level functions and efferent stimulation, or because they focused on other issues

(Fex, 1962; Wiederhold and Kiang, 1970; Wiederhold 1970; Teas et al., 1972; Gifford and Guinan 1983; Winslow and Sachs, 1987; Guinan and Gifford 1988a, 1988b, 1988c; Kawase et al., 1993). Winslow and Sachs (1987) used randomized level functions, but they randomized sound levels in the shocks and no-shocks level-functions separately, so that a comparison of these does not accurately show the efferent inhibition at high sound levels. This emphasizes the importance of simultaneously randomizing both sound level and the presence of efferent stimulation so that the expected amount of prior adaptation is similar for all points on the two resulting level functions. In addition, this procedure should equalize the influence of "slow" efferent effects similar to those reported by Sridhar et al. (1995). Finally, we note that even though most previous reports focused on efferent effects at low sound levels, there was clear evidence that some auditory-nerve fibers showed substantial inhibitions at high sound levels (Wiederhold 1970; Gifford and Guinan 1983; Guinan and Gifford 1988a).

Although previous reports did not use randomized paradigms, they provide some evidence relevant to the patterns of ΔL in the fast rising phases of level functions. Wiederhold (1970) found, in cats, that ΔL was relatively constant in the rising phases of most fibers, but Teas et al. (1972) found, in guinea pigs, that ΔL was greatest near threshold and decreased as sound level increased (the pattern we found for most high-SR fibers). One difficulty in interpreting results from these early reports is that they did not segregate fibers by spontaneous rate. Guinan and Gifford (1988a) measured the overall slopes of the rising phases of level functions and found that efferent stimulation increased the slope by 14.3% (on the average) in high-SR fibers and decreased the slope by 10.5% in medium-SR fibers and by 14.3% in low-SR fibers. These trends are consistent with our newer data from different SR groups (e.g. Fig. 2-7) considering that the sound-level ranges over which the fast rising phases occur increase as fiber SR decreases.

B. Is Efferent Inhibition Different across SR Groups?

Our data suggest that low-SR fibers are inhibited more by efferent stimulation than high-SR fibers, but these data do not completely settle the issue of whether efferent inhibition is different across SR groups. The level functions from fibers with CFs within 10% frequency bands (Fig. 2-8) indicate that there are not large systematic discrepancies in ΔL across SR

groups at low sound levels, but the noisiness of these data prevents stronger conclusions from being drawn. The overall average level functions (Fig. 2-7) provide a strong indication that ΔL is larger, on the average, in low-SR fibers than in high-SR or medium-SR fibers. However, this conclusion is tempered by the octave-band averages (Figs. 2-5, 2-6) in which the pattern is not so clear cut. Finally, there are statistically significant differences across SR groups in the efferent inhibition of firing rate at high levels (Fig. 2-9). If efferent inhibition at high sound levels were due solely to a process which produces a level shift, then this difference across SR groups might be due completely to differences in the slopes of the rate versus level functions at high sound levels. With this hypothesis, some fibers (e.g. Fig. 2-3) would require very large ΔLs at high sound levels (up to 50 dB) to explain the observed rate depression. In addition, the diversity of the ΔLs needed at high sound levels makes this hypothesis unattractive. An alternative hypothesis is that efferent inhibition is a combination of a ΔL and a reduction in rate (a ΔR), with the ΔR varying across fibers and being largest, on average, for low-SR fibers.

Although our data do not resolve the issue of whether efferent inhibition is different across SR groups, they provide alternate explanations for previous reports of such differences and thereby relieve some of the need to explain these differences. It seems likely that efferent-induced level shifts (which were measured at the midpoint of the rising phase of each level function) were larger in low-SR fibers than in high-SR fibers (Guinan and Gifford 1988a) because the low-SR level shifts were measured at higher sound levels where efferent inhibition is larger. A similar difference in the sound level at which they were measured may explain why efferent-induced threshold shifts were larger in low-SR fibers than in high-SR fibers (Guinan and Gifford 1988b) but the difference across groups is less at threshold (Figs. 2-6, 2-7). With sequential level functions, efferent stimulation reduced the plateau firing rate by 4.7% for high-SR fibers, 7.1% for medium SR fibers and 19.3% for low SR fibers Guinan and Gifford (1988a). It seems likely that if these had been randomized level functions, most of the plateaus would have been sloping saturations. Then the efferent-induced change at high sound levels would have been indistinguishable from a ΔL, as noted above for our measurements of the change in rate at 90-100 dB SPL. Differences in level-function slopes across SR groups might then account for the different plateau inhibitions

found by Guinan and Gifford (1988a). Although these suggestions may not fully account for the differences across SR groups found by Guinan and Gifford (1988a, 1988c), it seems likely that they at least account for some part of the difference.

C. The Mechanisms by which Medial Efferents Inhibit Auditory-Nerve Fibers All of the efferent effects reported here are likely to be due to medial efferents

with little or no effect from lateral efferents. We have stimulated efferents with electric shocks at 200/s. Such shocks are much more effective at stimulating the myelinated medial efferents than the unmyelinated lateral efferents (Gifford and Guinan, 1987). If any lateral efferents were stimulated, the most likely would be the crossed lateral efferents; these mostly innervate the apex of the cochlea but the pattern of effects we found was strongly biased toward the base, with a maximum near the location with the greatest medial-efferent innervation (Guinan et al., 1984). In addition, the effects we report here are similar in most basic respects to those reported by Guinan and Gifford (1988a) who used focal stimulation at the brainstem origin of medial-efferents, a technique which should not excite any lateral efferents. Finally, any hypothesis which would account for the depression of responses at high levels by lateral efferent synapses on auditory-nerve-fiber dendrites must account for the fact that, on the average, there was no inhibition at 90-100 dB SPL in high-SR fibers even though they receive lateral efferent synapses. All considered, it seems unlikely that lateral efferents had a major role in producing the efferent effects reported here.

A considerable body of evidence indicates that medial efferents inhibit auditory-nerve fibers mechanically through a depression of basilar-membrane motion. With this hypothesis, efferents act on OHCs to reduce basilar-membrane motion thereby reducing the sound drive to IHCs and inhibiting the responses of auditory-nerve fibers. Supporting this "mechanical hypothesis" are direct measurements showing efferent inhibition of basilar-membrane motion (Dolan and Nuttall, 1994) and indirect evidence from the efferent inhibition of OAEs (Mountain, 1980; Siegel and Kim, 1982). This mechanism also fits with the hypothesis that the high sensitivity and frequency selectivity of the cochlea is brought about by the fast motility of OHCs acting to amplify basilar-membrane motion, and the fact that medial

efferents synapse directly on OHCs. Medial efferents are well placed to regulate the action of OHCs.

Our data on the efferent inhibition of auditory-nerve fibers as a function of sound level do not fit with the hypothesis that this inhibition is caused solely by a reduction of basilar-membrane motion. The one report on efferent inhibition of basilar-membrane motion found that the biggest inhibitions were at low levels and the inhibition decreased as sound level increased (Dolan and Nuttall, 1994). A similar picture can be derived from many other measurements of basilar-membrane motion which show that near the best frequency, basilar-membrane motion is compressively nonlinear. Factors that reduce basilar-membrane motion do so by making the compressive nonlinearity more linear so that the greatest reductions of basilar-membrane motion are at low sound levels (e.g. Rhode 1973; Sellick et al., 1982; Ruggero and Rich, 1991).

The ΔLs from high-SR auditory-nerve fibers are largest at the lowest sound levels (ignoring the large ΔLs sometimes found just below a plateau), so they appear to match the expected change in basilar-membrane motion. In contrast, the ΔLs from low-SR and medium-SR auditory-nerve fibers (and from high-SR fibers if we consider the large ΔLs sometimes found just below a plateau) peak at moderate to high sound levels, a pattern which does not fit with the reported pattern (Dolan and Nuttall, 1994) of efferent inhibition of basilar-membrane motion. This discrepancy indicates that some mechanism, in addition to depression of basilar-membrane motion, also acts to provide efferent inhibition of auditory-nerve fibers, with the two mechanisms adding in some way.

In addition to the inhibition of basilar-membrane motion, there are several possible mechanisms by which medial efferents might suppress responses of auditory-nerve fibers. One possibility is that efferents produce a mechanical change (e.g. a distortion of the organ of Corti) that reduces the mechanical coupling of basilar-membrane motion to sound-frequency bending of IHC stereocilia (de Boer, 1990). However, if the efferent inhibition of basilar-membrane motion fully accounts for the efferent inhibition of auditory-nerve CAP responses at low sound levels (as indicated by Dolan and Nuttall 1994), then there would be little room for an additional reduction due to another mechanism which acts at low sound levels. The distortion in the organ of Corti would have to have little or no effect at low

sound levels, an effect up to 50 dB at moderate to high sound levels, and a lesser effect at 100 dB SPL. Such a pattern seems very unlikely.

Another possibility is that mechanical rectification in OHCs leads to a slow bending of IHC stereocilia (this might be the main method of exciting auditory-nerve fibers for high-frequency sounds; Evans et al., 1991), and efferent activity may inhibit by reducing the OHC rectification or the coupling of the resulting motion to IHCs. This hypothesis suffers from the same drawbacks as the previous possibility. It seems unlikely that such a mechanism would have little or no effect at low sound levels and very large effects at moderate to high sound levels.

A third possibility is that medial efferents change the firing of auditory-nerve fibers by an electrical effect (Geisler, 1974; Guinan and Gifford 1988b). Activation of medial efferents produces a potential (the MOC potential) which is positive within the organ of Corti and negative in the endocochlear potential space (i.e. is a reduction of endocochlear potential) (Fex 1967, Brown and Nuttall 1984; Gifford and Guinan, 1987). The MOC potential might lead to less transmitter being released by IHCs (by increasing the transmembrane potential, i.e. slightly hyperpolarizing the IHC; Brown and Nuttall, 1984). Alternately, the MOC potential in the region of the dendrites of radial auditory-nerve fibers may reduce the probability of action potentials in response to a given transmitter release. As with the previous possible mechanisms, an efferent electrical effect would have to produce almost no level shift at low sound levels and a very large level shift at moderate to high sound levels. However, these electrical mechanisms would act at or after IHC synapses and are thus more likely to be exerting an effect best understood as a change along the rate dimension than along the level dimension. For instance, an action on the dendrites of auditory-nerve fibers might reduce the firing a fixed percentage no matter what the sound level. Such an action would produce an effect which is equivalent to a much larger level shift at high sound levels when the slope of the rate-level function is low, than in the fast rising phase of the level function. This action might also have effects of different magnitudes in fibers of different SR groups because these fibers synapse on opposite sides of IHCs (Liberman, 1980) and are therefore at different distances from OHCs, the source of the MOC potential. Furthermore, the amplitude of the MOC potential varies as a function of sound level (Fex, 1967) which

provides yet another way in which electrical effects can vary with sound level.

Important information about the site of efferent action has been provided by recordings of IHC receptor potentials with and without efferent stimulation (Brown and Nuttall, 1984). Considering four pairs of level functions, with and without efferent stimulation, from IHC receptor potentials (Fig. 2-3 of Brown and Nuttall, 1984), three appear to have ΔLs which decrease approximately monotonically as sound level is increased, and one has a ΔL which is constant at low sound levels and increases dramatically at 50 dB SPL, similar to the pattern we have often seen in auditory-nerve-fibers. This suggests that at least some of the factors which cause the increase in ΔL at moderate to high sound levels are present at the level of IHC receptor potentials. Further experimental results are required to determine the actual combination of factors by which medial-efferents change auditory-nerve responses to high-level sounds.

Chapter 3

Medial Efferent Effects on Auditory-Nerve Responses to Tail-Frequency Tones I: Rate Suppression

I. Introduction

Stimulation of medial olivocochlear efferents that synapse on outer hair cells reduces activity in auditory-nerve fibers (ANFs) that contact inner hair cells. Understanding the mechanisms of this inhibition has stimulated much work (reviewed by Guinan,1996) because there are no known neuronal connections between medial efferents and afferents that contact inner hair cells, or between inner and outer hair cells. It is now widely believed that a major component of this inhibition is a reduction of the basilar-membrane motion.

Earlier investigations left the impression that efferents do not significantly affect responses of ANFs to stimuli from the broadly-tuned, insensitive, low-frequency "tail" region of tuning curves, even in fibers that show large inhibitions at the characteristic frequency (CF) – the frequency to which the fiber is most sensitive (Kiang, Moxon and Levine, 1970; Wiederhold, 1970; Guinan and Gifford, 1988a; but see also Guinan and Gifford, 1988c).

This impression was further reinforced by the evidence for a lack of a significant efferent effect on the inner-hair-cell d.c. potentials in response to tail-frequency tones (Brown and Nuttall, 1984). Most recently, this impression was supported by the report that efferent stimulation "had no apparent effect on the basilar-membrane displacement in response to tones at frequencies more than one-half octave below CF" (Murugasu and Russell, 1996).

However, a systematic study of efferent effects on responses to tail-frequency tones is lacking in the literature. Virtually all of the studies that reported on (the lack of) efferent effects at tail frequencies – whether it be at the level of ANFs, inner hair cells or basilar membrane – were focused on other aspects of efferent inhibition. The only exception is an exploration of efferent effects on ANF tuning curves (Guinan and Gifford, 1988c). That study concluded that efferents can sometimes significantly elevate tuning-curve tails, in addition to elevating their tips; the tail-frequency inhibition was small, averaging only 1 dB at 1 kHz. However, there are several important limitations to using tuning curves alone to draw conclusions about efferent effects at tail frequencies. First, tuning curves provide a measure of the efferent effect at threshold only, i.e., at the sound levels required to produce a just measurable change in the fiber's discharge rate. Second, the prolonged efferent stimulation – usually over several minutes – required to record a whole tuning curve with efferent stimulation, complicates data interpretations because of: (1) adaptation in ANFs and in the effects of efferent stimulation, (2) possible influences from the efferent slow effect (Sridhar et al., 1995), and (3) possible changes in properties of the stimulating electrode (Mountain, 1978).

The current study is the first extensive examination of efferent effects at tail frequencies. To overcome interpretational difficulties involved with the use of neural tuning curves, we recorded level series at specific tail frequencies. By simultaneously randomizing the presentation of sound level and efferent stimulation – while keeping the sound-on and shocks-on duty cycles low – adaptation was minimized both in the responses of ANFs to sound, and in the effects of efferent stimulation (Guinan and Stanković, 1996).

A careful study of efferent effects on ANFs at tail frequencies is an important part of any attempt to account for the efferent effects by theoretical models. Exploration of efferent effects at tail frequencies is also important for better understanding of the neural coding

of sound at the frequencies of conversational speech and at moderate-to-high sound levels. While this is important for all hearing people, it may be particularly relevant for the hearing impaired who are left with hearing at high sound levels only.

II. Methods

A. Surgical preparation

Healthy adult cats weighing between 1.5 and 3.0 kg, with no signs of middle-ear infections, were used in this study. Anesthesia was induced by intraperitoneal injection of 0.15 ml/kg diallyl barbiturate in urethane (100 mg/gl diallyl barbiturate, 400 mg/ml monethyurea, and 400 mg/ml urethane), and maintained by injections of 1/10 of the original dose, as needed.

Surgical procedures for a dorsal approach to the auditory nerve (Kiang et al., 1965) were used. Briefly, after insertion of a tracheal tube and cannulation of a femoral vein for the intravascular drip of a lactated Ringer's solution, ear canals were surgically exposed and the auditory bullae were opened. The bony septum between the bulla and middle ear was removed and the tendons of the middle ear muscles were cut using cautery or a surgical argon laser with a "Megabeam Endo-ENT Probe." The laser was used in the last four experiments from this series in an attempt to minimize acoustic trauma which sometimes resulted when middle ear muscles were cut using conventional cautery. Laser cutting gave excellent results without any detectable compromise in hearing. A posterior craniotomy was performed and the medial and lateral parts of the cerebellum were aspirated to expose the floor of the fourth ventricle and the exit of the auditory nerve.

The physiological state of the animals was continuously monitored throughout experiments using a custom-made LabView system that allowed real-time monitoring of electrocardiograms, electroencephalograms, breathing rate, CO_2 content in expired air, and rectal temperature. The monitoring system proved to be a more sensitive indicator of the deepness of anesthesia than the traditionally-used pinch-withdrawal reflex, and thus allowed us to maintain animals in a deeply anesthetized state.

To increase the efficacy of efferent stimulation without evoking motion, some animals

were paralyzed with an 8% solution of atracurium in saline dripped at 1 drop/5 s, and artificially respirated. Respirator parameters were adjusted so to maintain the breathing rate at 15-18 breaths per minute, and expired CO_2 at 3.5-5%.

Hearing was monitored by recording auditory-nerve compound action potentials (CAP) with an electrode on or near the round window. An automated procedure for obtaining a tone-pip audiogram was used (Guinan and Stanković, 1996). Sometimes, CAP audiograms were elevated when measured within 2 hours of middle-ear-muscle cutting, presumably due to trauma associated with the muscle cutting. However, in all animals reported here, CAP audiograms returned to the normal range by the time data acquisition started – usually ten or more hours after middle-ear-muscle cutting.

B. Stimulation and recording

Efferents were stimulated along the midline of the floor of the fourth ventricle using a multiprong electrode (Gifford and Guinan, 1987). The time course of efferent stimulation was as in Guinan and Stanković (1996). Briefly, shocks (0.3 ms pulses at 200/s) were coupled by a transformer (to avoid delivery of net charge) and then delivered through the pair of adjacent prongs which yielded the greatest inhibition of the click-evoked CAP response without evoking movement. The reduction in the CAP so obtained was equivalent to decreasing the sound level and it ranged from 10-20 dB over the course of gathering data reported here.

Recordings of single auditory-nerve fibers (ANFs) were made as in Kiang et al. (1965), using broad-band noise bursts as a search stimulus. Based on their spontaneous rate (SR), ANFs were grouped into three categories: low if SR$\leq$ 0.5, medium if 0.5<SR<18, and high if SR$\geq$18 spikes/s (Liberman, 1978). Fibers of all SRs were studied, with a bias toward high-SR fibers because they have the lowest tail thresholds. For high-SR fibers, (1) tuning curve tails could be recorded without exposing the ear to potentially traumatizing sound levels for an extended time period, and (2) a large portion of the fiber's dynamic range (defined as the range of levels over which firing rate increases) could be studied without causing acoustic trauma.

We were further biased towards studying fibers with characteristic frequencies CFs $\geq$

10kHz because (1) they had clearly defined tips and tails, and (2) the broadest range of the tail could be studied without eliciting a response in the tip region of a tuning curve, due to harmonic distortion in the tail-frequency stimulus[1]. Since harmonic distortion in the stimulus is an important issue when stimulating high-CF fibers with low frequencies, we were careful to estimate harmonic distortion in every experiment. In the last four experiments, harmonic distortion was measured during spike-data acquisition *in vivo* using the Fourier transform of the sound pressure recorded at the eardrum (in a closed acoustic assembly). Examples of the first five harmonics accompanying a 1 kHz stimulus are shown in Fig. 3-1; sixth and higher harmonics were below the noise floor. For earlier experiments, harmonic distortion was not measured *in vivo*, but instead was estimated from sound-pressure measurements in a closed cavity.

C. Data gathering

After making contact with a fiber (using a criterion that action potentials be at least 0.5 mV in magnitude), data were gathered in the following sequence:

1. A tuning curve was obtained. To increase the speed of data gathering, the point spacing in the tail (where response threshold is not a strong function of frequency) was courser (6 points per octave) than in the tip (30 points per octave)

2. Spontaneous firing was recorded for 20 s, and SR was calculated.

3. Level functions were run at a tail frequency. Contact time with a fiber permitting, multiple level functions were obtained at the same and/or a different tail frequency and/or at CF.

Rate-level curves (i.e., level functions) were obtained using a paradigm that allowed randomization of both sound level, and the presence/absence of efferent stimulation (as in Guinan and Stanković, 1996). Therefore, each randomized set of measurements yielded two rate-level curves – one "with efferents activated" and one "without efferents activated".

[1]Some fibers with CFs < 10kHz were also recorded, and they gave the same qualitative picture as fibers with CFs ≥ 10kHz. However, there are few data from fibers with CFs < 10kHz, so they were not analyzed in detail.

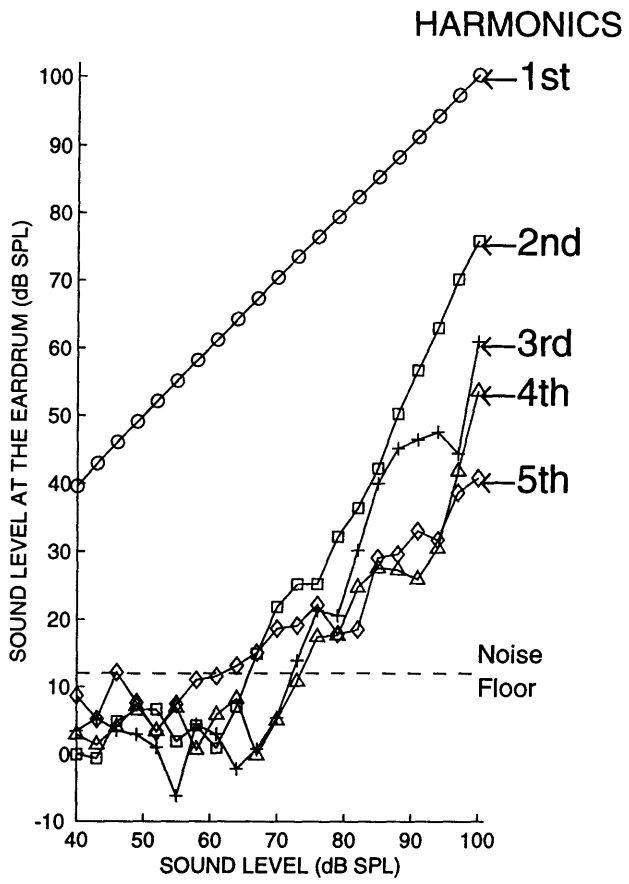

Figure 3-1: Harmonic distortion from a 1 kHz tone, as measured by taking a Fourier transform of the pressure waveform at the tympanic membrane. The abscissa is the sound pressure level determined from the attenuator setting, and the ordinate is the sound pressure level measured at the eardrum in a closed acoustic assembly. Cat TS43. The horizontal line at 15 dB indicates the noise floor.

Rate at each sound level in a randomized rate-level curve was obtained by presenting ten sequential tone bursts (50 ms on, 50 ms off, 2.5 ms rise/fall time), and averaging the responses (Fig. 3-2). For each tone burst, the time window for counting spikes included only the steady-state part of the response (where the response was delayed re. tone bursts), so that the window began 6 ms after the beginning of the rise of the tone burst and ended 1 ms after the end of the fall of the tone burst. Exclusion of the transient response, which can differ in phase from the steady-state response (Lin and Guinan, personal communication; see also Ruggero et al., 1996) did not substantially reduce the total number of spikes. For trials "with efferents activated", a train of efferent shocks started 100 ms before the onset of tone bursts and lasted throughout the duration of the tone bursts. Sets of tone bursts were presented and measurements made every three seconds. At tail frequencies, most randomized level functions covered the range from 40-100 dB SPL with 3 dB resolution. Exceptions include the first three experiments where some rate-level curves covered the range from 50-100 dB SPL with 2.5 dB resolution, 60-100 dB SPL with 2 dB resolution, or 70-100 dB SPL with 1.5 dB resolution. In the last three experiments, rate-level curves covered the range from 40-91 dB SPL with 3 dB resolution in order to minimize exposure to potentially traumatic sounds. At CF, randomized rate-level curves covered the range from 0-100 dB SPL with 5 dB resolution.

The most frequently used stimulus frequency was 1 kHz because (1) tuning-curve tails are often most sensitive around 1 kHz and (2) harmonic distortion accompanying a 1 kHz stimulus is often irrelevant for fibers with CF$\geq$ 10 kHz. A disadvantage of doing most runs at a single frequency, however, is that over many hours of recording, it can lead to hearing loss (evidenced by elevation of CAP thresholds) in the vicinity of that frequency. Data presented here are from fibers whose CFs spanned frequencies with stable hearing, i.e. frequencies at which CAP thresholds remained within 5-15 dB (most commonly within 10 dB) of the initial measurements. To rule out the possibility that hearing loss at low frequencies significantly affected our recordings from high-CF fibers, rate-level curves in the last 3 experiments were run only up to 91 dB. Efferent effects on rate-level curves in these last 3 cats, in which low-frequency hearing was preserved, were in agreement with the results from earlier experiments. Therefore, we pooled data across all cats (except two, see below),

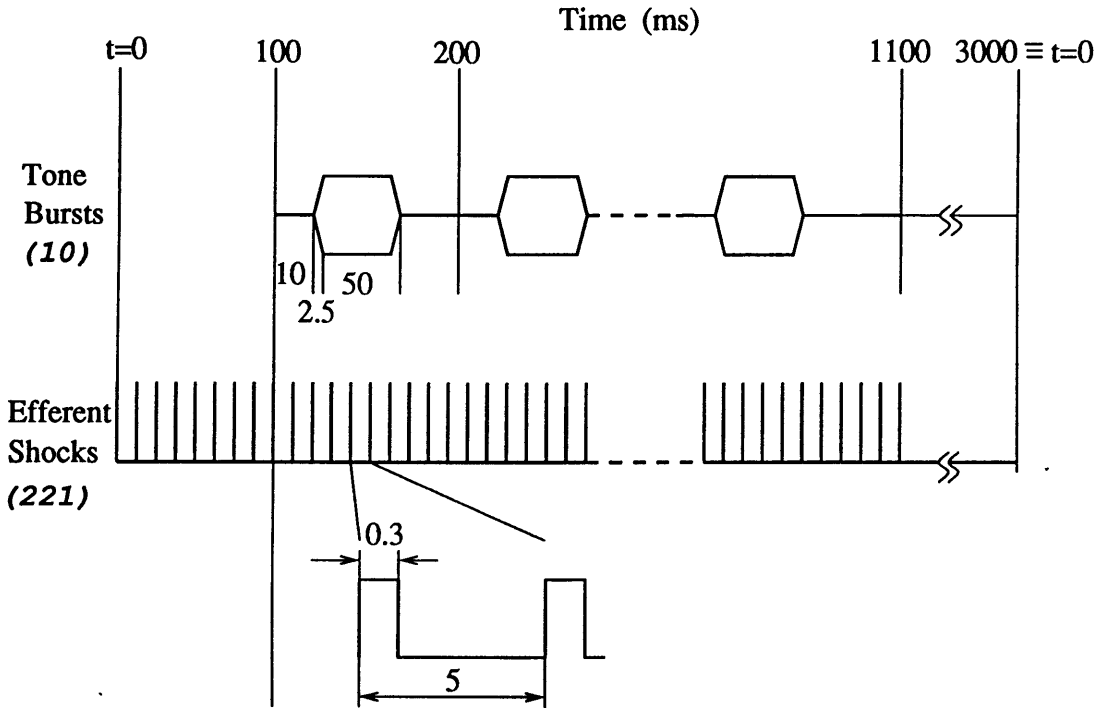

Figure 3-2: The stimulus paradigm used in recording rate-level curves of auditory nerve fibers. The plain-font numbers are times in ms. The numbers in italics are the numbers of tones bursts and shocks.

so that this report is based on ANFs from 17 cats. Data from two cats were not included: one because of loud audible noise associated with the respirator, the other because the cat had extremely sensitive hearing. In the latter cat, efferent stimulation caused an unusually large ($\approx$ 80%) suppression of SR, suggesting that "spontaneous" activity was in fact a response to animal-generated noise (as suggested earlier by Wiederhold and Kiang, 1970; Guinan and Gifford, 1988b; Kawase et al., 1993). Furthermore, rate-level curves in response to a single tail-frequency tone demonstrated dips characteristic of two-tone suppression (Abbas and Sachs, 1976), providing additional evidence that the cat was responding to sounds not present in the stimulus.

D. Data selection

We were careful to ensure that the data entered in the final pool were free of potential artifacts. Criteria for the inclusion/exclusion of data are summarized below.

- Tuning curves were compared with measurements (or estimates) of harmonic distortion at various levels and frequencies. Data were rejected if, for a given stimulus frequency and sound level, any of the first 5 harmonics exceeded a tuning-curve threshold.

- Fibers were included only if their CFs were from frequency regions of stable hearing (defined by CAP threshold remaining within 15 dB of the initial measurement, where CAP thresholds were measured approximately every 4 hours). Furthermore, only fibers with the difference between the tip and tail thresholds of at least 35 dB were included.

- For each data set, peri-stimulus-time histograms locked to the shock times were inspected to detect possible missed or extra triggers due to electronic artifacts at the recording electrode produced by the efferent shocks (as in Guinan and Stanković,1996). Only data free of such artifacts were included. We further selected for data that did not show evidence of missed short-interval spikes in inter-spike-interval histograms, based on visually detectable paucity of spikes at 1-2 ms intervals when compared to longer intervals.

E. Data analysis

All data analysis was done with Matlab5 software. For easier data handling in Matlab, sound-level spacing in all tail runs was "standardized" to the most commonly used sound-level spacing of 3 dB. This amounted to downsampling rate-level curves that had level spacings of 2.5 dB, 2 dB and 1.5 dB (and covered the ranges of 50-100 dB, 60-100 dB and 70-100 dB, respectively). For rate-level curves with the level spacings of 2.5 dB and 2 dB, linear interpolation was used between adjacent points to compute 3 dB steps counting down from 100 dB.

As an aid in evaluating the quality of the data in the figures, standard errors were displayed on top of data points. The standard error ($S.E.$) of the average rate-level curve – obtained from multiple sets of rate-level curves – was calculated as $S.E. = \sigma/\sqrt{n} = \sqrt{\frac{\sum_{i=1}^{n}(x_i-\bar{x})^2}{n-1}}/\sqrt{n}$ where σ is the standard deviation, n is the number of rate-level curves, x_i is an individual measurement in a rate-level curve, and $\bar{x}$ is the average. When only a single set of rate-level curves was available, a somewhat arbitrary formula for σ was used – a σ of 10 spikes/s was assigned if the driven firing rate (i.e., firing rate–SR) was less than or equal to 20 spikes/s; otherwise, a σ of 20 spikes/s was assigned. This simple formula that tends to overestimate σ was arrived at by selecting fibers for which σ could be calculated from multiple measurements, and then plotting σ as a function of the driven firing rate.

Some data were summarized in the form of scatter plots. To aid detecting trends in scatter plots, a loess fit (also known as local nonparametric regression) was used (Cleveland, 1993). Loess fit is characterized by two parameters – (1) a smoothing parameter that is related to the size of the smoothing window, and (2) the degree of the locally fitted polynomial (always set to 1 in the current study). In the figures where the loess fit is shown, the smoothing parameter was most commonly set to 0.2, which means that the smoothing window included 20% of the data.

F. Measuring time courses of efferent effects

The slow d.c. potentials produced by efferent stimulation were measured either with a chlorided silver wire on the round window, or by monitoring changes in endocochlear

potential with a KCl-filled electrode inserted into scala media through the round window. In both cases, the reference electrodes were chlorided silver wires placed on a neck muscle.

Efferent-induced changes in stimulus-frequency emissions (ΔSFEs) were determined from measurements of the ear canal sound pressures, using a B&K condenser microphone (4179 or 4132). The signal from the B&K amplifier was sent to a EG&G 5210 lock-in amplifier, and the in-phase and quadrature outputs of the lock-in were averaged as time-varying signals over 8 to 64 trains of efferent shocks. The amplitude and phase of the efferent-induced change in the SFE were computed by vector subtraction of the baseline sound pressure level (the level before the efferent shock train) from the time-varying sound pressure level (Guinan, 1986).

The cochlear microphonic (CM) was also measured by averaging in-phase and quadrature outputs of the EG&G 5210 lock-in amplifier. For measurements of both ΔSFE and the efferent-induced change in CM, the lock-in time constant was 30 ms. Measurements of efferent-induced changes in endocochlear potential and voltage at the round window were also filtered with a 30 ms time constant to make them comparable to the measurements of the CM and SFEs. Data on how efferents affect the spontaneous rates of single fibers was gathered in 1-min segments with 5-30 seconds between runs.

Although the slow efferent effect (Sridhar et al., 1995) was not directly measured in these experiments, it is unlikely to play an important role in our measurements, because the measurements were made over many minutes and the slow effect is transient and disappears after a few minutes of stimulation (Sridhar et al., 1997). The slow efferent effect is especially unlikely to have altered the patterns obtained using randomized rate-level curves for two reasons. First, by randomizing the presentation of sound level and efferent stimulation, possible contributions from the slow effect were balanced across sound levels. Second, by interleaving response measurements with baseline measurements (baseline measurements occurred < 50 ms before response measurements), possible contributions from the slow effect were balanced across the response and baseline measurements.

III. Results

Data presented here indicate that, contrary to a commonly held view, efferents can indeed inhibit ANF responses to tail-frequency tones. Because these data contradict the common wisdom, we were careful to rule out the possibility that the measured responses were artifacts arising from an imperfect stimulation and recording set-up. As described in the methods section in greater detail, we selected data with excellent triggering, free of shock artifacts, and free of contamination from harmonic distortion.

A. Individual examples

Examples of the typical range of efferent effects at tail frequencies are given in Figs. 3-3, 3-4, 3-5 and 3-6. In almost all cases (i.e., 162 out of 165 fibers), efferent stimulation reduced the response or had no appreciable effect, but in a few fibers (3 only), efferent stimulation clearly[2] enhanced the afferent response. Since these few fibers had sensitive tips and high-SR activity, this efferent enhancement was most likely due to efferent-induced removal of adaptation (Kawase et al., 1993) .

The fiber in Fig. 3-3 was substantially inhibited by efferent stimulation, especially at sound levels close to the tail threshold. This inhibition is demonstrated by the shift of the with-shocks rate-level curve to the right, meaning that a higher sound level was required with efferent stimulation to produce the same response as in the absence of efferent stimulation. Note that for this fiber, efferent stimulation not only shifted the original rate-level curve to the right, but also changed the slope of the rate-level curve. The change in slope made the efferent effect depend on sound level within the rising portion of rate-level curve. The 1 kHz response of the fiber in Fig. 3-4 was significantly inhibited by efferent stimulation. In this example, the largest efferent-induced inhibition occurred at sound levels away from response threshold. Fig. 3-5 demonstrates that efferents can also have a negligible effect at 1 kHz, even in the presence of a significant shift at CF. Fig. 3-6 is another example of a fiber with a minimal efferent effect at 1 kHz. In this example, two pairs of rate-level curves

[2]The enhancement was larger than what is expected from inherent noisiness of the data when efferents had no appreciable effect.

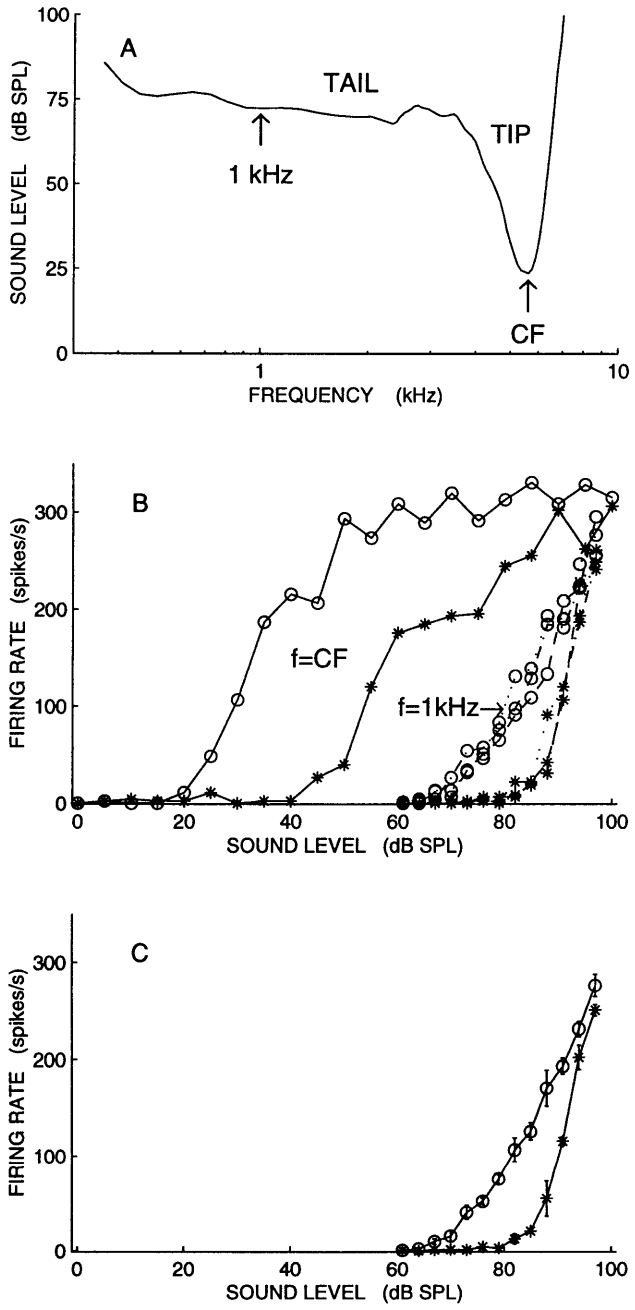

Figure 3-3: An example from a fiber with a large efferent-induced rate suppression in response to a tail-frequency stimulus of 1 kHz. (A) Tuning curve. Arrows indicate stimulus frequencies. Also, tip and tail regions of the TC are labeled. (B) Pairs of rate-level curves in response to tone bursts at CF (left), and in response to tone bursts at 1 kHz (right). Circles indicate no efferent stimulation and stars indicate efferent stimulation. To illustrate the reproducibility of the effect at 1 kHz, 3 sets of rate-level curves are shown. (C) Average rate-level curves from the 3 sets at 1 kHz shown in (B). Error bars indicate standard error of the mean. Fiber TS27-76,CF=5.62 kHz, SR=1.60 spikes/s.

illustrate the reproducibility of the minimal effect.

B. Level shift

As a measure of the efferent effect on rate-level curves, we used the level shift, ΔL. The level shift is defined as the amount (in dB SPL) by which the sound level must be increased with efferent stimulation to produce the same response as obtained without efferent stimulation. The procedure for calculating ΔL and its standard error is given in the caption of Fig. 3-7. Note that the standard error on ΔL is used as an aid in understanding the error in the measurement of ΔL, and it is also used in the statistical tests described later. An example of ΔL calculated from a pair of rate-level curves is given in Fig. 3-8(B).

Since we wanted to average ΔL-versus-sound-level curves from many fibers to look for trends, we needed to account for the fact that the overall strength of the efferent effect (estimated from CAP inhibition) varied over the course during which these fibers were recorded. Therefore, ΔL from every fiber was normalized to the CAP shift of 20 dB, which was the maximal CAP shift in this study. For example, when the CAP shift was 14 dB, ΔL was multiplied by 20/14 at every level. An example of such a normalized ΔL is shown in Fig. 3-8(C). Normalization to the CAP shift of 20 dB also makes this work directly comparable to an earlier studies by Guinan and Gifford (1988c) in which the same normalization was applied.

On average, ΔL (both raw and normalized) was found to be different from zero at a very highly significant level ($p<0.0001$), as determined from t-tests applied to data grouped according to stimulus frequency. Specifically, t-test was applied to all ΔLs (regardless of sound level) from fibers with CFs between 10-30 kH stimulated with: 500 Hz (9 fibers, average normalized ΔL=1.5 dB), 1 kHz (116 fibers, average normalized ΔL=3.6 dB), 2 kHz (28 fibers, average normalized ΔL=6.9 dB) and 3 kHz (10 fibers, average normalized ΔL=7.1 dB).

Based on the data from individual fibers it appeared that ΔL depended on both stimulus frequency and intensity, as well as characteristics of individual ANFs (i.e., CF and spontaneous rate). These dependences were explored for data pooled from many fibers and the results are summarized in the two sections that follow.

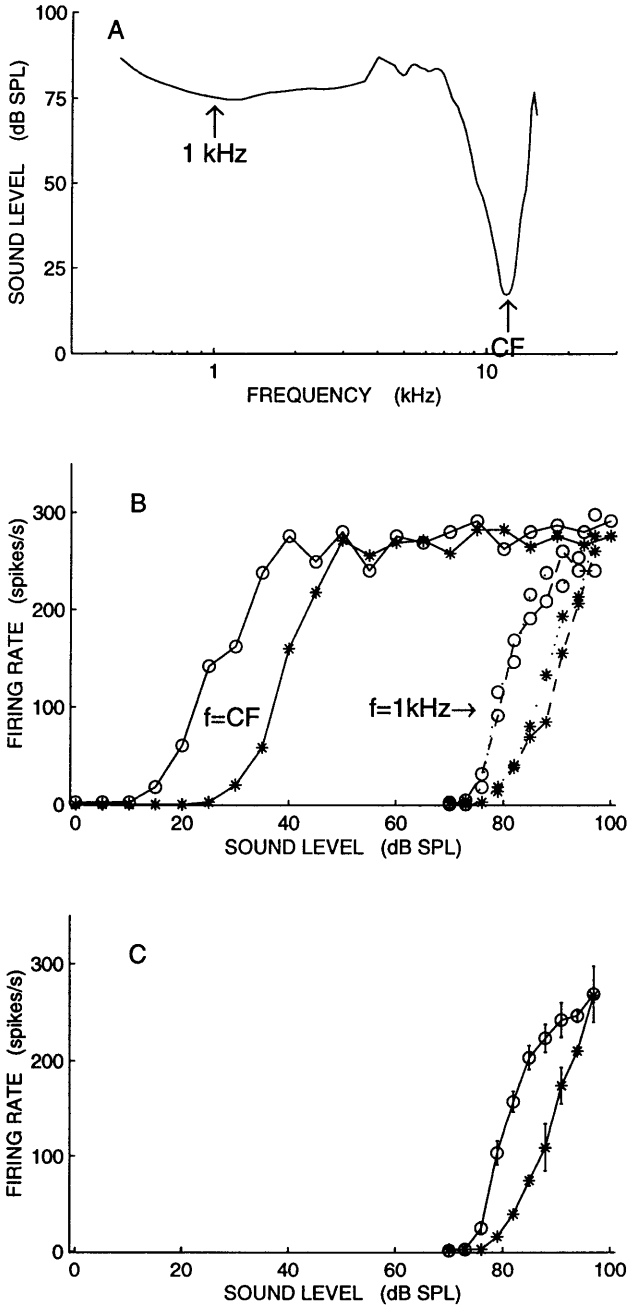

Figure 3-4: An example from a fiber with a medium efferent-induced rate suppression in response to a tail-frequency stimulus of 1 kHz. Figure layout as in Fig. 3-3. Note that the pair of rate-level curves in (C) is the average from two sets of rate-level curves in (B). Fiber TS28-86,CF=11.95 kHz, SR=0.9 spikes/s.

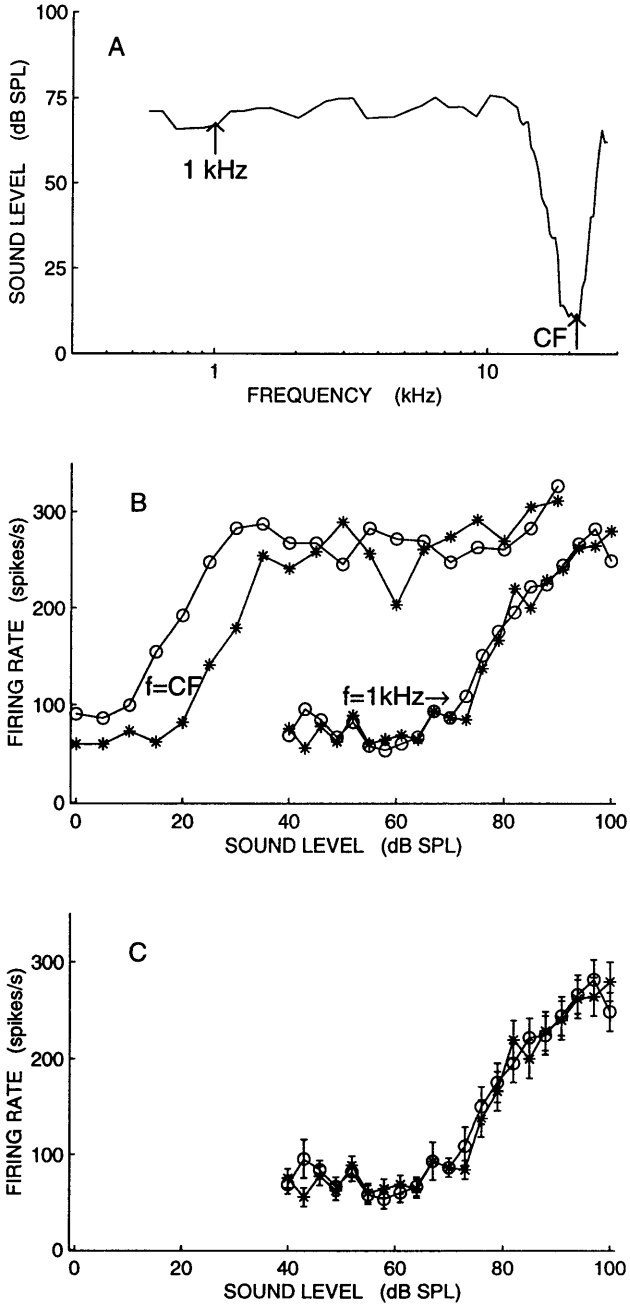

Figure 3-5: An example from a fiber whose firing rate in response to 1 kHz tone bursts was not affected by efferent stimulation. Figure layout as in Fig. 3-3, except that only one pair of rate-level curves in response to 1 kHz tone burst is shown in (B). Consequently, error bars shown in (C) were assigned, as described in the Methods section. Fiber TS46-20, CF=21.26 kHz, SR=71.2 spikes/s.

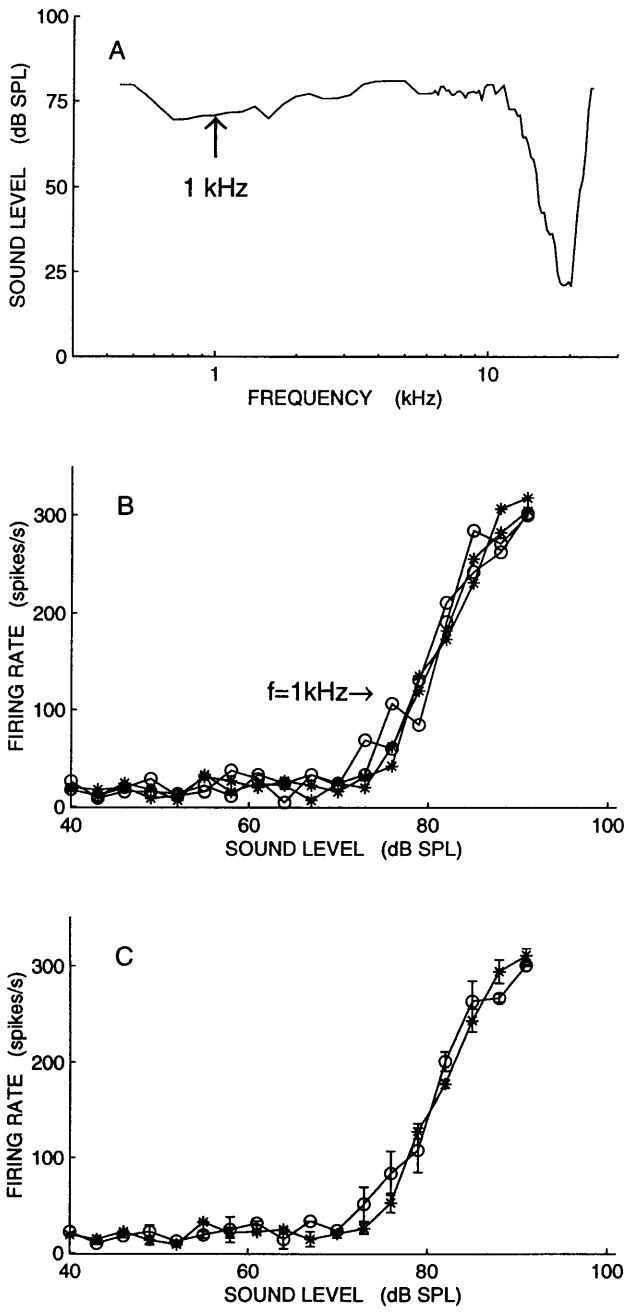

Figure 3-6: Another example from a fiber whose firing rate in response to 1 kHz tone bursts was not affected by efferent stimulation. Figure layout as in Fig. 3-3, except responses at CF were not measured. The curve in (C) is the average of the two sets of rate-level curves from (B). Fiber TS39-15, CF=18.84 kHz, SR=20.1 spikes/s.

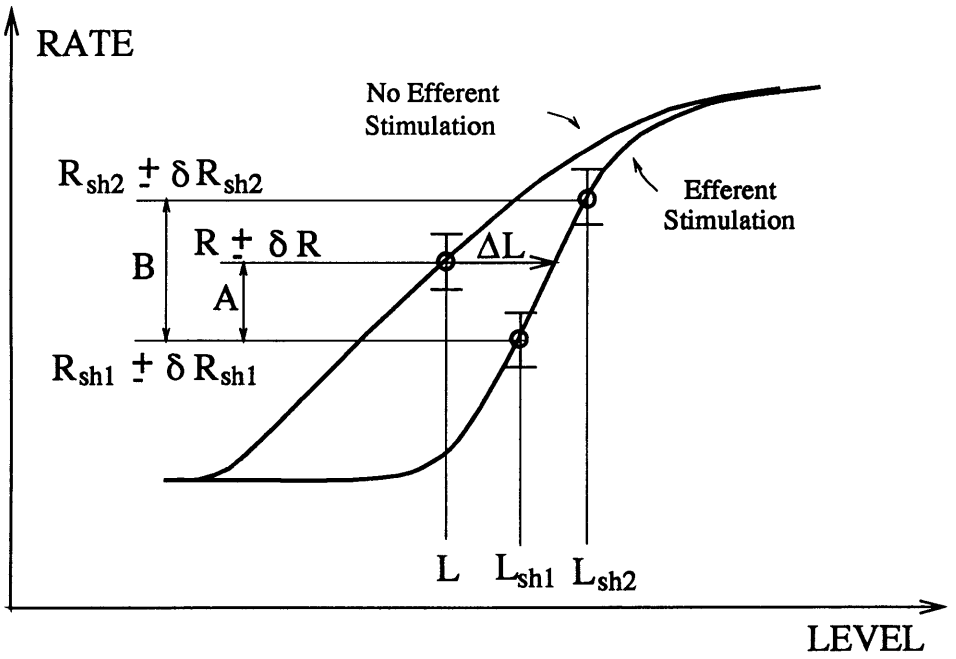

Figure 3-7: The computation of the efferent-induced level shift, ΔL. Only three points are labeled on a stylized pair of rate-level curves – one point with coordinates (R,L) on the rate-level curve without efferent stimulation, and two points with coordinates (R_{sh1}, L_{sh1}) and (R_{sh2}, L_{sh2}) on the rate-level curve with efferent stimulation. From the figure, $\Delta L = (L_{sh1} - L) + (\frac{A}{B})(L_{sh2} - L_{sh1})$, where $A = R - R_{sh1}$ and $B = R_{sh2} - R_{sh1}$. Standard error for ΔL ($\delta\Delta L$) can be calculated from standard errors of R, R_{sh1} and R_{sh2} (i.e., δR, δR_{sh1}, and δR_{sh2}). In particular, the main source of error in ΔL stems from the errors in determination of the firing rate, since errors associated with determination of the sound level are negligible in comparison. Because ΔL dependence on firing rate is expressed as a ratio of two independent variables A and B, the error in ΔL, $\delta\Delta L$, can be calculated from errors in A and B (Meyer, 1975). Specifically, $\delta\Delta L = (L_{sh2} - L_{sh1})(\delta\frac{A}{B}))$ where $\delta\frac{A}{B} = \sqrt{\frac{1}{B^2}((\delta A)^2 + (\frac{A}{B})^2(\delta B)^2)}$, $\delta A = \sqrt{(\delta R)^2 + (\delta R_{sh1})^2}$, and $\delta B = \sqrt{(\delta R_{sh2})^2 + (\delta R_{sh1})^2}$. This definition of ΔL is adequate only in the linear rising portion of rate-level curves. The beginning level for calculation of ΔL was determined by inspection. Given discrete sampling of rate-level curves, it was usually easy to define the rising phase as the first level point at which firing rate was clearly above spontaneous rate. Since in this study virtually no rate-level curve in the tail reached saturation, ΔL could be calculated up to the highest recorded level (or the highest level up to which harmonic distortion in the stimulus was not a problem). If at these highest levels the firing rate without efferent stimulation was higher that the highest rate with efferent stimulation (as in Fig. 3-3(C) at 97 dB SPL), ΔL was calculated by fitting a line through the last 3 points in the with-efferents rate-level curve and extrapolating to sound levels above 100 dB SPL. Error bars on extrapolated ΔL were estimated from the goodness of fit through the last 3 data points using a Matlab5 function "polyval."

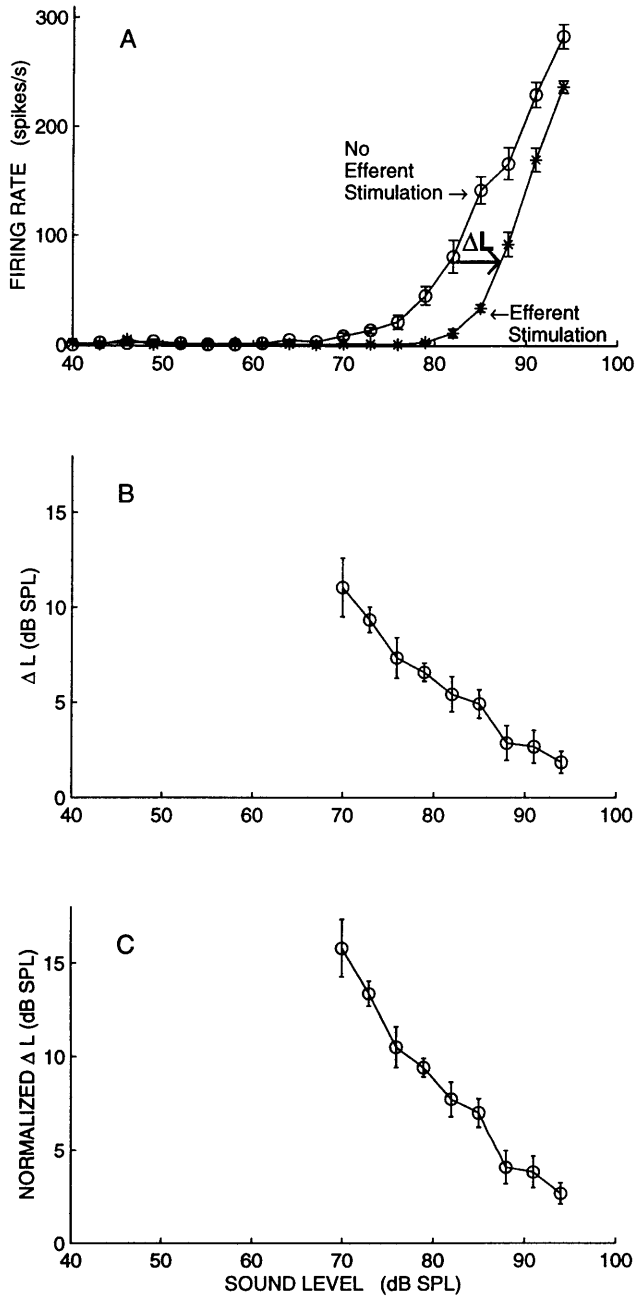

Figure 3-8: An example of ΔL calculated from a pair of rate-level curves. (A) Average rate-level curves from five individual pairs. (B) ΔL calculated from the rate-level curves in "A" using the procedure described in Fig. 3-7. (C) ΔL normalized to the CAP inhibition of 20 dB by multiplying ΔL from (B) with 20/14. Note that standard errors were also normalized using the same multiplicative factor (i.e., 20/14). Such normalization of standard error is likely an overestimate of the actual error.Fiber TS37-17, CF=10.59 kHz, SR=1.2 spikes/s.

C. Dependence of ΔL on sound level and spontaneous rate

To explore the dependence of ΔL on sound level and spontaneous rate – while controlling for the dependences on stimulus frequency and CF – we considered one stimulus frequency at a time with fibers grouped in CF bands. The majority of our data are from fibers with CFs greater than 10 kHz, responding to stimulus frequencies of 1 kHz (116 fibers), 2 kHz (28 fibers), 3 kHz (15 fibers) and 500 Hz (9 fibers). The grouping of fibers into CF bands was determined by the amount of data available for a given stimulus frequency. Narrow CF bands (of one half octave each) were used for the fibers responding to 1 kHz (Fig. 3-9), whereas a relatively broad (one octave) CF band was used when data were scarce (i.e., fibers responding to 2 kHz (Fig.3-10), 3 kHz (Fig.3-11) and 500 Hz (not shown)).

When considering responses from many fibers, there are two general ways of displaying the sound-level dependence of ΔL. One way is to superimpose ΔL-versus-sound-level curves from many fibers, and thereby generate a scatter plot (Fig. 3-10(A)). The other way is to group fibers according to SR and then plot the average ΔL-versus-sound-level curve for each SR group (e.g., Fig. 3-10(B)). An advantage of a scatter plot is that it can illustrate the inter-fiber variability of ΔL. However, a scatter plot has a disadvantage that it can easily start looking overcrowded if responses from too many fibers are superimposed, so that identification of individual fibers becomes extremely difficult. We have therefore shown scatter plots of ΔL only for stimulus frequencies used with a relatively small number of fibers (Fig. 3-10(A) and Fig. 3-11(A)). A way of summarizing scatter plots is to use the average ΔL-versus-sound-level curve (as in Fig. 3-10(B), Fig. 3-9 and Fig. 3-11(B)). An advantage of the average ΔL curves is that they allow a quick visual appraisal of the differences among the SR groups for a given stimulus frequency, as well as a quick visual comparison of the trends in the average ΔL across sound levels and for different stimulus frequencies. A disadvantage of the average ΔL curves is that they may mask patterns present in individual fibers and may produce artificial "trends" due to sampling different fibers at different sound levels.

Based on the visual inspection of Figs. 3-9, 3-10 and 3-11, it appears that responses from fibers of different SR groups are not grossly different, and that ΔL tends to depend on sound level. To test these visual impressions, we performed several statistical analyses. The

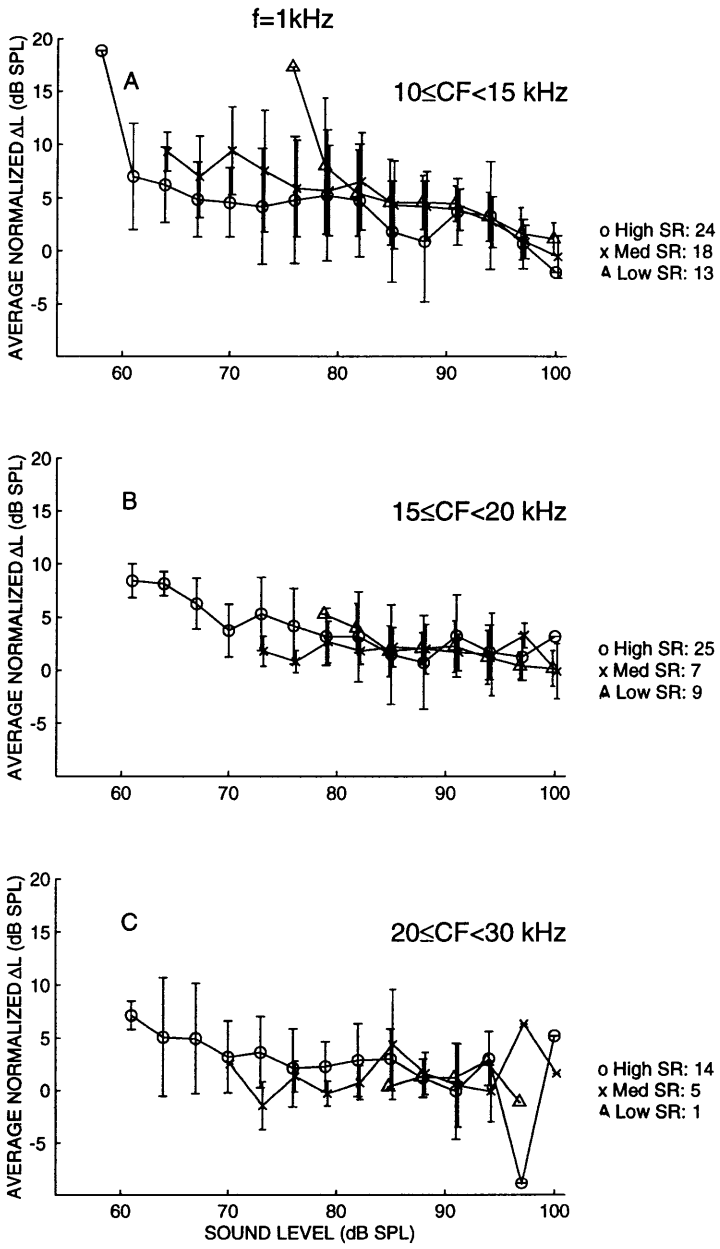

Figure 3-9: ΔL versus sound level for ANFs from 3 CFs regions (10–15 kHz, 15–20 kHz and 20–30 kHz) stimulated with a tail-frequency tone of 1 kHz. Each curve represents the average at one sound level for a given SR group, with the total number of fibers in each SR group shown on the right. Differences in the lowest initial sound level among the SR groups reflect differences in tail thresholds. Bars on individual points indicate standard deviation, and therefore are a measure of spread. Points without bars are from one fiber only. To allow easier identification of error bars associated with data of different SR groups, sound levels for medium-SR data were shifted to the right by 0.2 dB SPL, and sound levels for low-SR data were shifted to the left by 0.2 dB SPL. The overall small size of ΔL for fibers with CFs between 20−30 kHz reflects, at least partly, decreased efferent innervation for that frequency region (reviewed by Guinan, 1996 and Warr, 1992).

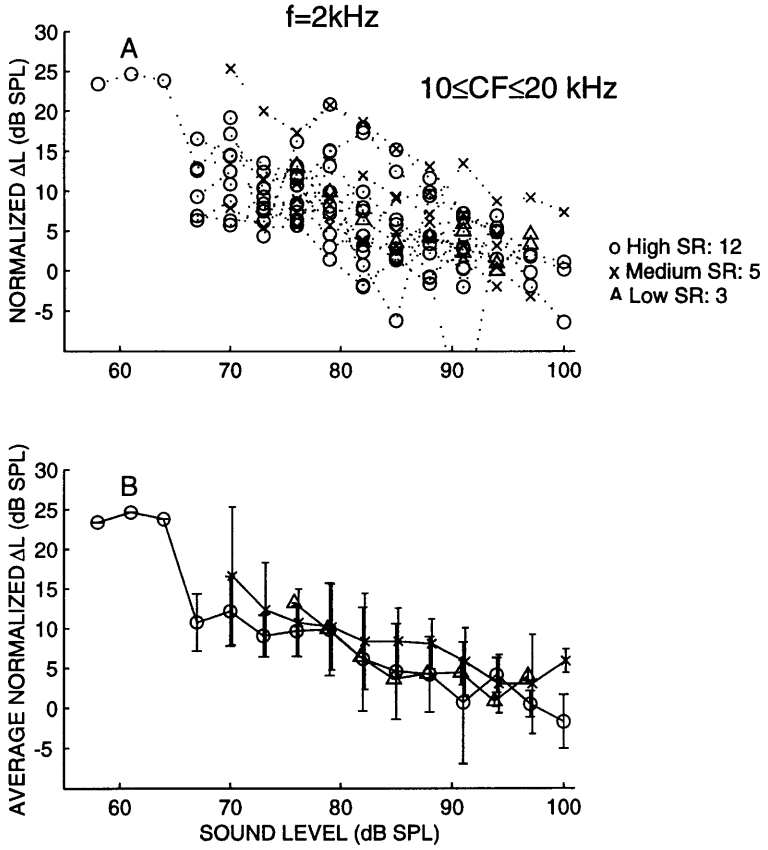

Figure 3-10: ΔL versus sound level for ANFs with CFs from 10–20 kHz, stimulated with a tail-frequency tone of 2 kHz. (A) Superimposed responses from individual fibers. Text on the right of the figure indicates how many fibers of each SR group are shown on the figure. Responses from one fiber are connected by dotted lines. Note that the sound-level range of the normalized ΔL varies from fiber to fiber. Differences in the lowest initial sound level reflect differences in tail thresholds of individual fibers; differences in the highest sound level reflect differences in availability of the data. (B) The average curves for each SR group, based on fibers from (A). Bars on individual points indicate the standard deviation of the mean at a given level, and give a feel for the spread in data. Points without bars are from one fiber only. As in Fig. 3-9, sound levels for medium-SR data were shifted to the right by 0.2 dB SPL, and sound levels for low-SR data were shifted to the left by 0.2 dB SPL.

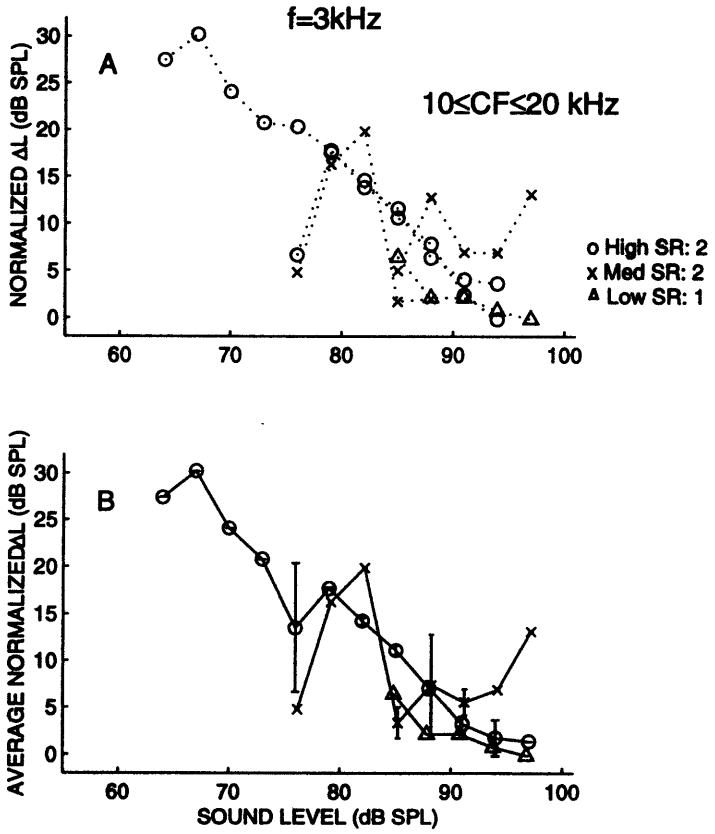

Figure 3-11: ΔL versus sound level for ANFs with CFs from 10–20 kHz, stimulated with a tail-frequency tone of 3 kHz. Even though there are too few fibers to make strong statistical statements about trends in the data, the figure illustrates that efferents can have a substantial (level-dependent) effect for a tail-frequency stimulus of 3 kHz. Layout as in Fig.3-10.

tests were aimed at addressing the question of whether there are significant changes in ΔL across SR groups and across sound levels. The answers to these questions are important in evaluating hypotheses about the mechanisms that underlie the efferent effects described here.

To look for statistical significance across SR groups, we used permutation tests with p values estimated by Monte Carlo shuffling ("resampling", Efron and Tibshirani(1993)); Note 3 gives a summary of the method[3]. Statistically significant differences across SR groups were not detected at the p=0.05 level (Table 3.1 and Note 4 provide details[4]). Because there were no significant differences among SR groups, data were pooled across SR groups for subsequent tests.

To statistically determine whether ΔL varies with sound level, we again used permutation tests (Note 3). As summarized in Table 3.2, ΔL was found to significantly depend on sound level for some, but not all fibers. Specifically, a significant dependence of ΔL on sound level was found for fibers with CFs between 15-20 kHz stimulated with 1 kHz, and for fibers with CFs between 10-20 kHz stimulated with 2 or 3 kHz. Although for fibers with CFs between 10-15 kHz stimulated with 1 kHz tones ΔL did not vary significantly with

[3]A major advantage of using a permutation test (Efron and Tibshirani, 1993) is that it makes no assumptions about the underlying distribution of samples, unlike the assumptions required in applying traditional methods (e.g., assumptions about a Guassian distribution in ANOVA or t-test), since permutation tests are based on the creation of artificial data sets by repeated shuffling from the original data and drawing inferences from these artificial data sets. On a single trial of a permutation test, data from individual fibers are randomly assigned to categories of high-SR, medium-SR or low-SR (without regard to their original SR) with the number of fibers in each category the same as the number in the original data. For each trial, one or more statistics are calculated. For each statistic, a histogram is formed from the results across many trials (we used 1000 trials). The statistical significance of the original data is then judged according to where these data fall in the histogram.

[4]We additionally tested for a significant difference among SR groups using an alternative method of permutation tests – for each trial, the ΔL-vs.-sound-level points from *each fiber* were fitted with a single straight line (the fitting procedure is described in the caption of Table 3.1). From the slopes and intercepts of these lines, the mean slope and intercept was calculated for each SR group. Statistics similar to the ones described in Table 3.1 were then computed. This method also failed to detect a statistically significant change between SR groups. Note that, overall, this method is less favored compared to the method where lines were fitted through data from all fibers of the same SR group (Table 3.1) because line fits are more robust descriptors of the behavior of a group of fibers (when a multitude of data is available), rather than of single fibers (when, sometimes, only two data points are available). Finally, to compare results of permutation tests and t-tests, we used t-tests to the determine whether slopes (or intercepts) of the lines fitted to the ΔL-vs.-sound-level points from individual fibers were significantly different between SR groups (two SR groups were considered at a time). Results of t-tests were in complete agreement with the results of permutation tests (i.e., there was no statistically significant difference across SR groups).

Tests for a Significant Change in ΔL vs. L across SR Groups					
	f=1 kHz			f=2 kHz	f=3 kHz
CF range (kHz)	10.0–14.9	15.0–19.9	20.0–30.0	10.0–20.0	10.0–20.0
Levels (dB SPL)	76–100	79–100	85–97	76–97	85–97
# Fibers (H+M+L)	23+18+13	24+7+9	9+4+1	12+5+3	2+2+1
Difference in SLOPE of ΔL vs. L between SR groups:					
H – M	p=0.55	p=0.42	p=0.41	p=0.70	p=0.12
H – L	p=0.86	p=0.76	p=0.23	p=0.27	p=0.71
M – L	p=0.69	p=0.59	p=0.72	p=0.54	p=0.33
Difference in INTERCEPT of ΔL vs. L between SR groups:					
H – M	p=0.45	p=0.40	p=0.39	p=0.67	p=0.12
H – L	p=0.81	p=0.81	p=0.24	p=0.29	p=0.71
M – L	p=0.67	p=0.55	p=0.73	p=0.57	p=0.39

Table 3.1: Statistical results aimed at determining the probability that the apparent differences among SR groups (H=high-SR, M=medium-SR, L=low-SR fibers) arose by chance. Permutation tests were used with p values estimated by Monte Carlo shuffling. **Choice of sound-level range:** Note that ΔLs from individual fibers span variable sound-level ranges because factors that determine the exact lower and upper sound-level limits (i.e., threshold and availability of the data, respectively) vary among fibers and depend on SR; high-SR fibers tend to have the largest, and low-SR fibers the smallest number of points per fiber. As a consequence, the sound-level range over which, for a given stimulus frequency, ΔLs from most fibers overlap is typically very narrow (<10 dB), such that statistical comparisons of SR groups across such a range may give biased results. We, therefore, chose to compare SR groups across the sound-level range over which the *average* ΔL-vs.-L curves (one curve per SR group) overlapped (e.g., see Fig. 3-9). This means, that if, e.g., the average ΔL for a given SR group included 9 points (76-100 dB, with 3 dB spacing between points), individual fibers that contributed to the average could have anywhere from 2 to 9 points; most fibers considered in the tabulated tests had approximately 7 points per fiber. **Method:** The results summarized in the table are based on a method where, for each trial, the data from *all fibers assigned to the same SR group* were fitted with a single straight line, using least-squares fitting, with points weighted by the errors of individual measurements (Press et al., 1992) . The lines produced a slope (ΔL/L) and intercept (ΔL at L=0) for each SR group. The slopes and intercepts were used to generate 6 different statistics, e.g., [(slope through high-SR fibers) – (slope through medium-SR fibers)], [(intercept through high SR fibers) – (intercept through medium-SR fibers)] and similarly for the other pairs of SR groups. The tabulated results show that statistically significant differences were not detected among SR group at the p=0.05 level. Similar results (i.e., no statistical significance among SR groups) were obtained when data from *all* sound levels were considered, not only data from sound level ranges shown in the table. Results of additional statistical tests that gave similar results are summarized in Note 4.

Tests for a Significant Change in Slope of ΔL vs. L (SR Groups collapsed)					
	f=1 kHz			f=2 kHz	f=3 kHz
CF range (kHz)	10.0–14.9	15.0–19.9	20.0–30.0	10.0–20.0	10.0–20.0
Levels (dB SPL)	58–100	61–100	61–100	58–100	64–97
# Fibers (H+M+L)	24+18+13	25+7+9	14+5+1	12+5+3	2+2+1
Significance of SLOPE of ΔL vs.L	p=0.275	p=0.002	p=0.783	p<0.001	p=0.017

Table 3.2: Tests for a statistically significant change in the slope of ΔL vs. sound level. Permutation tests were used with p values estimated by Monte Carlo shuffling. All fibers were considered together, without regard to SR groups. All available data were used, without any restrictions to the sound-level ranges considered. On a single trial of a permutation test, the ΔL at a given sound level was randomly assigned to a sound level, L, chosen from the original set of sound levels. The calculated statistic was a slope through the data, determined by using least-squares fitting, weighted by the errors of individual measurements (Press et al., 1992). This statistic was used to determine the statistical significance of the original slope, as summarized in Note 3.

sound level when fitted with a straight line through all sound levels, visual inspection of the average trend suggested a downward slope between 90-100 dB SPL (see Fig. 3-9). This visual impression was confirmed statistically by a permutation test restricted to 90-100 dB SPL, which found a very highly significant ($p<0.001$) dependence of ΔL on sound level for this sound-level range.

D. Dependence of ΔL on stimulus frequency

We wanted to explore whether ΔL depends on stimulus frequency. Conceptually, doing such an exploration in a single fiber may seem straightforward. Practically, however, there are several important limitations to studying a whole range of tail frequencies in a single fiber. A major limitation is the danger of acoustic trauma. Specifically, since tail thresholds are not uniform across frequency, rate-level curves in response to some frequencies may have only a few (or no) points in their rising portion, before a threshold for acoustic trauma is reached. Another limitation is harmonic distortion which, for a high-level tail-frequency stimulus, can elicit a response in the tip region of the tuning curve. Harmonic distortion severely limits the study of tail frequencies 1-2 octaves below CF. A final limitation is a finite contact time with fibers. To obtain multiple sets of rate-level curves at multiple frequencies, holding times of at least 1/2 hour are needed.

Given the technical difficulties in exploring a broad range of tail frequencies in a single fiber, our data base on the topic is small (13 fibers were stimulated at 3 or more tail frequencies). Nonetheless, the available data suggest that for a given fiber, ΔL depends on stimulus frequency. Two examples are shown in Fig. 3-12 and Fig. 3-13. For the fiber in Fig.3-12, efferent inhibition changed from minimal at 500 Hz, to small at 1 kHz, larger at 2$-$2.2 kHz, maximal at 2.5$-$3 kHz, and back to minimal at 4 kHz. This fiber is also interesting because without-efferent-stimulation rate-level curves at 2$-$3 kHz seem to have two rising portions separated by a small plateau. At these frequencies, efferents appear to inhibit the lower rising portion substantially more than the upper rising portion[5].

Another example of a fiber stimulated at multiple tail frequencies is shown in Fig. 3-13. Even though the overall efferent effect for this fiber was substantially smaller than in Fig. 3-12, frequency dependence of the effect can still be appreciated. Specifically, the effect changed from minimal at 500 Hz to small at 1$-$1.5 kHz, somewhat bigger at 1.7$-$2 kHz, and back to minimal at 3 kHz.

To get around the difficulties involved with stimulating a single fiber at multiple tail frequencies, we pooled data across many fibers. One way of data pooling was illustrated in Fig. 3-9, 3-10 and 3-11, where fibers of similar CFs were grouped and one stimulus frequency was considered at a time. Based on a visual inspection of these figures, it appears that, on average, efferent inhibition was greater at 2 kHz (and 3 kHz) than at 1 kHz for fibers with CFs between 10-20 kHz. These visual impressions were supported by the results of a statistical test that revealed a very highly significant change in ΔL with frequency. In particular, we used the analysis of variance (ANOVA) to test whether there was a change in ΔL with frequency for high-SR fibers with CFs between 10$-$20 kHz, stimulated with 1 kHz, 2 kHz and 3 kHz tone bursts (i.e., data from Fig. 3-9(A) and (B), Fig. 3-10 and Fig. 3-11). We considered only high-SR fibers whose ΔLs spanned the sound-level range of 67$-$82 dB SPL, because it appeared that the main differences in ΔL across frequency occurred at the lowest sound levels. Based on 19 fibers stimulated at 1 kHz, 6 fibers

[5]The transition from the lower to the upper rising portion in the rate-level curves was not accompanied by abrupt changes in the response phase, defined as the first Fourier component of a period histogram. Instead, the response phase gradually decreased with sound level, and was similarly affected by efferent stimulation across all sound levels.

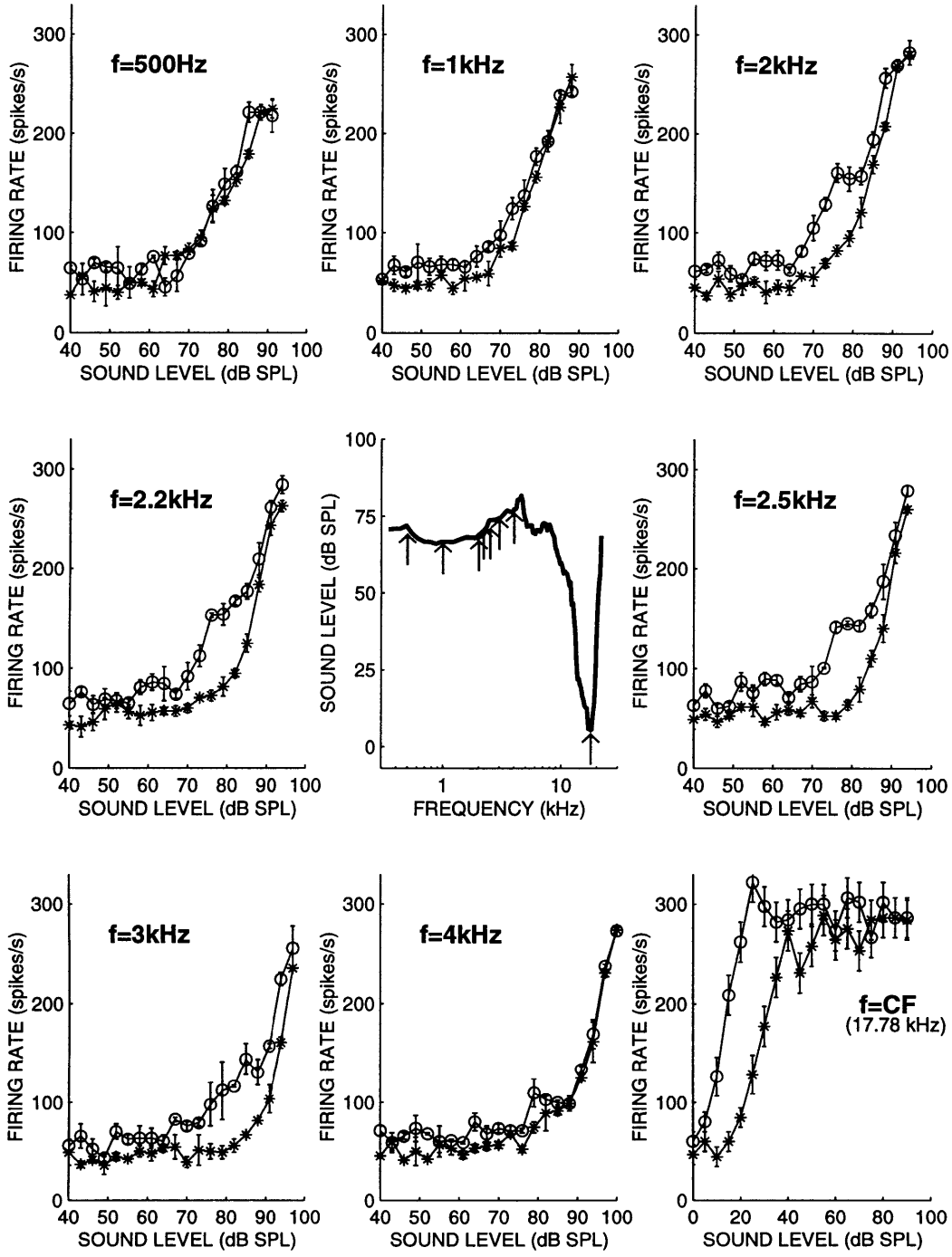

Figure 3-12: An example demonstrating that efferent inhibition in the tail depends on sound frequency. Different stimulus frequencies are indicated on the tuning curve in the central panel (arrows), and in the upper left corner of the other panels. Every pair of rate-level curves in this figure (except the CF run) is an average of multiple runs. Consequently, bars on individual points indicate standard error of the mean. Fiber TS37-24, CF=17.78 kHz, SR=69.4 spikes/s.

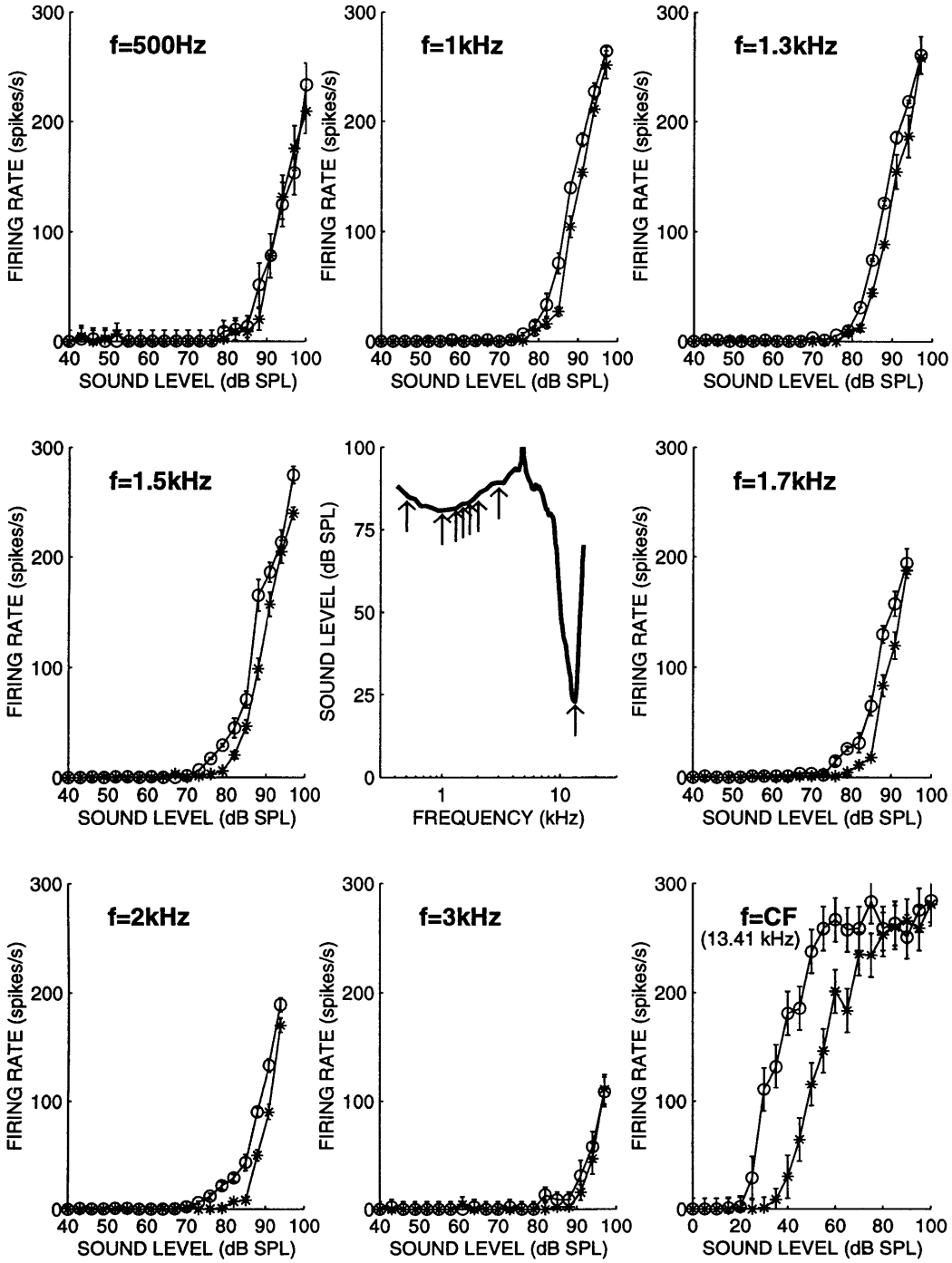

Figure 3-13: Another example of a fiber demonstrating that efferent inhibition in the tail depends on tail frequency. Figure layout is the same as for Fig. 3-12. As in Fig. 3-12, rate-level curves in each panel (except the last) are averages of multiple runs, and bars on individual points indicate standard error Note that overall, this fiber was much less affected by efferent stimulation than the fiber in Fig. 3-12. Nonetheless, the magnitude of efferent inhibition still exhibited frequency dependence. Fiber TS37-22, CF=13.41 kHz, SR=0.2 spikes/s.

stimulated at 2 kHz and one fiber stimulated at 3 kHz, the ANOVA revealed a very highly significant change ($p \leq 0.0001$) in ΔL with frequency, as well as a very highly significant change ($p \leq 0.0001$) in ΔL with sound level and across fibers.

To focus on the frequency dependence of ΔL, we averaged ΔL across sound levels and thereby collapsed the level dependence of ΔL into a single, average ΔL value – the "average normalized ΔL". The details of the sound-level collapsing are described in the caption of Fig. 3-14. Note that the averaging was done only up to 85 dB SPL to focus on sound levels for which ΔL tended to be large. Since fibers from different SR groups have different tail thresholds, ΔL was typically averaged down to lower sound levels for high-SR fibers than for medium-SR and low-SR fibers. Since ΔL tended to be larger at low sound levels than at high sound levels (Figs. 3-9, 3-10 and 3-11), the averaging procedure introduced a bias in the average normalized ΔL across SR groups, and thereby precluded comparisons across SR groups. Therefore, the frequency dependence of the average normalized ΔL was analyzed with fibers of all SRs considered together.

When analyzing the frequency dependence of the average normalized ΔL, there are several ways of expressing frequency. One way is to use absolute units (i.e., kHz), as done in Fig. 3-14. The figure illustrates a substantial scatter in the average normalized ΔL for fibers with CFs between 10–30 kHz (Fig. 3-14 (A)). Despite the scatter, it appears that, on average, the efferent inhibition grew with frequency from 500 Hz to 2–3 kHz, and then declined as stimulus frequency continued to increase (Fig. 3-14 (B)). The apparent downward trend should be interpreted with caution because it is determined by only a few fibers.

A different way of analyzing the frequency dependence of the average normalized ΔL is to express stimulus frequency relative to CF. Expressing stimulus frequency in this way (i.e., as f/CF) is often used in theoretical analyses (e.g., Zweig, 1976; Siebert, 1968)) as a way of aligning tuning curves. By expressing stimulus frequency as f/CF, we use data obtained at a few frequencies in fibers of many CFs to explore different locations within the tuning curve tails. The result is shown in Fig. 3-15. Plotted this way, the data show somewhat less scatter than in Fig. 3-14(A), and show a trend reminiscent of the trend from Fig. 3-14. In particular, Fig. 3-15 illustrates that the average normalized ΔL tends: to grow

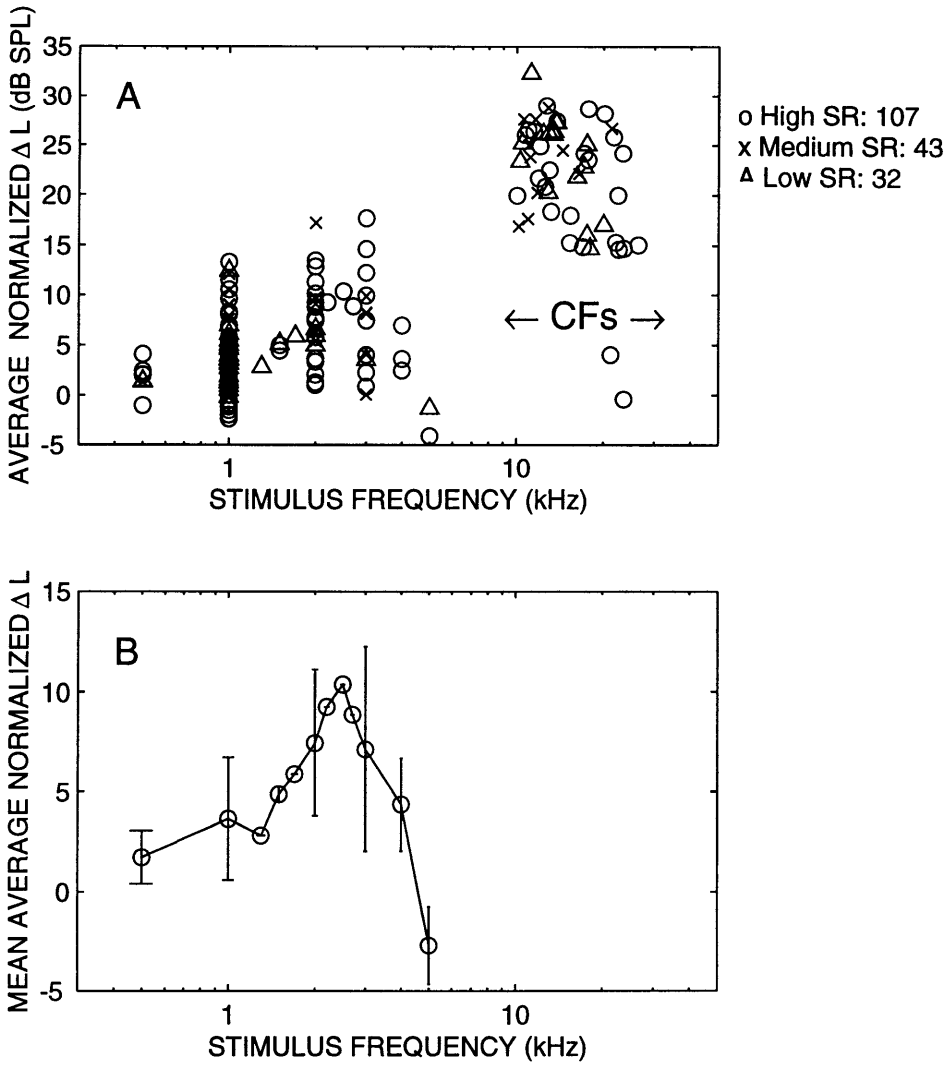

Figure 3-14: Average normalized ΔL versus stimulus frequency for fibers with CFs between 10–30 kHz. (A) A scatter plot where each fiber produced one tail-frequency point, and sometimes one CF point. The number of tail-frequency points is shown in the legend on the right, where different symbols indicate fibers of different SR groups. Note that the total number of fibers (117) is smaller than the total number of points (182) because some fibers were stimulated at multiple tail frequencies. Each point in the tail represents the normalized ΔL averaged over all available values for which the sound level L $\leq$ 85 dB SPL (exact lower sound-level limit depended on tail threshold and exact upper sound-level limit depended on availability of the data). Each point at CF represents ΔL averaged for L$\leq$ 85 dB SPL, where exact lower and upper limits for a given fiber depend on the fiber's dynamic range. Note that there are fewer points at CF than at tail frequencies because rate-level curves at CF were not obtained for all fibers. (B) The average curve derived from the tail-frequency data in (A). Each point is the mean of the average normalized ΔL at a given frequency; bars indicate standard deviation of the mean. Note that responses from all SR groups were averaged together because the data in Figs. 3-9, 3-10 and 3-11 suggested that the SR groups were not grossly different.

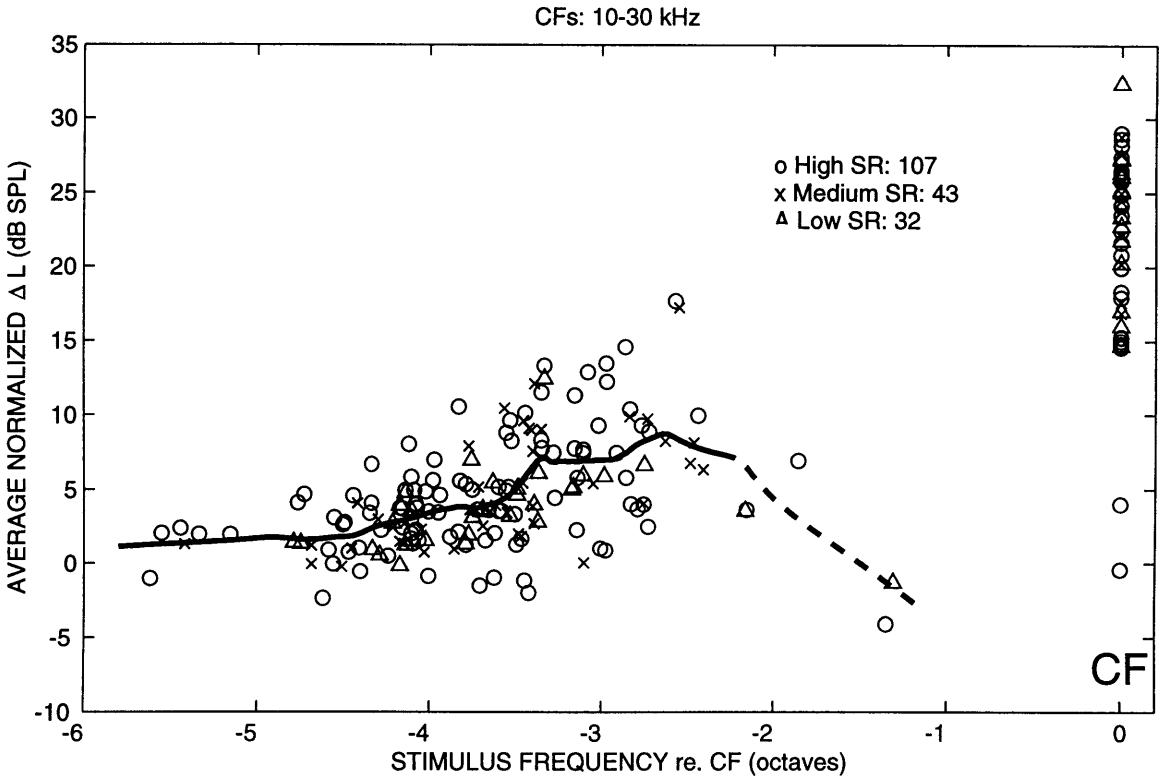

Figure 3-15: Average normalized ΔL versus stimulus frequency relative to CF. Each point represents the sound-level average of the normalized ΔL from one fiber, as explained in Fig. 3-14. Symbols identify fibers of different SR groups, as in Fig. 3-14. To guide the eye, a loess fit (smoothing factor=0.2) to the data is shown by the thick line. The dashed part of the line indicates uncertainty in the trend due to paucity of data. Stimulus frequencies ranged from 500 Hz to 5 kHz. Fibers had CFs between 10–30 kHz.

as stimulus frequency increases from 6 to 3 octaves below CF, to peak at about 2.5 octaves below CF, and to decline at higher tail frequencies. As in Fig. 3-14, caution is warranted when interpreting the downward trend in the average normalized ΔL because the trend is determined by only a few fibers. Nonetheless, the downward trend is consistent with data from single fibers (e.g., Fig. 3-12 and 3-13) - data that are included in Fig. 3-15.

E. Time courses of efferent effects

To explore the mechanisms that underlie the above-described efferent effects at tail frequencies, we took advantage of the fact that efferent effects have several time courses. In particular, we have previously shown (Guinan and Stanković,1995) that in response to

efferent stimulation of one second or longer, the time course of the efferent-evoked change in cochlear d.c. potentials (the "MOC potential") is quite different from other efferent-evoked changes, either a.c. electrical (measured by changes in cochlear microphonic, CM) or mechanical (measured by changes in stimulus frequency emissions, ΔSFE), as shown in Fig. 3-16. In particular, changes in the MOC potential (measured as changes in endocochlear potential, EP, or as changes in d.c. voltage at the round window) decay during efferent stimulation and overshoot upon the cessation of efferent stimulation. In contrast, changes in CM and ΔSFE are sustained during efferent stimulation and show little or no overshoot upon the cessation of efferent stimulation. These results suggest that an efferent-induced increase in the basolateral conductance of outer hair cells – thought to be responsible for the changes in CM – is not the only determinant of the MOC potential.[6] Moreover, the data suggest a way to separate contributions of efferent effects on basilar-membrane motion – thought to be largely reflected in efferent-induced changes in ΔSFE (reviewed by Guinan, 1996) – from efferent effects acting via mechanisms that do not change basilar-membrane motion.

Earlier authors (Geisler, 1974; Sewell, 1984; Guinan and Gifford, 1988b) have suggested that EP mediates an electrical coupling between outer and inner hair cells. This electrical coupling is distinct from mechanical coupling through basilar-membrane motion, OHCs stereocilia and the tectorial membrane. It is important to note that mechanical and electrical couplings are not exclusive, although one type of coupling may predominate under certain conditions. We have previously shown (Guinan and Stanković,1995) that efferent suppression of "true spontaneous activity" (i.e., activity not due to responses to sound) is most likely mediated electrically, through changes in EP. Evidence for this (see Fig.3-17) comes from similarities between the time course of the efferent-induced change in EP and the time course of the efferent inhibition of the true spontaneous activity (when mechanical amplification of basilar-membrane motion is presumed not to influence the firing of ANFs). A mechanism that could account for the suppression of spontaneous activity via changes in EP is that efferent reduction of EP leads to a decrease in inner-hair-cell potentials, a

[6]This finding, therefore, challenges the assumption of several cochlear models that the efferent-induced change in the basolateral conductance of outer hair cells completely accounts for both the change in CM and the change in EP (Fex, 1967; Geisler, 1974).

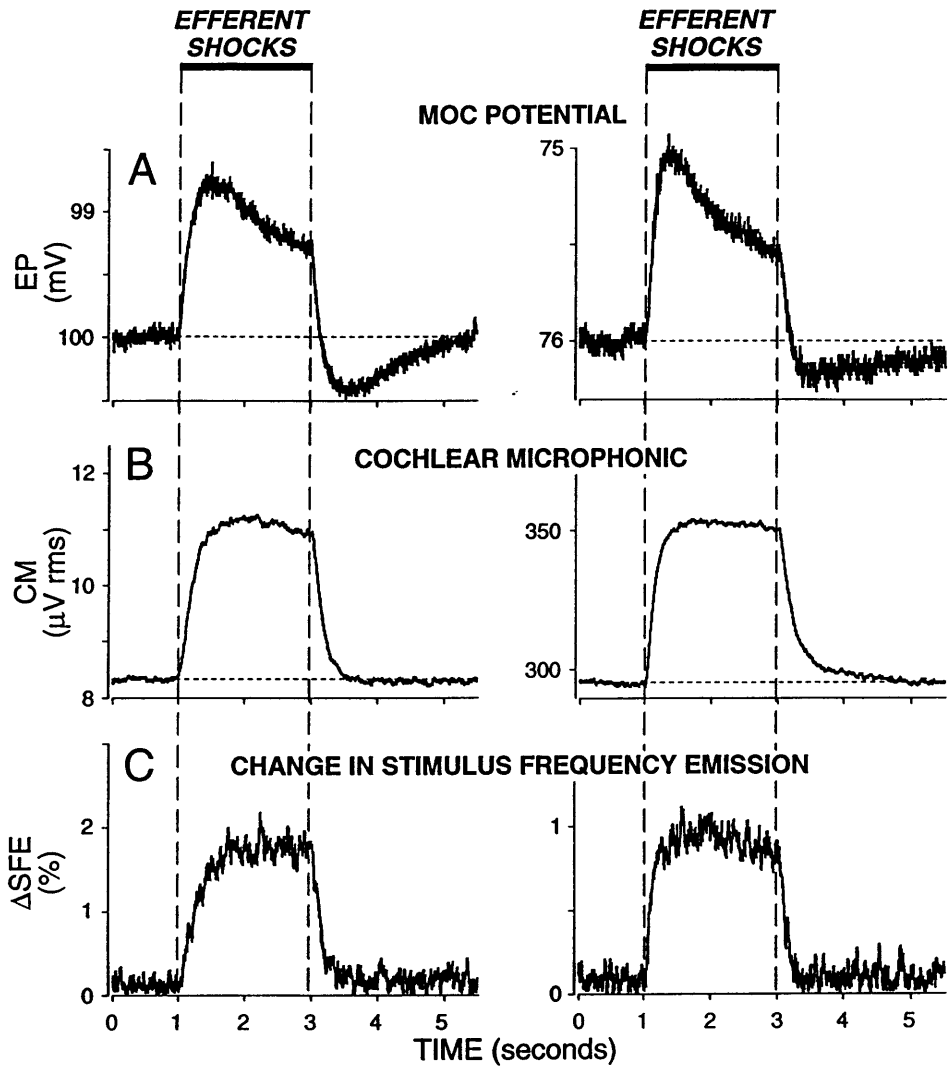

Figure 3-16: Time courses of efferent effects from two cats. **Top row:** The MOC potential as seen in the change in endocochlear potential (EP). Note that the ordinate is reversed, with smaller values plotted upward, to ease comparison with other plots in the figure. **Middle row:** The magnitude of the cochlear microphonic (CM) generated by an 80 dB SPL tone. Left column: 220 Hz tone; CM recorded from an electrode near the round window. Right column: 330 Hz tone; CM recorded from a scala media electrode. Low-frequency tones were used so that there would be little or no efferent-induced change in basilar-membrane motion at the base of the cochlea. Thus, the change in CM reflects only electrical changes produced by efferent synapses on outer hair cells. **Bottom Row:** The magnitude of the efferent-induced vector change of ear-canal sound pressure of a 20 kHz tone at approximately 60 dB SPL. This change represents the inhibition of Stimulus Frequency Emissions (SFEs) which add with the stimulus tone in the ear canal (Guinan 1986). The SFEs were measured with high-frequency tones so that they would reflect mechanical effects which originate in the cochlear base, near the EP electrode. Left column – cat G67; right column cat TS16. Efferent stimulation lasted 2 seconds.

decrease in inner-hair-cell transmitter release, and a decrease in excitation of ANFs (Sewell, 1984).

To investigate the role of the efferent-induced change in EP on tail-frequency responses, we compared efferent effects on rate-level curves during and after efferent stimulation. If the change in EP underlies efferent effects on ANFs, rate-level curves should be shifted in one direction during efferent stimulation and in the opposite direction shortly after the cessation of efferent stimulation (Fig. 3-18). In particular, if responses of ANFs were inhibited during efferent stimulation, they should be *enhanced* shortly after efferent stimulation. Although conceptually simple, this hypothesis can be difficult to test in practice, as discussed below. The overshoot in EP upon the cessation of efferent stimulation varies from cat to cat and is usually only a fraction of the EP change during efferent stimulation (see Fig. 3-16 and also Fig. 3-17). Therefore, the expected efferent-evoked enhancement of a fiber's response should be a fraction of the fiber's inhibition. Since for fibers with CFs between 10-20 kHz efferent inhibition of a 1 kHz response is on average $\approx$ 5 dB (Fig. 3-9), the expected efferent enhancement is only 2 dB or less.

For such a small shift to be detected convincingly, multiple measurements need to be averaged. The need for multiple measurements, and therefore longer holding times, is further reinforced by the fact that fewer tone bursts (i.e., 4 as opposed to the normally used 10) must be used to sample the time window of maximal overshoot.

The overall data base for the comparison of rate-level curves during and after efferent stimulation is small – 13 healthy fibers from 2 cats, plus 8 more fibers with only $\approx$ 30dB difference between tip and tail thresholds. A clear-cut example of rate-level enhancement upon the cessation of efferent stimulation was observed in one fiber only (Fig. 3-19). More frequently, rate-level curves were not affected upon the cessation of efferent stimulation (Fig. 3-20; second column), or there was only a hint of a small enhancement (Fig. 3-20; first column).

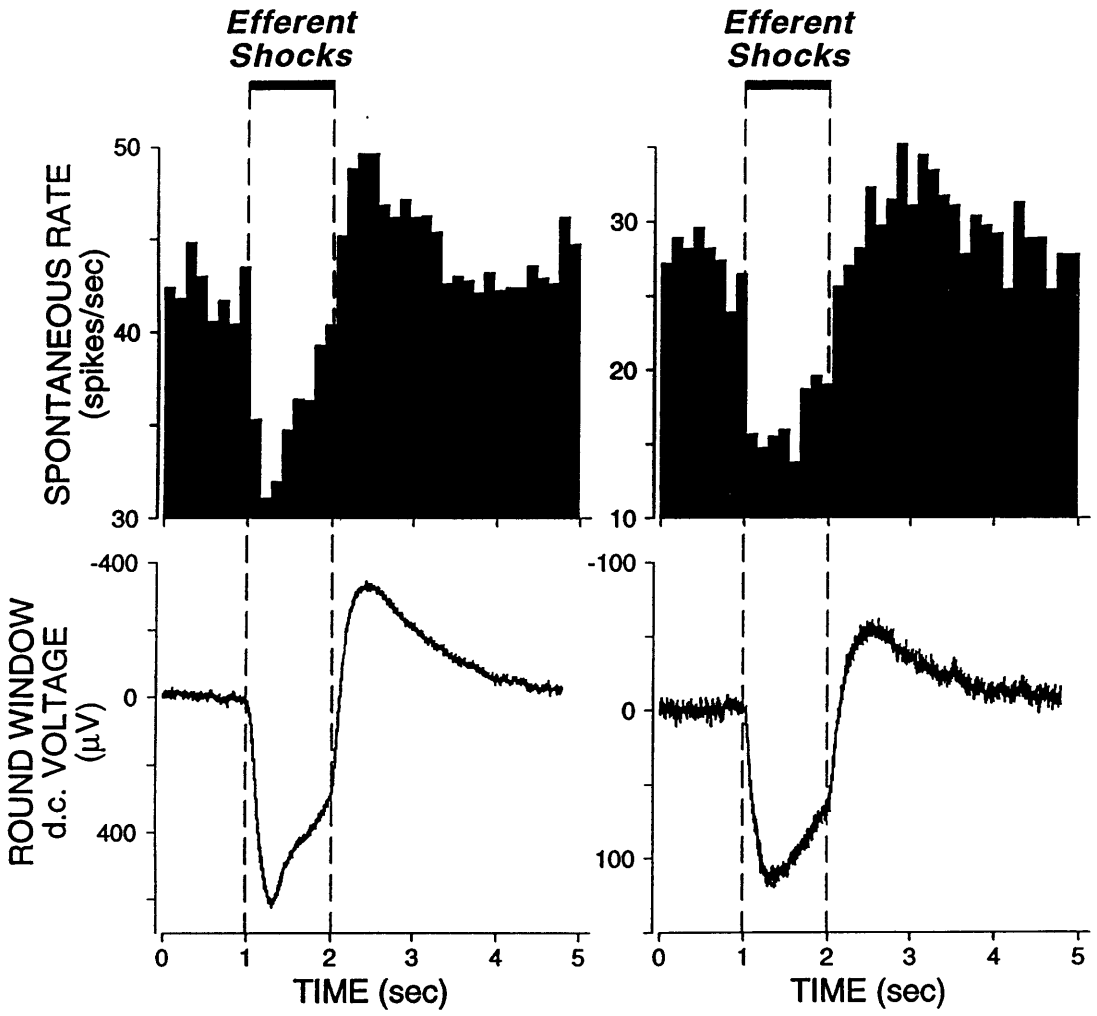

Figure 3-17: Examples from two cats of the time courses of efferent-induced changes in the spontaneous rate of a single auditory nerve fiber (top) and the simultaneously-measured d.c.voltage at the round window (V_{rw}, bottom). Note that the change in V_{rw} is opposite in sign but has, to a first approximation, the same time course as the efferent-induced change in EP (Fex, 1967) shown in Fig. 3-16. Since these fibers were not especially sensitive (thresholds: 31.0 dB SPL (left) and 12.5 dB SPL (right)), it is likely that most, or all, of their firing is "true spontaneous" firing and not a response to low-level sound. Efferent stimulation lasted 1 second. The histograms are averages of many runs. Left: Fiber TS11-8, CF=20.0 kHz Right: Fiber TS14-27, CF=9.8 kHz

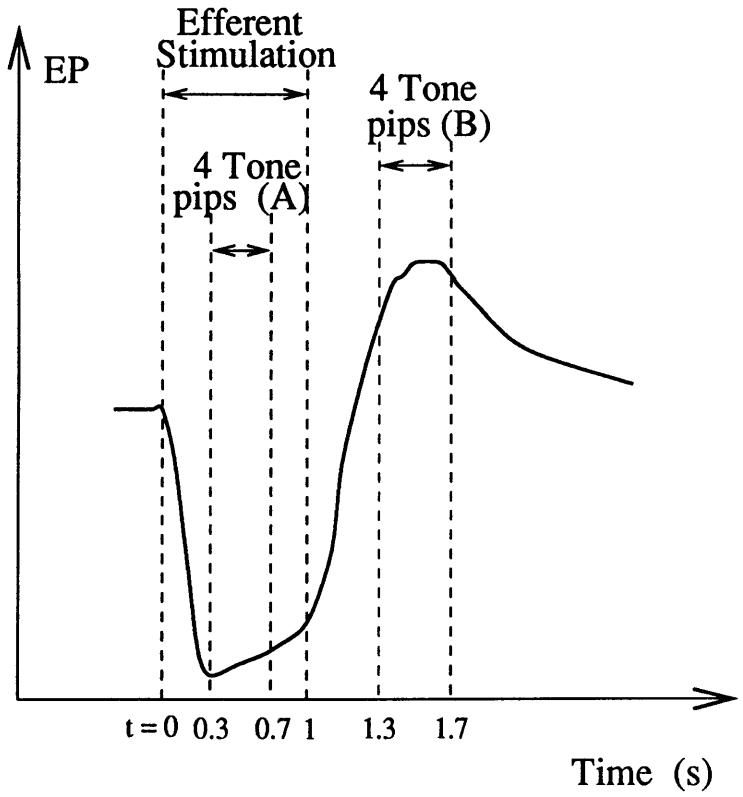

Figure 3-18: Comparison of efferent-induced changes in endocochlear potential (EP) during and after efferent stimulation. Following the onset of efferent stimulation (at t=0 s), EP quickly declines and then starts to slowly increase, despite continued efferent stimulation. After the cessation of efferent stimulation (at t=1 s), EP overshoots the baseline and reaches the maximal overshoot at t=1.3-1.4 s. Efferent effects on ANFs should have a similar time course if they are due to the change in EP. To test this hypothesis, we compared how efferents shifted rate-level curves during time windows A (i.e., when the efferent effect peaks) and B (i.e., during EP overshoot). Four tone pips (with timing as in Fig. 3-2) were presented during each time window. To test sensitivity of the results on the exact position of the sampling window B, for a few fibers the window was shifted to the left by 100 ms (so that it went from 1.2-1.6 s). The window shift did not produce a striking change in the results.

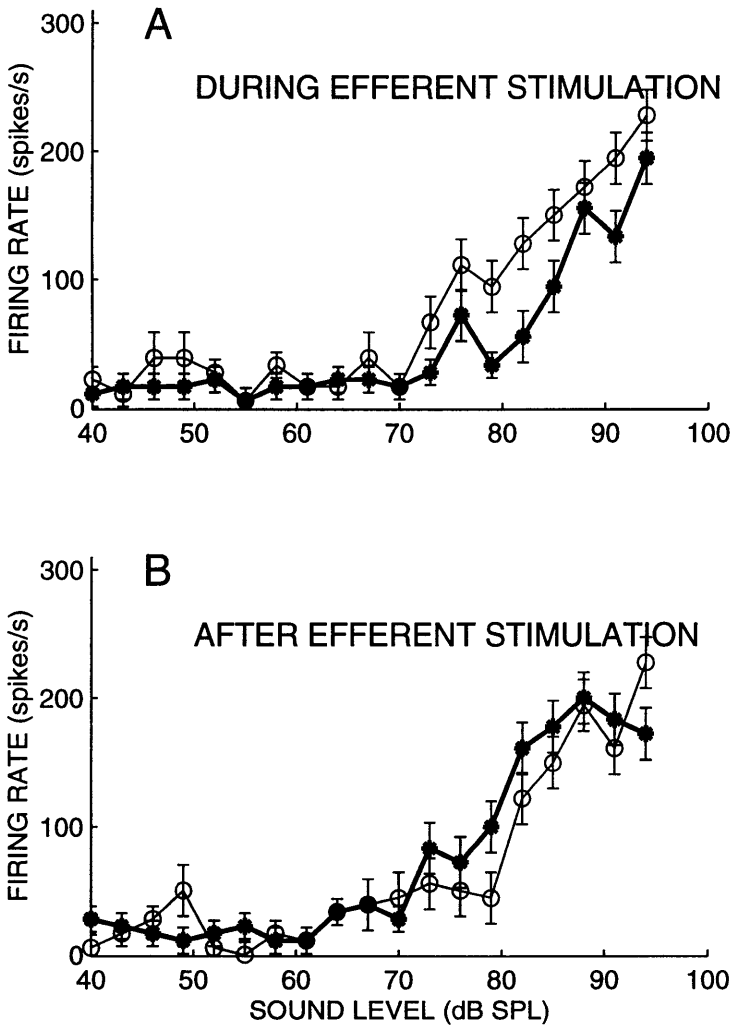

Figure 3-19: Enhancement of a fiber's response upon termination of efferent stimulation. During efferent stimulation (A) the rate-level curve was shifted to the right, and upon the cessation of efferent stimulation (B) the rate-level curve was shifted to the left. The shifted curve is shown in by the thick line. Fiber TS40-18, CF=11.5 kHz, SR=18.6 spikes/s.

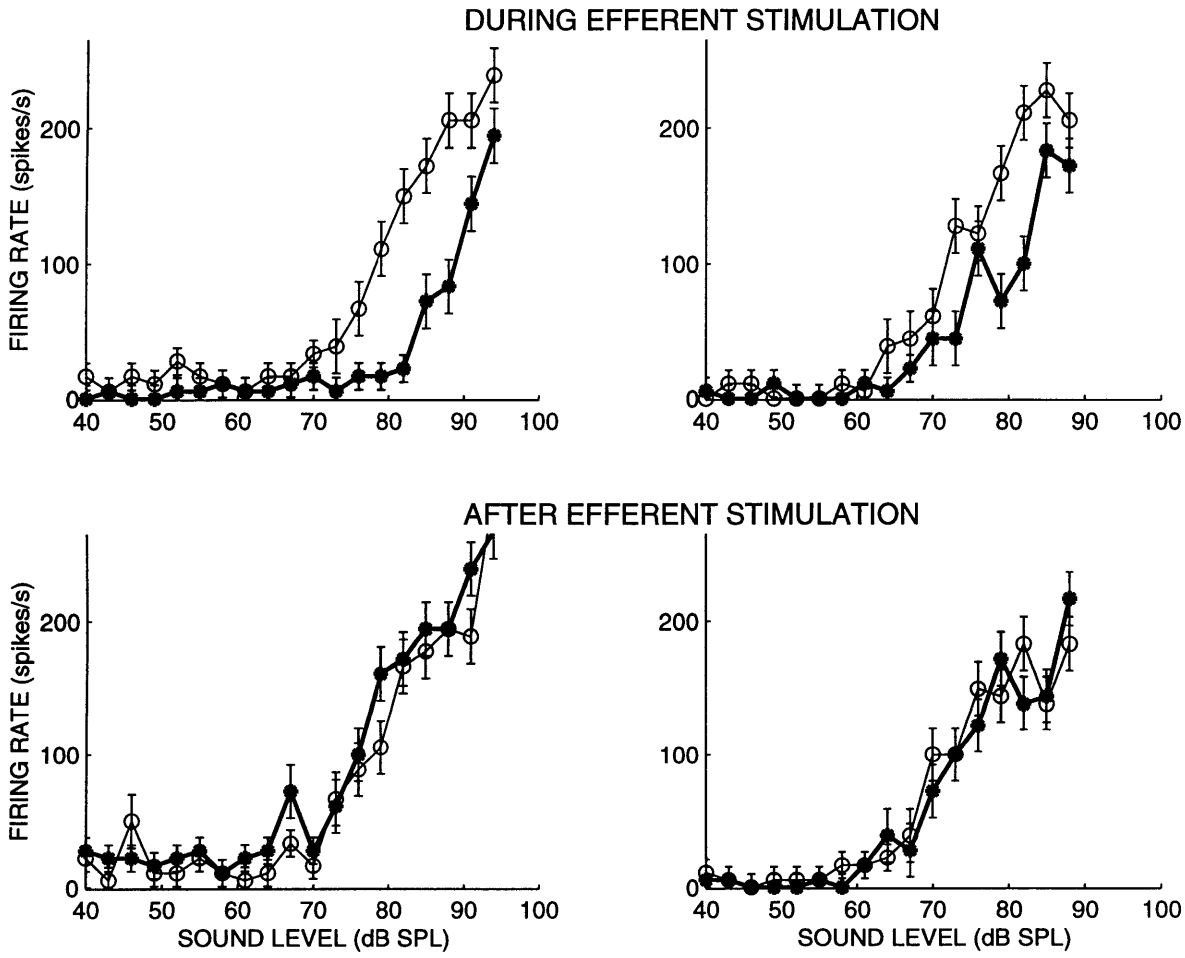

Figure 3-20: Typical efferent effects on rate-level curves upon the cessation of efferent stimulation, illustrated on two examples. There was usually only a hint of enhancement (fiber in the left column), or no effect (fiber in the right column) Left column: Fiber TS40-10, CF=11.7 kHz, SR=15.0 spikes/s. Right column: Fiber TS40-25, CF=10.5 kHz, SR=4.8 spikes/s.

IV. Discussion

A. The observed results are most likely due to medial olivocochlear efferents

There are several compelling reasons to believe that efferent effects on ANFs reported in the current study are due to stimulation of medial olivocochlear (MOC) efferents that synapse on outer hair cells, rather than lateral olivocochlear (LOC) efferents that synapse on ANF dendrites contacting inner hair cells:

1. MOC neurons are much more likely than LOC neurons to be stimulated with shock levels used in the current study because they are myelinated, and therefore have lower thresholds for extracellular electrical stimulation than unmyelinated LOCs.

2. We used high shock rates (200/s), and unmyelinated fibers (such as LOCs) do not follow shock rates > 20-50/s (Gifford and Guinan, 1987).

3. We recorded from neurons from the cochlear base, and the greatest density of crossed LOC efferent innervation is at the cochlear apex.

4. With electrical stimulation at the floor of the fourth ventricle, efferent effects on ANF responses to tones are fully explained by stimulation of MOC neurons alone (Gifford and Guinan, 1987).

B. Possible mechanisms of the observed effect

The mechanisms of efferent inhibition at tail frequencies are not yet known but a prime consideration is whether the inhibition involves depression of basilar-membrane (BM) motion, or not. Although the current measurements cannot definitively answer that question – because ANFs reflect responses from all stages of cochlear signal transduction, not just BM motion – they can provide constraints on various possibilities. Importantly, our results remain interesting regardless of the basilar-membrane involvement. For clarity, however, ramifications of the current results are considered depending on whether on not depression of BM motion is involved in producing the effect.

Could the reported inhibition of ANFs be due to efferent depression of basilar-membrane motion?

There are only two published reports of efferent effects on basilar membrane at tail frequencies, and these reports provide opposing views. In particular, Murugasu and Russell (1996), reported that efferents did not affect BM motion at frequencies more than 1/2 octave below CF. However, the major focus of that study was not on tail frequencies and the observations appear to be very limited in scope. Motivated by our preliminary data on the presence of, sometimes substantial, efferent inhibition of ANF responses to tail frequencies (Stanković and Guinan, 1997), Russell and Murugasu reexamined their BM measurements, and recently presented a conference paper (Russell and Murugasu, 1997b) suggesting that efferents may indeed inhibit BM motion at tail frequencies. However, the authors warn that their data are from a single preparation and "capricious." Therefore, it remains to be seen what, if any, fraction of the ANF inhibition at tail frequencies is produced by efferent inhibition of the BM motion.

If our measurements of efferent effects on ANFs at least partly reflect efferent effects on BM motion, it is possible that some of the effects that we observed were undetectable in BM measurements because of differences in experimental techniques. In particular, recordings from ANFs are not invasive to the cochlea, whereas BM measurements are. Consequently, ANF recordings may be more telling than BM measurements.

Our data allow for the possibility that efferents indeed reduce BM motion at tail frequencies and that this reduction *entirely* accounts for the efferent inhibition of ANFs. Implications of such a possibility are that some common assumptions about cochlear mechanics at tail frequencies need to be reexamined. One assumption is that outer hair cells (OHCs) do not influence BM displacement at tail frequencies. Since medial efferent synapses end on OHCs and act through changes in OHCs, the efferent inhibition of BM displacement would imply that OHCs affect BM displacement at tail frequencies.

Another assumption is that BM displacement at tail frequencies is always linear. There is convincing evidence from several species that this is indeed the case in the absence of efferent stimulation (guinea pig (Sellick et al., 1982), chinchilla (Ruggero et al., 1986; Ruggero et

al., 1997), and cat (Cooper and Rhode, 1992)). Note, however, that even the most detailed measurements of BM velocity to date (that reflect responses of the most sensitive and stable cochleae, Ruggero et al., 1997), may not be accurate below a tail-frequency stimulus of 3 kHz (i.e., the frequencies that were the main focus of the current study). As Ruggero et al. (1997) point out, their results for 1-3 kHz tones should be viewed with caution because of the artifact associated with the use of laser velocimetry (first described by Cooper and Rhode, 1992).

Our data indicate that, at least for some stimulus conditions, there is a highly significant change in ΔL across sound levels (Fig. 3-9, Fig. 3-10, Fig. 3-11). Presuming that BM motion is indeed linear without efferent stimulation, the sound-level dependence of ΔL suggests that BM displacement is not linear when efferents are stimulated. Specifically, if BM displacement were linear with efferent stimulation, and if efferent effects on the BM alone could entirely account for the efferent inhibition of ANFs, ΔL should not depend on sound level, i.e., rate-level curves should be parallelly shifted upon efferent stimulation. If, however, efferent effects on ANFs result from a combination of the effects on the BM and on subsequent stages of cochlear signal transduction, BM motion at tail frequencies could still be linear with efferent stimulation. If BM motion is remains linear at tail frequencies, the nonlinearity of ΔL must result from nonlinearities occurring beyond the basilar membrane, such as nonlinearities involving inner or outer hair cell stereocilia, outer-hair-cell voltage to motion transduction, synaptic mechanisms and/or possibly nonlinearities in other structures. A delineation of the contribution of different mechanisms would be aided by systematic measurements of efferent effects on BM motion at tail frequencies.

What if the basilar membrane is not involved?

If efferents do not affect BM displacement at tail frequencies, then our finding of efferent inhibition of ANFs at tail frequencies implies that efferent synapses on OHCs can affect ANFs by some other (non-BM-motion) mechanism. These other mechanisms might involve almost any step in the transduction of sound post BM motion, including: (1) alteration of cochlear micromechanics (i.e., the processes that couple BM displacement to the bending of inner-hair-cell (IHC) stereocilia), perhaps by a change in OHC elasticity (Dallos et al.,

1996); (2) reduction of the IHC receptor potential produced by bending of IHC stereocilia; (3) reduction of the transmitter released by an IHC receptor potential; or (4) reduction of the excitation of ANFs produced by an IHC transmitter release.

Comparisons of efferent inhibition across SR groups can be useful is evaluating the hypothesis that the inhibition is due to an electrical effect via the MOC potential (Geisler, 1974; Guinan and Gifford, 1988b, Guinan and Stanković). In particular, activation of MOC efferents produces the MOC potential that can be measured as a reduction of the endocochlear potential (Fex, 1967; Brown and Nuttall, 1984; Gifford and Guinan, 1987; Guinan and Stanković, 1995) or an enhancement of a potential within the organ of Corti. The reduction of endocochlear potential might cause a reduction of the IHC receptor potential, leading to a reduction of neurotransmitter release and a reduction in excitation of ANFs (Sewell, 1984). Another way in which the MOC potential might inhibit ANFs is through changes in extracellular potential around ANFs, so to reduce the probability of action potentials in response to a given transmitter release. Regardless of the way in which the MOC potential might inhibit ANFs, the inhibition should vary across fibers of different SR groups – which have different thicknesses and locations around an IHC – if there is a significant difference in amplitude of the MOC potential on modiolar vs. pillar side of an inner hair cell. It seems likely that such a difference in the MOC potential exists, but the size of the difference is unknown. If, however, the MOC potential does not vary significantly within the organ of Corti, or if mechanisms other than (or in addition to) the MOC potential shape ANF responses at tail frequencies, significant differences across SR groups would not be expected.

Based on visual inspection, our data on ΔL dependence on sound level suggest that responses from fibers of different SR groups are similar (Figs. 3-9, 3-10, 3-11). This visual impression was confirmed by statistical tests (Table 3.1) which failed to detect a significant difference between SR groups at p=0.05 level. The lack of a detectable difference, however, does not preclude the possibility that there is a real difference between SR groups, but could not be detected for the given data sets. Some limitations of the current data sets are: (1) some tests were based on a small number of fibers, (2) because of differences in tail thresholds across SR groups, our data are not well suited for comparisons across SR groups,

and (3) there is certain arbitrariness to how fibers were grouped into CF bands, and how the sound-level range was selected for the analysis of ΔL. Despite these limitations, our data provide some constraints on the possibility that efferent inhibition at tail frequencies arises from the MOC potential. In particular, if efferent inhibition at tail frequencies is due to the MOC potential, the lack of a statistically significant differences across SR groups suggests that the MOC potential does not vary substantially within the organ of Corti. Alternatively, if the MOC potential varies within the organ of Corti, the lack of a difference across SR groups suggests that efferent inhibition at tail frequencies is not primarily due to the MOC potential.

The possibility that efferent effects on ANFs at tail frequencies might arise from mechanisms that do not invoke changes in BM motion is consistent with the data indicating that the tails of ANFs are not entirely determined by mechanical tuning in the BM. Evidence for this comes from several sources. First, in the most recent report on BM measurements from very sensitive cochleae, Ruggero et al. (1997) concluded: "The neural and mechanical tuning curves resemble each other closely at near-CF frequencies but the resemblance is weaker if frequencies well below CF are taken into account." Second, furosemide, an ototoxic loop diuretic, had no apparent affect on tails of mechanical tuning curves (Ruggero and Rich, 1991), but it substantially elevated tails of neural tuning curves (Sewell, 1984). Third, acoustic trauma did not significantly affect tails of mechanical tuning curves (Ruggero at al., 1993), but it caused prominent hyposensitivity or hypersensitivity of neural tails (Liberman and Kiang, 1978). Finally, even death, which completely destroys hearing, had only a minor effect on tail-sensitivity of mechanical tuning curves (Nuttall and Dolan, 1996).

By looking at the time course of the efferent inhibition at tail frequencies (Figs. 3-18, 3-19, 3-20), we tried to evaluate the hypothesis that efferent-induced suppression of EP plays a key role in inhibiting ANFs at tail frequencies. Our data on this topic are few, and therefore not definitive, primarily because of difficulties in acquiring adequate data. However, the available data suggest that efferent-induced suppression of EP plays a minor role in inhibiting ANFs at tail frequencies. This conclusion is indirectly supported by the data of Sewell (1984) that correlate a furosemide-induced change in EP with a shift in tail

threshold of neural tuning curves. The particular correlation is 0.3 dB elevation in tail threshold per 1 mV decrease in EP. This implies that an efferent-induced change in EP of $\approx$ 2 mV should cause a 0.6 dB change in tail threshold, if the shift in tail threshold were due to the change in EP. Since the average level shift in this study was $\approx$ 5 dB, occasionally being as large as 25 dB, this suggests that efferent-induced suppression of EP plays a minor role in inhibiting ANFs at tail frequencies.

C. Frequency dependence of ΔL

Examples from individual fibers, as well as from data pooled across many fibers suggest that efferent inhibition in the tail depends on the stimulus frequency. Regarding the pooled data, the frequency-dependent pattern is somewhat clearer when stimulus frequency is expressed relative to CF (Fig. 3-15), rather than in absolute units (Fig. 3-14). It is difficult to see how this frequency dependence of the efferent effect at tail frequencies would arise directly from electrical coupling via changes in endocochlear potential (EP). Specifically, an efferent-induced change in EP is a d.c. change which does not depend on frequency, and yet our data from single fibers (Figs. 3-12, 3-13) demonstrate that efferent effects in the tail depend on sound frequency. This suggests that efferents might alter the shape of a neural tail so to introduce frequency dependence of the efferent effect. Alternatively, the frequency dependence of the efferent inhibition allows for the possibility that tuning curve tails are produced by more than one excitatory factor, each factor being differently affected by efferent stimulation.

Our results suggesting that tails of neural tuning curves might be affected differently at different frequencies are consistent with several earlier reports indicating that manipulations of the cochlear electrochemical environment differently affected different parts of neural tails. Siegel and Relkin (1987) showed that, in chinchilla, perilymphatic perfusion by Mg^{2+} caused elevation of tuning curve tails in a frequency-dependent manner; the greatest elevation was seen in the region close to the notch where tails meet tips. Those authors concluded that the frequency dependence was not primarily a synaptic phenomenon since Mg^{2+} is thought to act synaptically to block transmitter release, and there is "no reason to assume that ... Mg^{2+}" action "should depend on the frequency of the acoustic stimulus." Sewell (1984)

found that, in cat, intravenous administration of furosemide also elevated neural tails in a frequency-dependent manner.

It is useful to compare our results on the frequency dependence of the efferent-induced level shift (Fig. 3-15) with the shape of the tails of neural tuning curves. Such a comparison addresses the issue of whether frequency dependence of ΔL can be entirely explained by the frequency dependence of tail thresholds. To avoid the clutter that would result from superimposing tuning curves of all fibers with $10 \leq$ CFs ≤ 30 kHz, we selected three "averaged" tuning curves that span the CF region of the data (see Fig. 3-21). The result of plotting these "averaged" tuning curves superimposed on top of the trend from Fig. 3-15 is shown in Fig. 3-22. Based on Fig. 3-22, it appears that the frequency dependence of ΔL has some resemblance to, but cannot be predicted from the frequency dependence of tail thresholds. In particular, the figure illustrates that ΔL at two tail frequencies with similar thresholds can be very different (e.g., compare points with the abscissa of -4 and -2.6 of the tuning curve labeled "CF $\approx$ 11 kHz"). The figure also illustrates that, on average, the largest ΔL occurs at frequencies above "tail CF." The examples from individual fibers shown in Fig. 3-12 and 3-13 (as opposed to the pooled data in Fig. 3-22) also support the idea that the tuning-curve tail threshold is not the only determinant of ΔL, and that the largest efferent effects at tail frequencies occur above "tail CF".

It is very unlikely that the dependence of ΔL on tail frequency resulted from sound-evoked efferent activity, either due to stimulation of the ipsilateral ear, or due to stimulation of the contralateral ear by acoustic crosstalk (as described in Warren and Liberman 1989). This is unlikely because when cats are anesthetized as deeply as in our study, efferent sound-evoked activity is minimal (Liberman, 1989; Puria et al., 1996). In one cat we attempted to measure inhibition due to sound-evoked efferent activity (as in Warren and Liberman, 1989), but could not detect any, despite a prominent inhibition at tail frequencies when efferents were stimulated electrically.

D. Functional implications

Even though our measurements were not designed to test specific hypotheses about functional roles of efferents, they can, nonetheless, be used to comment on this issue. However,

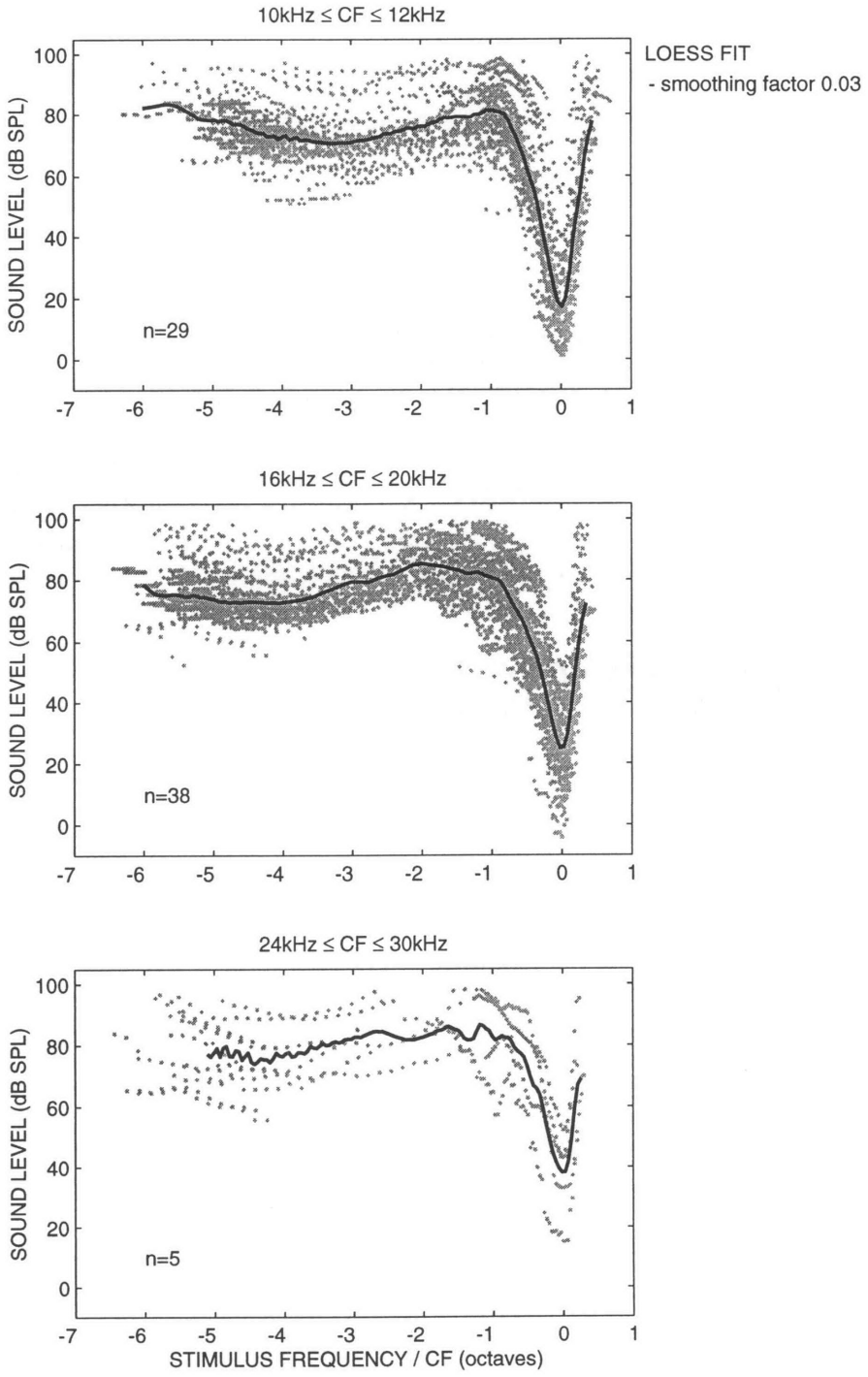

Figure 3-21: "Averaged" tuning curves for 3 frequency ranges indicated above each panel. In each panel, individual tuning curves are shown in dotted gray lines. The total number of fibers with CFs within a given frequency region is shown in the lower left part of each panel. To guide the eye, thick lines indicate the "averaged" tuning curves, i.e., the loess fits (with a smoothing factor of 0.03) through the data.

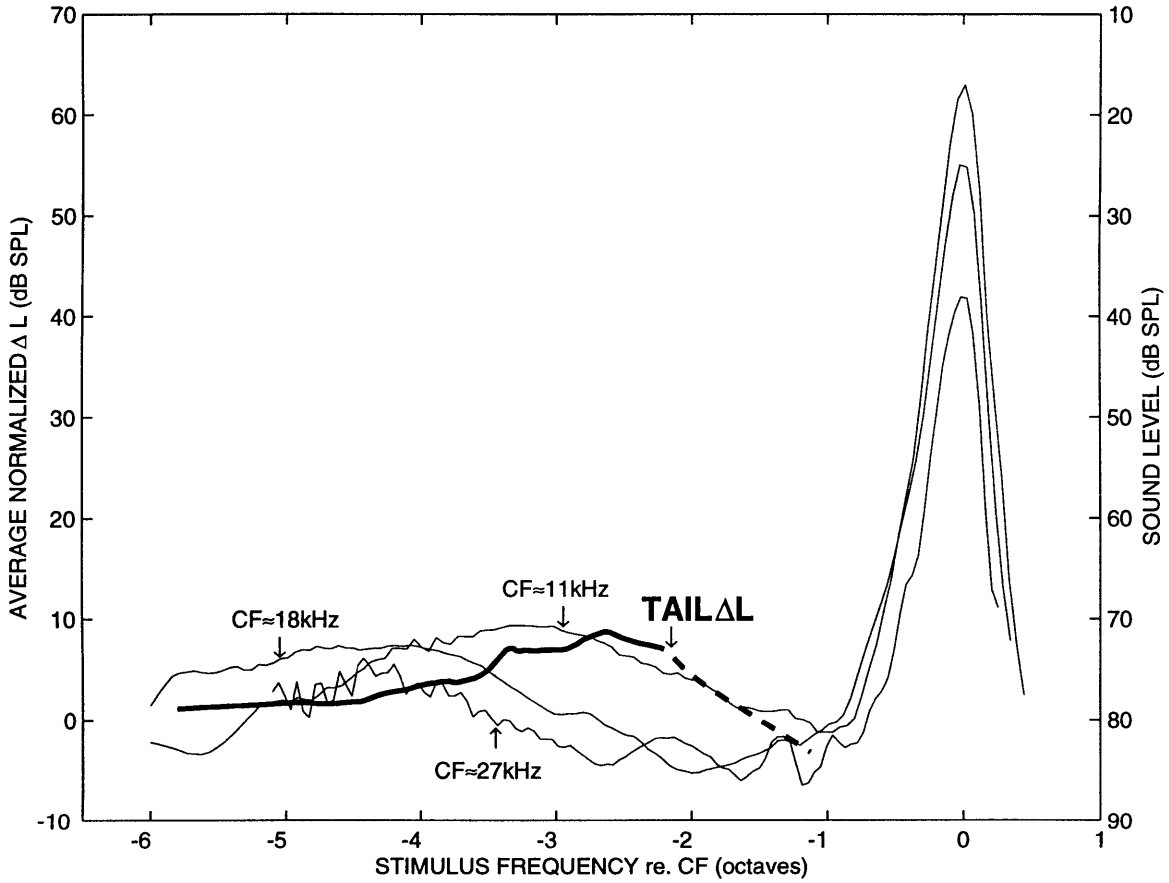

Figure 3-22: Comparison between the frequency dependence of ΔL and tails of neural tuning curves. The thick curve is the the fitted ΔL curve from Fig. 3-15 (ordinate shown at left). Thin curves are "averaged" tuning curves from Fig. 3-21, (ordinate shown at right). For simplicity, labeling in the figure was abbreviated so that CF $\approx$ 11kHz means 10kHz $\leq$ CF $\leq$ 12kHz, CF $\approx$ 18kHz means 16kHz $\leq$ CF $\leq$ 20kHz, and CF $\approx$ 27kHz means 24kHz $\leq$ CF $\leq$ 30kHz.

since our data were recorded in anesthetized cats with artificial stimulation of olivocochlear efferents, our inferences about functional implications for behaving humans are speculative.

The current results indicate that efferent inhibition in the tail is on average much smaller than in the tip. It is also possible, however, that functional implications of a small inhibition in the tail are similar to those of a big inhibition in the tip. This view is consistent with the finding that high levels of background noise do not substantially affect responses to tail-frequency tones, whereas they can routinely saturate responses in the tip (Kiang and Moxon, 1974). Since efferents play a role in facilitating detection of transients in a noisy background (Kawase and Liberman, 1993 and Kawase et al., 1993) – presumably by decreasing adaptation to noise – small effects in the tail could be functionally relevant. This view is further supported by the finding that efferents similarly enhanced single fibers' detection of tail-frequency transients and tip-frequency transients in a broadband noise (Kawase et al., 1993). It is possible that efferent effects at tail frequencies may be especially important in various pathologies that destroy sensitive tips.

V. Conclusions

Efferents can inhibit responses of ANFs to tail-frequency tones. The existence and characteristics of this inhibition provide new constraints on common concepts of how the cochlea works.

Chapter 4

Medial Efferent Effects on Auditory-Nerve Responses to Tail-Frequency Tones II: Alteration of Phase

I. Introduction

In the previous chapter, we demonstrated that, contrary to the common belief, medial olivocochlear (MOC) efferents can inhibit the firing rate of auditory-nerve fibers (ANF) responding to tones in the broadly-tuned tail region of tuning curves. In this chapter, we will explore efferent effects on fibers' response phases. As in the previous chapter, our focus will be on fibers tuned to high frequencies (i.e., fibers with high characteristic frequencies, CFs), stimulated by low-frequency tones from the broadly-tuned tail region of tuning curves.

A description of the efferent effects on response phase is an important component of any attempt to understand the system behavior, as illustrated by several examples below. First, phase measures are dominated by the a.c. receptor potentials of inner hair cells (IHCs), whereas rate measures are dominated by the d.c. receptor potentials (e.g., Palmer and Russell, 1986; Cheatham and Dallos, 1992; reviewed by Ruggero, 1992). Therefore,

studying efferent effects on response phase provides insights that cannot be gained from studying efferent effects on rate only. In particular, phase measurements provide additional constraints on models attempting to account for efferent effects in the cochlea. Second, there is compelling evidence that the response phase of ANFs cannot be accounted for by the phase of basilar membrane movement (e.g., Ruggero et al., 1996) and that mechanisms acting beyond the basilar membrane likely play an important role in shaping response phase of ANFs. Thus, exploring efferent effects on ANF response phase sheds light of the mechanisms that underlie the efferent effect at tail frequencies. Third, studying efferent effects on response phase provides a test for whether the efferent effect at tail frequencies is equivalent to an attenuation of sound. This is interesting because efferent inhibition of the firing rate is consistent with an attenuation of afferent response. If the phase change and the rate change both are equivalent to an attenuation, this has strong implications regarding the mechanisms involved. Based on the measurements from low-CF ANFs stimulated by tip-frequency tones, Gifford and Guinan (1983) concluded that efferent effects on response phase were inconsistent with an attenuation of sound. Since different mechanisms may be involved in producing efferent inhibition near CF versus at tail frequencies, we explored whether similar conclusions held for high-CF ANFs stimulated by tail-frequency tones.

II. Methods

The surgical preparation, single-fiber recordings and the stimulation paradigms are described in the previous chapter. Important differences and additions are discussed below.

A. Single fiber recording and data analysis

For each level series – in which both sound level and efferent stimulation were randomized – the occurrence times of all action potentials were automatically stored during data acquisition. To minimize the uncertainty in the timing of spikes, a custom-made spike-peak trigger was used. Its main advantage over the basic Schmidtt trigger is that it produces an output at the peak of the spike, rather than on an arbitrary point on the rising edge of the spike. Data for period histograms were from the steady-state part of the response (where

the response was delayed re. tone bursts), i.e., from 6 ms after the onset of the 50-ms long tone burst, to 1 ms after the offset of the tone burst. When appropriate, the sampling window was slightly adjusted to insure that it included an integer number of cycles.

The stored spikes were used during off-line analysis to construct histograms of action potentials relative to the zero-crossing of the stimulus waveform, i.e., post-zero-crossing or period histograms. Each histogram had 400 bins per tone cycle. For the figures presented here, data were re-binned into 25 bins per tone cycle to make the histograms smoother. For a given stimulus frequency and sound level, two different period histograms were constructed at each sound level – one in the presence, and one in the absence of efferent stimulation. Contact time with a fiber permitting, multiple level series were recorded. Period histograms (based on 400 bins/cycle) were used to define (1) synchrony, and its measure known as the synchronization index (as in Goldberg and Brown, 1969; Johnson, 1980), which is the amplitude of the fundamental Fourier component of the histogram normalized by the firing rate and (2) response phase as the phase of the fundamental Fourier component of the histogram.

The 95% confidence interval of the phase was calculated according to the procedure described by Mardia (1972). The basic assumption of the procedure is that data can be described by a von Mises distribution, which is similar to the normal distribution, except that it describes directional data. A key step is to estimate the "concentration parameter", κ, that characterizes the von Mises distribution (κ is similar to the inverse of "standard deviation" in a normal distribution). For a histogram that has a significant synchrony, $\bar{S}$, we approximated the maximum likelihood estimate of κ, $\hat{\kappa}$, as $\hat{\kappa} = 10^{(-1.402+7.310\hat{S}-12.997\hat{S}^2+8.473\hat{S}^3)}$. This approximation was obtained by fitting a curve to data from a look-up table (Appendix 2.3. of Mardia, 1972) that provides the maximum likelihood estimate of κ for given $\bar{S}$ in the von Mises distribution. The 95% confidence interval of phase (in degrees) was then calculated for a histogram of n spikes as $\frac{360^o}{2\pi}\frac{1.96}{\sqrt{\kappa'}}$ where $\kappa' = n\bar{S}\hat{k}$. The latter formula is appropriate for $n > 30$, but is an underestimate for $n < 30$ and $\kappa' < 4$. To avoid resorting to a second look-up table (Appendix 2.7a of Mardia, 1972) when the formula did not hold, and because the error was always large for this condition, the 95% confidence interval of phase was then arbitrarily set to 180°. The standard error of the phase was defined as

(95% confidence interval)/1.96, by analogy to the normal distribution for which 95% confidence interval = $1.96 \cdot$ (standard error). The standard error of the phase was used to define a criterion for rejection of phase data. Specifically, only data for which the standard error of phase, $S.E._{\Phi}$, was $-30 \leq S.E._{\Phi} \leq 30^{o}$ for at least two adjacent phase points in a sound-level series were accepted, because when the criterion for $S.E._{\Phi}$ was not met, phase data were too noisy to allow accurate determination of phase.

An estimate of the standard deviation of synchrony, $\sigma_{\bar{S}}$, was calculated using the empirical approximation of Johnson (1974): $\sigma_{\bar{S}} = (\frac{1-e^{-10\bar{S}}}{4} + \frac{\sqrt{4-\pi}}{2})/\sqrt{n}$. Synchrony data were accepted if they met the arbitrary criterion of $\bar{S} \geq 0.3$ and $\sigma_{\bar{S}} \leq 0.1$. This criterion was relaxed somewhat for Figs. 4-2 and 4-3 to show more data.

The other criteria for the acceptance of data were the same as described in the previous chapter. In summary, data were selected for: (1) minimal likelihood of artifactual responses due to harmonic distortion in the stimulus (based on a criterion that none of the first 5 harmonics of exceeds a tuning-curve threshold), (2) excellent triggering, (3) the absence of a shock artifact in histograms, and (4) no evidence of lost short-interval spikes in inter-spike-interval histograms. The fibers that entered this study are a subset of the fibers reported in the previous chapter. Overall, data are from 13 cats, which is four cats fewer than in the previous chapter, because we were not set up to record phase during initial experiments. The same two cats that were ignored in the previous chapter are also ignored here because of inadequate recording conditions (for one cat, there was loud audible noise associated with the respirator; the other cat had extremely sensitive hearing and it appeared to be responding to sounds not present in the stimulus).

A vast majority of the data are from high-spontaneous rate (SR) fibers with CFs $\geq$10 kHz stimulated with a tail-frequency stimulus of 1 kHz. The major reasons for such recording conditions are described in detail in the previous chapter, and are only summarized here, along with an additional reason relevant for the current study. First, by stimulating at 1 kHz, a large fraction of a fiber's rate-level curve can be sampled without producing acoustic trauma, because tail thresholds of high-CF fibers usually have a minimum around 1 kHz. Second, harmonic distortion accompanying a 1 kHz stimulus is usually of no consequence for fibers with CFs greater than 10 kHz. Third, fibers usually exhibit excellent phase locking

to a 1 kHz stimulus, so that the need for multiple data runs (and therefore long contact time with a fiber) is minimized, because phase can be reliably extracted from histograms with a relatively small number of spikes.

To determine whether several apparent trends in the data were statistically significant, permutation tests were used with p values estimated by Monte Carlo shuffling ("resampling", Efron and Tibshirani, 1993); in some cases the analysis of variance (ANOVA) test was applied, using the statistics package "DataDesk[4]." The loess fit (Cleveland, 1993) was sometimes used in scatter plots to aid the eye in detecting trends in data. All these methods were described in a greater detail in the previous chapter.

B. Measurements of the cochlear microphonic

We also measured efferent effects on the magnitude and phase of the cochlear microphonic (CM). Since the recording electrode was on the round window, or on the niche of the round window, there were two potentially complicating artifacts: (1) contamination of the CM with an evoked neural response, and (2) electronic artifacts at the recording electrode produced by the efferent shocks. To avoid the first artifact, forward masking with broad-band noise, attenuated 45 dB relative to the maximal output of the noise generator, was used. To avoid the second artifact: (1) efferents were stimulated between tone bursts, but not when CM was recorded, and (2) the shock frequency (227.27 Hz) was chosen to be incommensurate with stimulus frequencies. Given the long time constant of the efferent effect, interleaved efferent stimulation had little consequence on the overall strength of the efferent effect. This was confirmed in two experiments where CM was recorded between, and then during efferent stimulation. A schematic of the stimulus paradigm for the CM measurements is shown in Fig. 4-1.

Cochlear microphonic was measured by averaging in-phase and quadrature outputs of a EG&G 5210 lock-in amplifier. Overall, 32 responses to the 100-ms long repetition period (Fig.4-1) were averaged. Level series were run up to 85 dB (starting at 40-52 dB), and were obtained by either randomizing the presentation of sound level and efferent stimulation (2 cats) or by sequentially increasing sound level and, at each level, averaging responses without, then with efferent stimulation (1 cat). As expected, randomization did not significantly

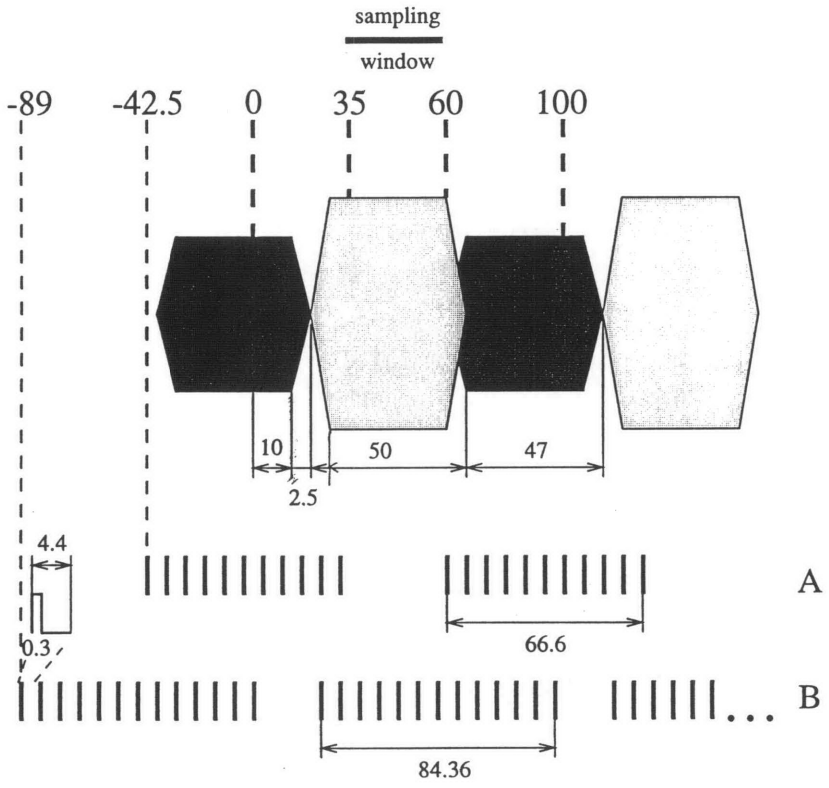

Figure 4-1: Schematic of the stimulus paradigm for recording efferent effects on the phase of the cochlear microphonic. Big numbers on top indicate time in ms relative to the reference counter, and smaller numbers in the lower half of the figure indicate duration in ms. White boxes stand for tone bursts (50 ms long with 2.5 ms rise time), and black boxes stand for noise bursts (47 ms long with 2.5 ms rise time). The time window over which CM was sampled is shown as a thick horizontal bar labeled "sampling window." Efferent shocks are shown as a sequence of short vertical bars at the bottom of the figure. Efferents were usually stimulated between (A), and sometimes during (B) tone bursts.

affect the overall response because CM shows little, if any, adaptation.

III. Results

A. Efferent effects on period histograms

Usually, efferent stimulation delayed the peak of the period histograms to later in the cycle. This is illustrated in Fig. 4-2(A−K) and Fig. 4-3(A−J) that show efferent effects on level series of period histograms from two fibers. Note that although these two fibers show typical responses, they are not typical fibers because they were recorded for a long time, so that a multitude of data is available for them. The period histograms in Fig. 4-2 and Fig. 4-3 illustrate that the variation of spike rate during the cycle typically showed only one peak and resembled a rectified sinewave. This means that actions potentials were preferentially triggered at a single phase of the stimulus sinusoid. Similar shapes of period histograms have been reported earlier for ANFs (e.g., Rose, 1967; Anderson, 1970; Johnson, 1980) in the absence of efferent stimulation. The current data on period histograms with efferent stimulation suggest that efferent stimulation does not produce major changes in the shapes of the period histograms.

Although efferent activation most commonly delayed the peak of period histograms (i.e., in 86/108=80% of fibers), this was not the only effect observed. Sometimes, efferent stimulation had no apparent effect on period histograms (i.e., in 13/108=12% of fibers), as illustrated in Fig. 4-4. In the remaining number of fibers (9/108=8%), efferent stimulation shifted period histograms to earlier in the cycle (Fig. 4-5).

Although a vast majority of the period histograms in this study had a single peak per stimulus cycle, we occasionally observed period histograms that showed two peaks per cycle − the behavior known as "peak splitting" (Kiang et al., 1965). Peak splitting was seen only at high sound levels in some fibers stimulated with 500 Hz tones. This is consistent with earlier reports that peak splitting occurs in high-CF fibers only when stimulus frequencies less than 1 kHz are used (e.g., Kiang, 1990; Ruggero et al., 1996). Since most of our data are in response to a stimulus frequency of 1 kHz, we have little data that show peak splitting. In this small data set (i.e., 7 fibers out of 14 stimulated with 500 Hz tones), there appears to be

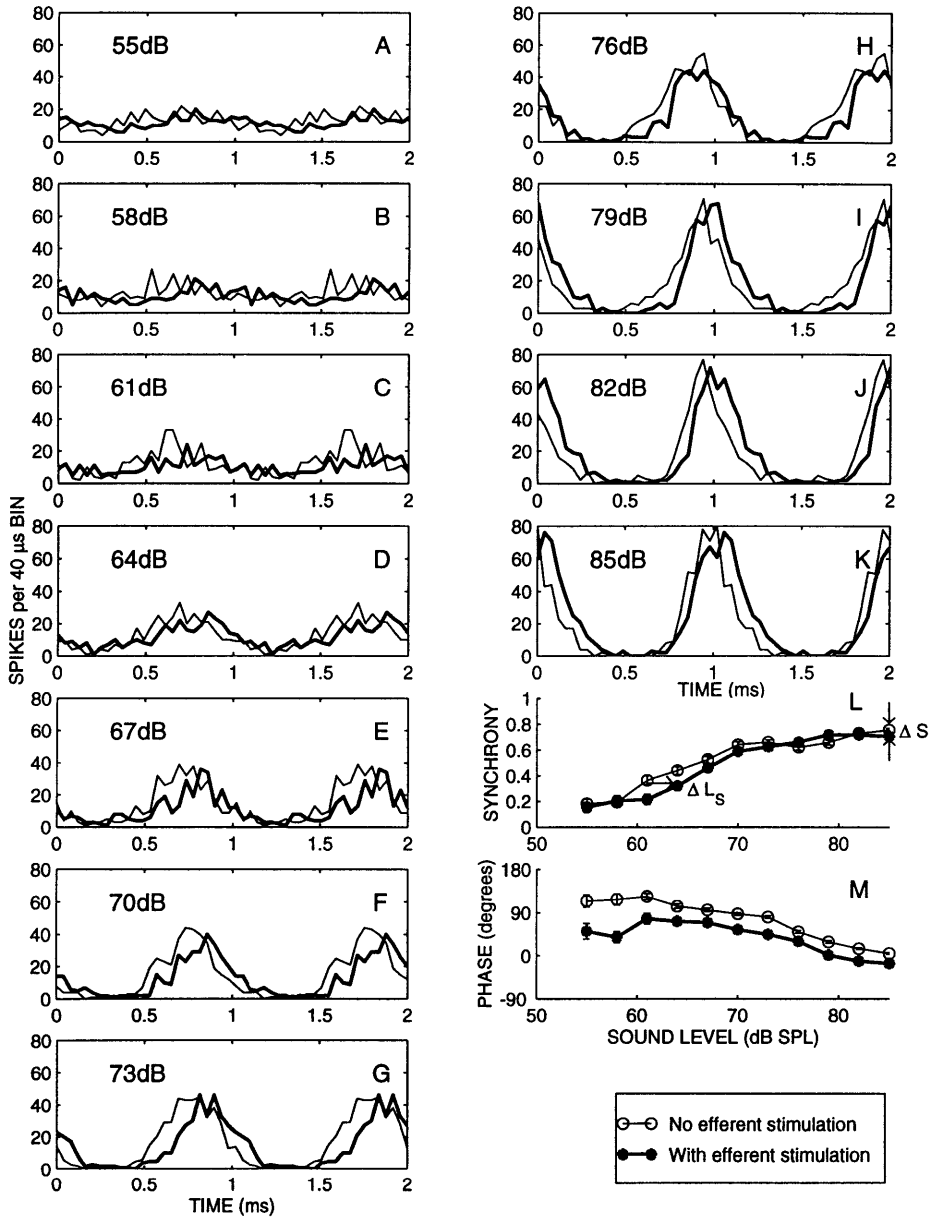

Figure 4-2: An example of a fiber whose response phase at 1 khz was delayed by efferents. Each histogram in panels A-K is a one-period histogram that, for clarity, is shown over two cycles by duplicating the one-period response. At each sound level (indicated in the upper left corner of each panel), responses in the absence (thin line) and presence (thick line) of efferent stimulation are shown. These period histograms were obtained by combining responses from 6 runs. Panel (L): synchrony derived from the above histograms in the absence (circles connected by a thin line) and presence (stars connected by a thick line) of efferent stimulation. Panel (M): response phase derived from the above histograms. Symbols are as in (L). Bars in (L) indicate standard deviation, and in (M) indicate standard error of the mean. Most of the error bars are smaller than the symbol size. Unit TS37-15, CF=17782 Hz, SR=118.9 spikes/s.

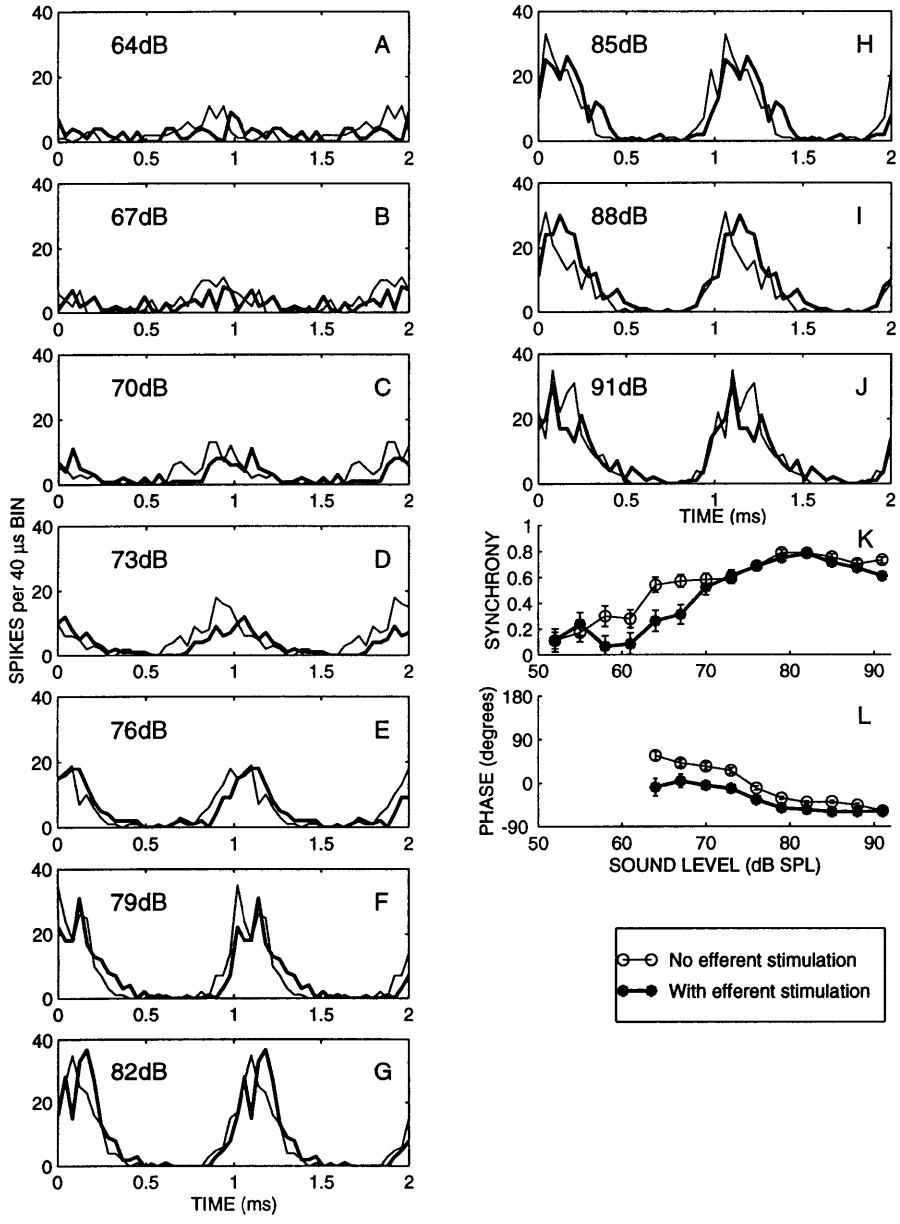

Figure 4-3: Another example of a fiber whose response phase at 1 kHz was delayed by efferents. The period histograms were obtained by combining responses from 3 runs. Figure layout as in Fig. 4-2. Unit TS37-13, CF=16692 Hz, SR=57.0 spikes/s.

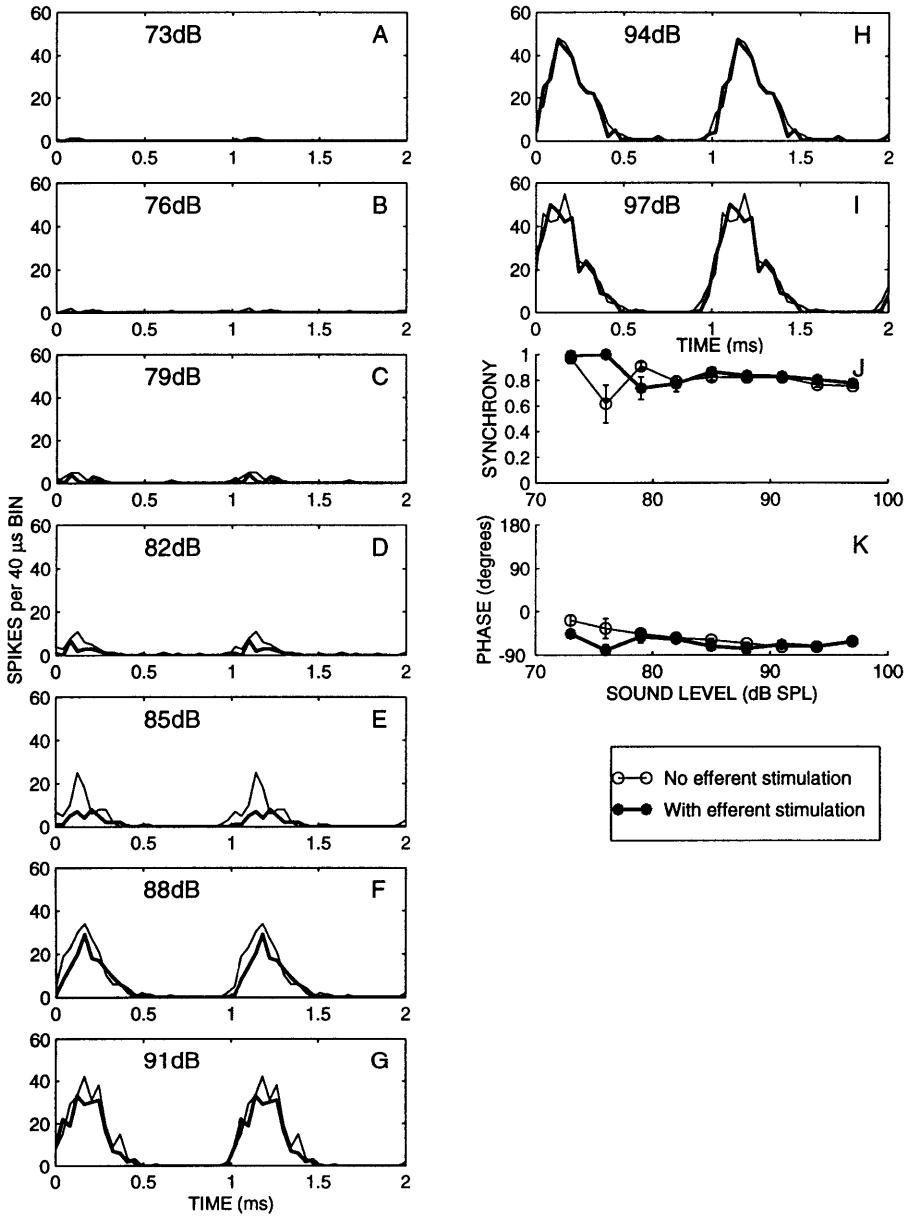

Figure 4-4: An example of a fiber whose response phase at 1 kHz was not affected by efferents. The period histograms were obtained by combining responses from 3 runs. Figure layout as in Fig. 4-2. Unit TS37-22, CF=13412 Hz, SR=0.2 spikes/s.

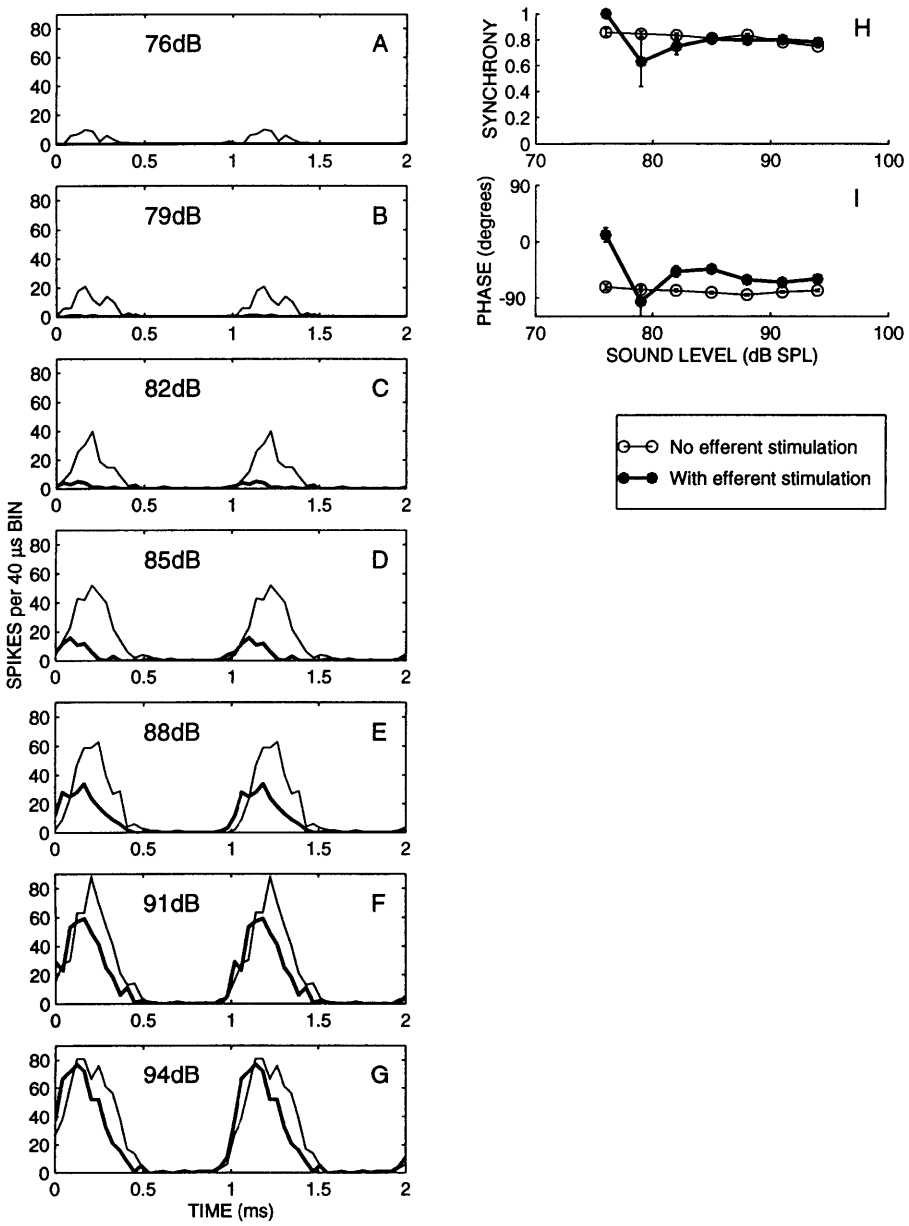

Figure 4-5: An example of a fiber whose response phase at 1 kHz was advanced by efferents. The period histograms were obtained by combining responses from 5 runs. Figure layout as in Fig. 4-2. Unit TS37-17, CF=10592 Hz, SR=1.2 spikes/s.

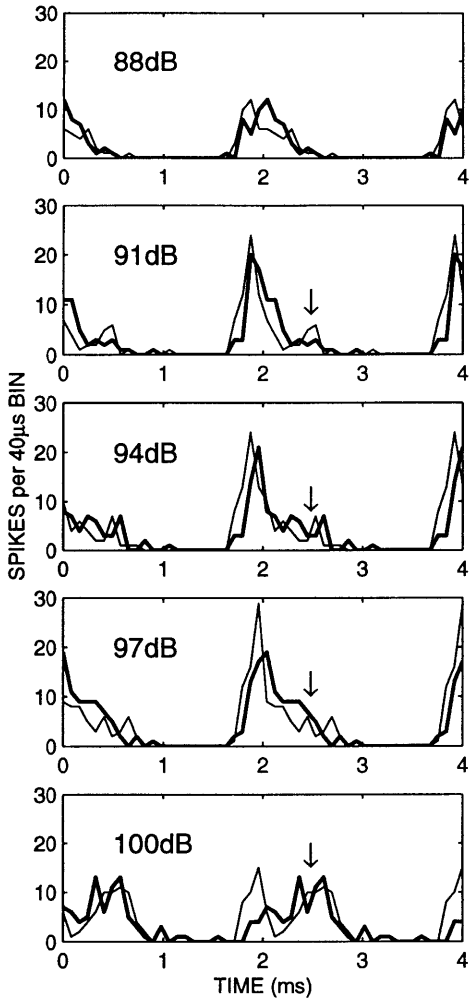

Figure 4-6: An example of efferent effects on responses that show peak splitting. Period histograms without (thin line) and with (thick line) efferent stimulation in response to a stimulus frequency of 500 Hz. This fiber started to show signs of peak splitting at 91 dB and higher (arrows). Histograms are based on a single run. Unit TS44-15, CF=21752 Hz, SR=50.3 spikes/s.

little effect of efferents on the shape of the period histograms. In particular, the histograms that show peak splitting without efferent activation also show peak splitting with efferent stimulation (Fig. 4-6 and Fig. 4-7). Furthermore, there is no clear indication in our data that there are differences in the relative amplitude of the peaks due to efferent stimulation. However, the data set is too small to draw definitive conclusions.

Since, with a few exceptions, period histograms in this study were single-peaked and their shape was not obviously changed with efferent activation, they can be characterized by their first Fourier component (as previously done by e.g., Goldberg, 1969; Johnson, 1980;

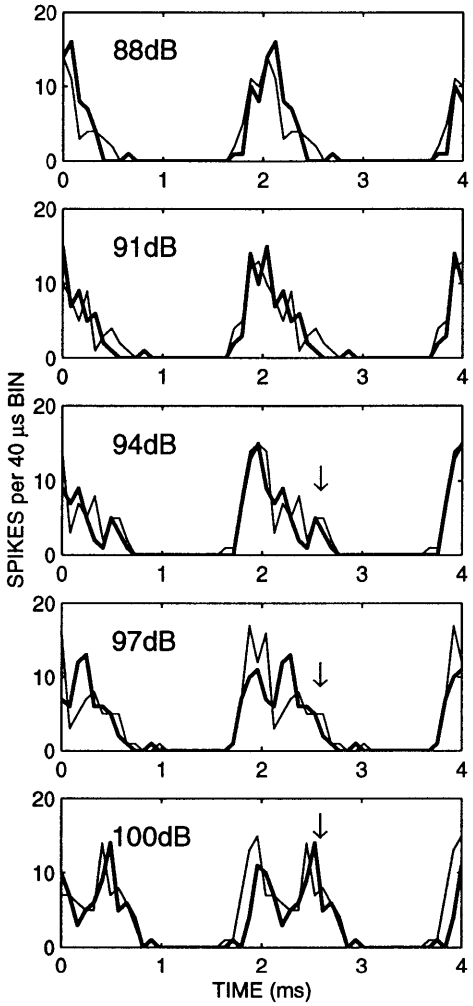

Figure 4-7: Another example of efferent effects on peak splitting. This fiber exhibited peak splitting (shown by arrows) at sound levels of 94 dB and higher in response to tone bursts at 500 Hz. Figure layout as in Fig. 4-6. Unit TS44-16, CF=23442 Hz, SR=44.1 spikes/s.

reviewed by Ruggero, 1992). The first Fourier component has two measures – (1) synchrony (also known as synchronization index or vector strength), which is the magnitude of the first Fourier component, normalized by the mean firing rate, and (2) response phase, which is the phase of the first Fourier component. Synchrony is a measure of phase-locking of spikes to the stimulus – synchrony of zero indicates no phase locking, i.e., flat period histograms; synchrony of one indicates perfect phase locking such that all spikes occur within a single time bin of the histogram (reviewed by Ruggero, 1992). Response phase and synchrony are related since phase cannot be measured unless there is adequate synchrony. For conceptual simplicity, however, we have separately considered efferent effects on synchrony and response phase in the sections that follow.

B. Efferent effects on synchrony

Since synchrony is a function of sound level (e.g., see Fig. 4-2(L)), it is of interest to explore efferent effects on synchrony across a range of sound levels. In particular, it is of interest to explore how efferents affect synchrony in the rising portion of its growth with sound level, and at high sound levels at which synchrony "saturates", or only weakly depends on sound level; the quotation marks around "saturates" serve as a reminder that synchrony often declines with sound level after reaching a peak (Johnstone, 1980), so that saturation is not flat. It turns out that most of the synchrony data are from high sound levels because the criterion for an accurate determination of synchrony (see Methods section) was usually reached only when synchrony almost saturated. Based on the data from the few fibers in which our measurements of synchrony was available over a range of sound levels, it appears that spikes from at least three runs needed to be combined to allow reliable detection of synchrony in the rising portion of sound-level curves. Most data in this study, however, are based on one or two runs so that our synchrony measure was usually not measurable in the rising portion of the sound-level curves. For low-SR and medium-SR fibers, even when spikes were combined from three runs, synchrony was never measurable in the rising portion of sound-level curves, because the low firing rates of these fibers near the threshold prevented acquisition of enough spikes.

As a measure of the efferent effect on synchrony, we used the level shift, ΔL_S – a measure

similar to the level shift for rate, ΔL, described in the previous chapter (Fig. 3-7). The ΔL_S is the amount by which the sound level must be increased with efferent stimulation to produce the same synchrony as obtained without efferent stimulation (Fig. 4-2(L)). Note that ΔL_S is meaningfully defined only in the rising portion of the sound-level dependence of synchrony, before synchrony saturates. We therefore used a different measure at high sound levels – the efferent-induced synchrony difference, ΔS. The synchrony difference was calculated by subtracting, at a given sound level, synchrony with from synchrony without activated efferents (Fig. 4-2(L)).

A question of interest is whether the efferent effect on synchrony is equivalent to attenuating the sound. To address that question, it is useful to consider ΔL_S: a positive ΔL_S is consistent with efferent attenuation of sound, whereas a negative ΔL_S is inconsistent with that view. Based on our small data set of ΔL_S, it appears that efferent stimulation most commonly (i.e., in 12 out of 13 cases) caused a positive ΔL_S, consistent with an efferent-induced attenuation of sound. This is illustrated in the examples from two fibers (Fig. 4-2(L) and Fig. 4-2(K)), as well as in the summary plot for ΔL_S from all fibers for which adequate data to plot ΔL_S were obtained (Fig. 4-8). Figure 4-8 also suggests that fibers with positive ΔL tended to have positive ΔL_S (see the figure caption for details on how the plotted points were calculated). However, because of the paucity and scatter of the data, strong conclusions about correlations between ΔL and ΔL_S are not warranted.

At high sound levels, efferent activation had only a minor effect on synchrony, as illustrated in (Figs. 4-2, 4-3, 4-4 and 4-5). To determine whether these minor effects were statistically significant across different spontaneous rate classes, we obtained a single measure of ΔS for each fiber. The measure was ΔS averaged across sound levels of maximal, or just past maximal ΔS (since synchrony tends to decline after reaching a peak, Johnstone, 1980). This amounted to averaging across 79–85 dB SPL for high-SR fibers, and across 85–91 dB SPL for medium- and low-SR fibers, which had higher synchrony thresholds than high-SR fibers. For a few high-SR fibers that had high synchrony thresholds, similar to medium- and low-SR fibers, ΔS was averaged across 85–91 dB SPL. For a few fibers with especially high synchrony thresholds, and also for a few fibers with synchrony data available only up 79 dB SPL, ΔS was averaged across the highest 3 sound levels. Regarding responses

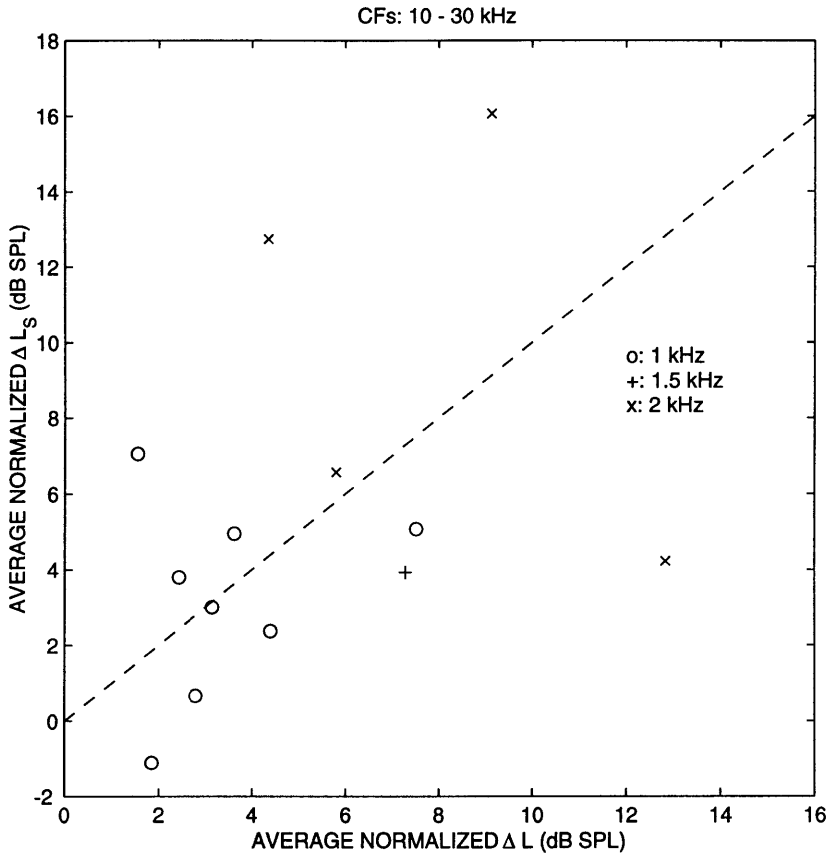

Figure 4-8: Average normalized level shift for synchrony, ΔL_S, versus average normalized level shift for rate, ΔL. Note that both ΔL and ΔL_S were normalized to account for the fact that the strength of the efferent effect (estimated from the inhibition of the compound action potential, CAP) varied across cats, and with time in a single cat. As in the previous chapter, the normalization was done to the CAP shift of 20 dB. For example, when the CAP shift was 16 dB, ΔL and ΔL_S were multiplied with 20/16 at every sound level. To ease comparison between the normalized ΔL and ΔL_S – both of which depended on sound level, but often across different sound-level ranges – we averaged the normalized ΔL and ΔL_S across sound levels. The normalized ΔL was averaged from the lowest available sound level up to 85 dB SPL to focus on sound levels where ΔL tended to be large (as in the previous chapter). The normalized ΔL_S was averaged across all sound levels at which ΔL_S was calculated. Note, however, that this amounted to averaging ΔL_S across at most three sound levels; most "average" normalized ΔL_S are, in fact, from a single sound level. Symbols identify stimulus frequencies, as shown in the legend. The dashed line indicates the slope of one.

from fibers with CFs between 10–30 kHz (69 high-SR, 25 medium-SR and 17 low-SR fibers), stimulated with frequencies between 500 Hz and 3 kHz (but most frequently with 1 kHz), the average ΔS was not statistically different from zero (p=0.1172; base on t-test) and there were no statistically significant differences across SR groups (p=0.8261; based on ANOVA method). The mean average ΔS for each SR group, along with the standard error of the mean were: -0.0098 ± 0.0006 for high-SR fibers, -0.0044 ± 0.0100 for medium-SR fibers, and -0.0029 ± 0.0161 for low-SR fibers.

C. Efferent effects on response phase

Most frequently, efferent activation shifted the response phase downward, i.e., toward (more) negative values (80% of fibers), as illustrated in Fig. 4-2(M) and 4-3(L). Sometimes (12% of fibers), response phase was minimally affected by efferent stimulation (Fig. 4-4). In a few fibers (8%), response phase was shifted toward more positive values (Fig. 4-5(I)). There was no clear correlation between the direction of the efferent shift in phase and (1) phase measured at the lowest sound levels, or (2) the degree to which phase varied with sound level.

Note that, without efferent stimulation, response phase usually changes with sound level. The change is such that the response phase advances as sound level decreases (Fig. 4-2(M) and 4-3(L)). Similar sound-level dependence of phase was reported by Ruggero at al. (1996) in chinchilla, after correcting for the difference in the definition of response phase[1].

Because phase shows a sound-level dependence, we can ask the question: "Is the efferent effect equivalent to attenuating the sound?" If the answer were affirmative, efferent stimulation would be expected to cause a phase advance, because phase advances as sound level decreases in the absence of efferent stimulation. In contrast, our data indicate that efferent stimulation usually caused a phase delay (Fig. 4-2(M) and 4-3(L)), which is inconsistent with an attenuation of sound. There are certainly exceptions to this most common trend. In particular, in a few fibers whose response phase varied with sound level, efferents caused a phase advance. Note that the example of an efferent-induced phase advance in Fig. 4-5(I)

[1]We define phase relative to zero-crossings of the stimulus sinusoid, whereas Ruggero et al. (1996) define phase relative to maximal rarefaction of the stimulus sinusoid.

is not simply explained as being due to an effect equivalent to an attenuation of sound, because the response phase of that fiber only weakly varied with sound level. When the response phase does not vary with sound level, an efferent effect that is equivalent to an attenuation of sound is expected not to affect the phase (as in Fig. 4-4(K)). Note, however, that in fibers whose phase was not affected by efferent stimulation, the phase often varied with sound level.

As a measure of the efferent effect on response phase, we used phase difference, $\Delta\Phi$. The phase difference is the amount by which phase has to be increased with efferent stimulation to produce the same response as that obtained without efferent stimulation (see Fig. 4-9). Note that the phase difference is a measure different from a "shift", where "shift" is defined as a change measured along the sound-level axis. The level shift was used to characterize efferent effects on rate (ΔL) and synchrony (ΔL_S) in the rising portion of their growth with sound-level. Even though response phase also often changes with sound level, the change is qualitatively different from a simple growth with a fast rising portion. Hence we used phase difference, not a level shift, as a measure of the efferent effect on response phase. Note that the error bars on $\Delta\Phi$ derived from a single fiber are shown in Fig. 4-9 as an aid in appreciating the error in the measurement of $\Delta\Phi$. Such error bars are used in some statistical tests described below and, for clarity, are omitted from later plots (Fig. 4-10(A) and Fig. 4-11(A)).

On average, $\Delta\Phi$ was found to be different from zero at a very highly significant level ($p<0.0001$), as determined from t-tests applied to data grouped according to stimulus frequency. Specifically, t-test was applied to all $\Delta\Phi$s (regardless of sound level) from fibers with CFs between 10-30 kH stimulated with: 500 Hz (8 fibers, average $\Delta\Phi = 10.5^o$), 1 kHz (67 fibers, average $\Delta\Phi = 15.3^o$) and 2 kHz (24 fibers, average $\Delta\Phi = 16.2^o$); for only 3 fibers stimulated at 3 kHz, the average $\Delta\Phi$ did not significantly differ from zero ($p=0.98$).

Data from individual fibers suggest that $\Delta\Phi$ depends on both stimulus variables (i.e., stimulus intensity and frequency), and fiber characteristics (i.e, CF and spontaneous rate). Considering our data on $\Delta\Phi$ pooled across many fibers, these four parameters were varied to variable extents. The results on the degree to which $\Delta\Phi$ depended on these parameters are described in the two sections that follow.

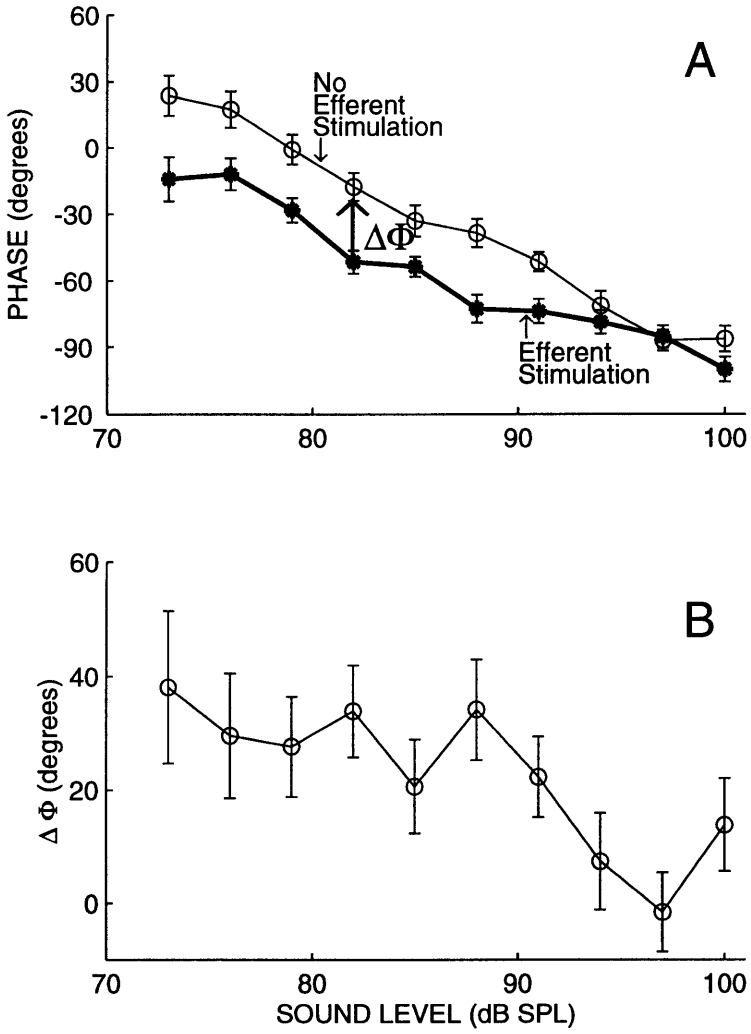

Figure 4-9: Definition of efferent-induced phase difference $\Delta\Phi$. (A) Response phase as a function of sound level in the absence (circles connected by thin lines) and presence (stars connected by thick lines) of efferent stimulation. Phase difference is the amount by which the response phase without efferent stimulation has to be increased to obtain the response phase with efferent stimulation. Panel (B): $\Delta\Phi$ derived from curves in (A). Bars on individual points indicate standard error ($\delta\Delta\Phi$) as determined from standard errors of individual phase measurements without ($\delta\Phi_{NoShs}$) and with ($\delta\Phi_{Shs}$) efferent stimulation as $\delta\Delta\Phi = \sqrt{(\delta\Phi_{NoShs})^2 + (\delta\Phi_{Shs})^2}$. Unit TS44-34, CF=16032 Hz, SR=55.3 spikes/s.

D. Dependence of $\Delta\Phi$ on sound level and spontaneous rate

To investigate the dependence of $\Delta\Phi$ on sound level and spontaneous rate – while controlling for CF and stimulus frequency – fibers were grouped into CF bands, and one stimulus frequency was considered at a time. The data are largely from fibers with CFs greater than 10 kHz, stimulated by 1 kHz tones (most fibers), 2 kHz tones (some fibers) and 500 Hz (a few fibers). Fiber grouping into CF bands depended on the number of fibers stimulated by a given frequency. In particular, fibers stimulated by 1 kHz tones were grouped into two CF bands (one an octave wide, the other one-half octave wide, Fig. 4-10) whereas fibers stimulated by 2 kHz tones were grouped into a single one-octave wide band (Fig. 4-11).

The sound-level dependence of $\Delta\Phi$ was depicted in two ways. One way was to superimpose $\Delta\Phi$ from many fibers, so to illustrate the inter-fiber variability of $\Delta\Phi$ (Fig. 4-10(A) and 4-11(A)). The other way was to plot the average $\Delta\Phi$ for each SR group (Fig. 4-10(B) and (C); Fig. 4-11(B)). Although a plot of the average $\Delta\Phi$ masks patterns present in individual fibers, it facilitates comparisons across SR groups, across sound levels and across stimulus frequencies.

A visual examination of Fig. 4-10 and Fig. 4-11 suggests that the $\Delta\Phi$ depends on sound level but does not depend on spontaneous rate. These visual impressions were tested statistically using permutation tests with p values estimated by Monte Carlo shuffling (Efron and Tibshirani (1993); also see Note 3 from the previous chapter, caption of Table 4.1 and Note 2 for details)[2]. This method has the advantage (over traditional methods such as

[2].We additionally tested for a significant difference among SR groups using an alternative method of permutation tests – for each trial, the $\Delta\Phi$-vs.-sound-level points from *each fiber* were fitted with a single straight line (the fitting procedure is described in the caption of Table 4.1). From the slopes and intercepts of these lines, the mean slope and intercept was calculated for each SR group. Statistics similar to the ones described in Table 4.1 were then computed. Results of this method agreed with the results in Table 4.1) with the exception that low-SR fibers with CFs between 10-15 kHz, stimulated with 1 kHz tones, were found to be significantly different ($p<0.001$) from medium-SR and high-SR fibers. Note, however, that this method – as compared to the method where lines were fitted through the data from all fibers of the same SR group (Table 4.1) – has a disadvantage that all slopes through individual fibers are weighted equally in calculating the mean for a given SR group, and yet reliability of a slope estimate for a given fiber depends on how many points (sometimes only two) the line was fitted through. Therefore, the method described in Table 4.1 is preferred because line fits are more accurate descriptors of the behavior of a group of fibers (when many data points are available) rather than of single fibers. Finally, to compare results of permutation tests and t-tests, we used t-tests to determine whether slopes (or intercepts) of the lines fitted to the $\Delta\Phi$-vs.-sound-level points

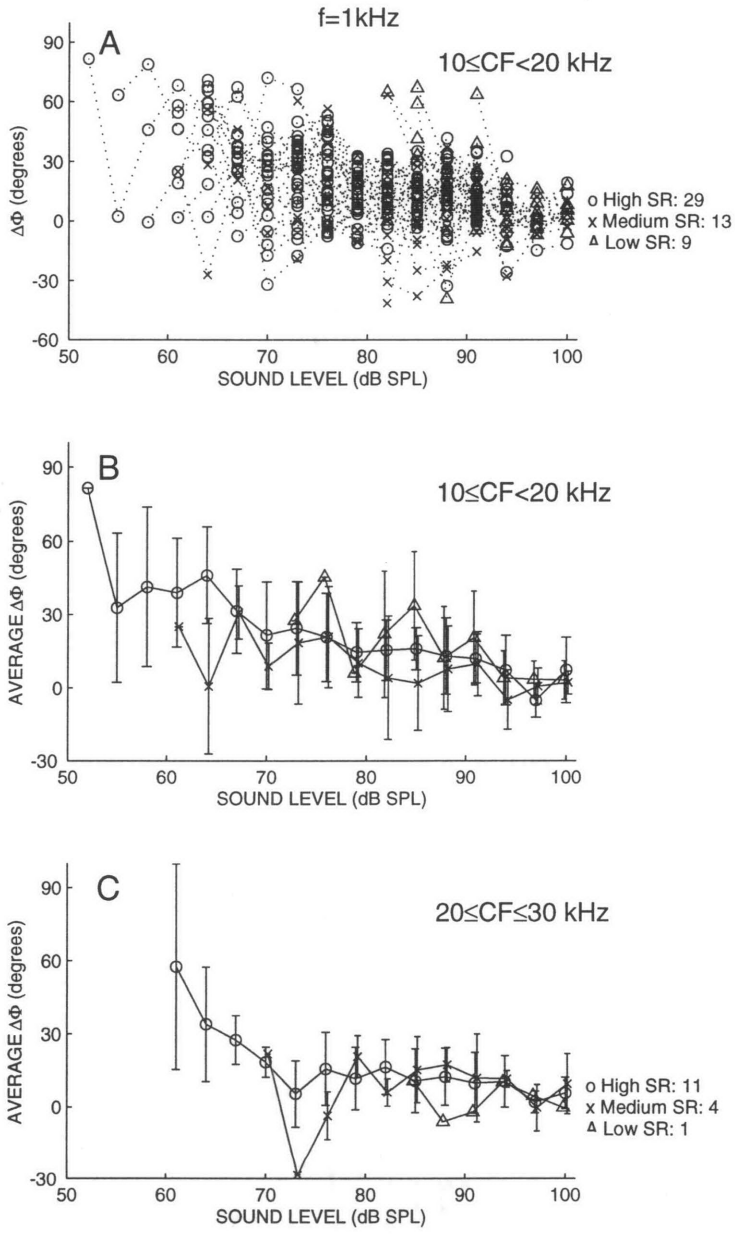

Figure 4-10: $\Delta\Phi$ as a function of sound level for a stimulus frequency of 1 kHz and two CF regions – – 10–20 kHz (A,B) and 20–30 kHz (C). (A) Superposition of $\Delta\Phi$-versus-sound-level curves from many individual fibers. Responses from a single fiber are connected by dotted lines. Symbols code fiber SR: circles=high-SR, x=medium-SR, triangles=low-SR. Text on the right of the figure indicates how many fibers of each SR group are shown in the figure. Differences in the lowest initial sound level reflect differences in synchrony thresholds, i.e., the levels at which phase error is $< 30^{o}$. (B) Average $\Delta\Phi$ for each SR group, based on fibers from (A). Bars on individual points indicate standard deviation, and give a feel for the spread in data. Points without bars result from one fiber only. (C) Average $\Delta\Phi$ for fibers with $20 \leq$ CF $\leq$ 30kHz, grouped according to SR. Symbols as in (B).

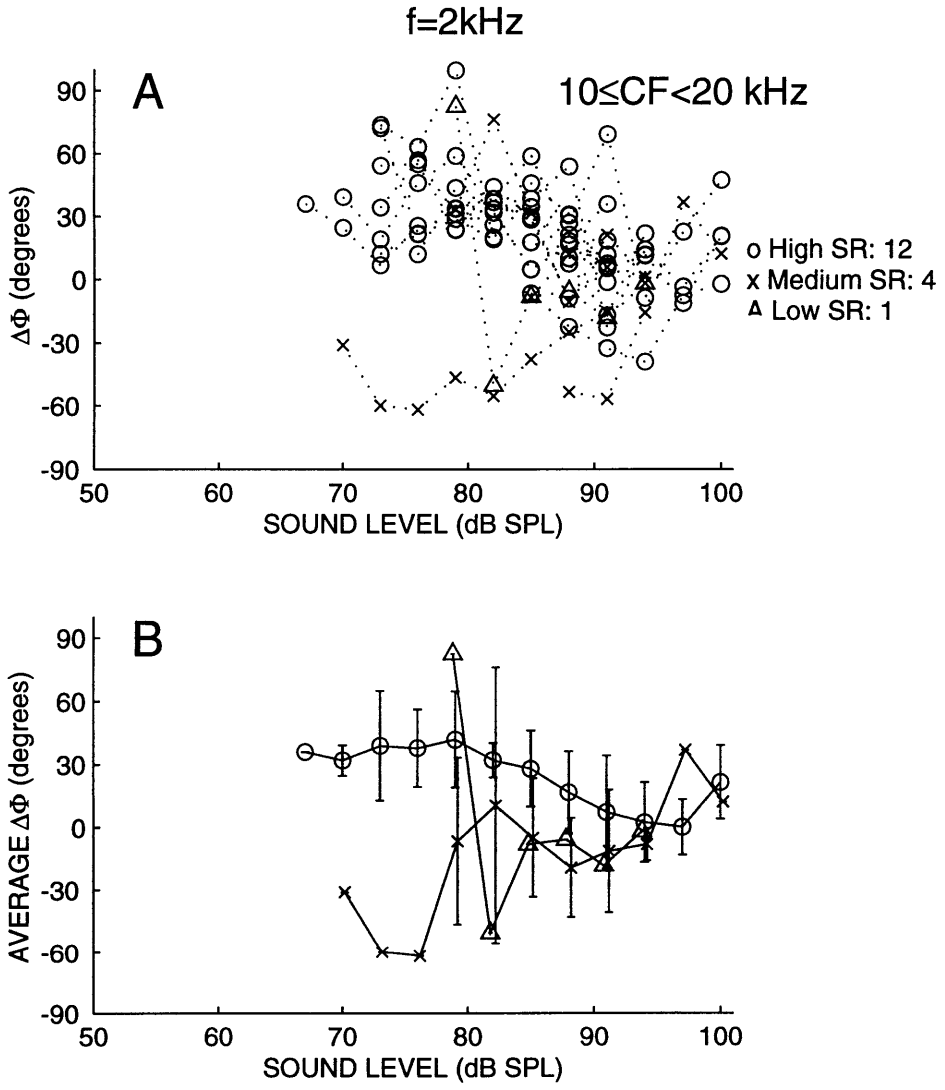

Figure 4-11: $\Delta\Phi$ as a function of sound level for stimulus frequency of 2 kHz and fibers with CFs from 10–20 kHz. Symbols as in Fig. 4-10.

ANOVA) that it does not assume a Gaussian distribution of samples. For most cases, no statistically significant difference was seen between SR groups (Table 4.1). The only difference detected between SR groups – using permutation tests based on straight line fits through the data from all fibers of a given SR – is the difference between high- and medium-SR fibers with CFs between 10-20 kHz, stimulated with 2 kHz tones (p=0.01). Since this result is based on only 4 medium-SR fibers, it needs to be interpreted with caution.

Next, we wanted to determine the dependence of $\Delta\Phi$ on sound level. Since we found that there was no significant difference among SR groups when data on $\Delta\Phi$-vs.-sound level were analyzed (or in the one case that appeared to be significant, there were few fibers in one of the SR groups), we considered all fibers together, without regard to SR, in determining the dependence of $\Delta\Phi$ on sound level. Permutation tests revealed that $\Delta\Phi$ significantly depended on sound level for all conditions considered (Table 4.2).

E. Dependence of $\Delta\Phi$ on stimulus frequency

Ideally, the frequency dependence of $\Delta\Phi$ should be studied in a single fiber at a time. Practically, however, there are several limitations that hinder such a study at tail frequencies, as explained in the methods section. Briefly, the limiting factors are: (1) the danger of acoustic trauma when stimulating with tones for which the fiber has high thresholds; (2) harmonic distortion in the stimulus which, for some frequencies, can elicit a response in the tip region; (3) a decrease in phase-locking for higher stimulus frequencies, and (4) a finite contact time with a fiber. Given these technical difficulties, we have pooled data across many fibers to explore how $\Delta\Phi$ depends on stimulus frequency.

To concentrate on the frequency dependence of $\Delta\Phi$, we averaged $\Delta\Phi$ across sound levels. The averaging was done only up to 85 dB SPL to focus on sound levels where $\Delta\Phi$ tended to be large. The details of the averaging are provided in the caption of Fig. 4-12. Note that the averaging produced a bias across SR groups because, when compared with medium-SR and low-SR fibers, averaging for high-SR fibers was typically done down to lower sound

from individual fibers were significantly different between SR groups (two SR groups were considered at a time). Results of t-tests were in complete agreement with the results of permutation tests when lines were fitted through $\Delta\Phi$-vs.-sound-level points from *each fiber*.

Tests for a Significant Change in $\Delta\Phi$ vs. L across SR Groups			
	f=1 kHz		f=2 kHz
CF range (kHz)	10.0–20.0	20.0–30.0	10.0–20.0
Levels (dB SPL)	73–100	85–100	79–94
# Fibers (H+M+L)	29+13+9	11+4+1	11+4+1
Difference in SLOPE of $\Delta\Phi$ vs. L between SR groups:			
H – M	p=0.50	p=0.61	p=0.01
H – L	p=0.38	p=0.63	p=0.93
M – L	p=0.17	p=0.52	p=0.27
Difference in INTERCEPT of $\Delta\Phi$ vs. L between SR groups:			
H – M	p=0.24	p=0.60	p=0.01
H – L	p=0.36	p=0.61	p=0.80
M – L	p=0.09	p=0.46	p=0.27

Table 4.1: Results of statistical tests aimed at determining the probability that the apparent differences among SR groups (H=high-SR, M=medium-SR, L=low-SR fibers) arose by chance. Permutation tests were used with p values estimated by Monte Carlo shuffling. **Choice of sound-level range:** Similar to the previous chapter (Table 3.1), SR groups were compared across the sound-level range over which the *average* $\Delta\Phi$-vs.-sound-level curves (one curve per SR group) overlapped (e.g., see Fig. 4-10(B,C)). This choice of sound level range was deemed most appropriate for the least biased comparison of SR groups. Specifically, since $\Delta\Phi$s from individual fibers span variable sound-level ranges, the range of overlap of most fibers (for a given stimulus frequency) is typically very narrow (<10 dB), such that statistical comparisons of SR groups across such a range may give biased results. Fibers considered in the tests typically spanned a subset of the sound-level range of the average $\Delta\Phi$ for a given SR group. For example, if the average $\Delta\Phi$ included 10 points (73-100 dB, with 3 dB spacing between points), individual fibers that contributed to the average could have anywhere from 2 to 10 points; most fibers considered in the tabulated tests had approximately 6 points per fiber. **Method:** The results summarized in the table are based on a method where, for each trial, the data from *all fibers assigned to the same SR group* were fitted with a single straight line, using least-squares fitting, with points weighted by the errors of individual measurements (Press et al., 1992) . The lines produced a slope ($\Delta\Phi$/L) and intercept ($\Delta\Phi$ at L=0) for each SR group. The slopes and intercepts were used to generate 6 different statistics, e.g., [(slope through high-SR fibers) – (slope through medium-SR fibers)], [(intercept through high SR fibers) – (intercept through medium-SR fibers)] and similarly for the other pairs of SR groups. The statistics obtained from the real data were then compared with the distribution of statistics from 1000 permutation trials to estimate the p value of the real data. The tabulated results show that statistically significant differences were not detected among SR group at the p=0.05 level, with one exception (high-SR and medium-SR fibers with CFs between 10-20 kHz appeared to be different when stimulated with 2 kHz tones. Statistically the same results were obtained when data from *all* sound levels were considered, not only data from sound level ranges shown in the table. Results of additional statistical tests that gave similar results are summarized in Note 2.

Tests for a Significant Change in the Slope of $\Delta\Phi$ vs. L (SR groups collapsed)			
	f=1 kHz		f=2 kHz
CF range (kHz)	10.0–20.0	20.0–30.0	10.0–20.0
Levels (dB SPL)	52–100	61–100	67–100
# Fibers (H+M+L)	29+13+9	11+4+1	11+4+1
Significance of SLOPE of $\Delta\Phi$ vs. L	$p<0.001$	$p<0.001$	$p<0.001$

Table 4.2: Tests for a statistically significant change in the slope of $\Delta\Phi$ vs. sound level. Permutation tests were used, with p values estimated by Monte carlo shuffling. All fibers were considered together, without regard to SR. No restrictions were imposed on the sound-level range considered, so that all available data were used. On a single trial of a permutation test, the $\Delta\Phi$ at a given sound level was randomly assigned to a sound level chosen from the original set of sound levels. The calculated statistic was a slope through the data, determined by using least-squares fitting, weighted by the errors of individual measurements (Press et al., 1992). The distribution of slopes from 1000 permutation trials was used to determine the statistical significance of the original slope, using the procedure outlined in Note 3 from the previous chapter.

levels, where $\Delta\Phi$ tended to be large. Because of this bias, a comparison across SR groups was not warranted. Consequently, fibers of all SR groups were considered together in the analyses of the frequency dependence of the average $\Delta\Phi$.

When the average $\Delta\Phi$ is plotted as a function of stimulus frequency for fibers with CFs between 10–30 kHz, the variability in the size of $\Delta\Phi$ becomes apparent. (Fig. 4-12). This variability is not surprising in light of the data shown in Fig. 4-10 and Fig. 4-11. Despite the variability, data in Fig. 4-12 illustrates that in a large majority of fibers, efferents caused a positive $\Delta\Phi$, consistent with an efferent-induced phase delay. The plot also suggests, although weakly, that $\Delta\Phi$ tends to grow with frequency from 500 Hz to $\approx$ 2.5kHz, and tends to decline at 3 kHz. This apparent decline should be interpreted with caution given the scatter in the data, and the paucity of the fibers stimulated by 3 kHz tones.

An alternative way of analyzing the frequency-dependence of $\Delta\Phi$ is to express stimulus frequency relative to CF – the frequency that characterizes a given fiber. In this way, tuning curves could be aligned (e.g., Zweig, 1976; Siebert, 1968), so that our data in response to a few stimulus frequencies in fibers of many CFs could be used to explore different locations within the tuning curve tails. The result is shown in Fig. 4-13. Despite a substantial scatter in the figure, there is a hint of a trend somewhat similar to the trend from Fig. 4-12. In particular, it appears that the average $\Delta\Phi$ tends to grow slowly as stimulus frequency

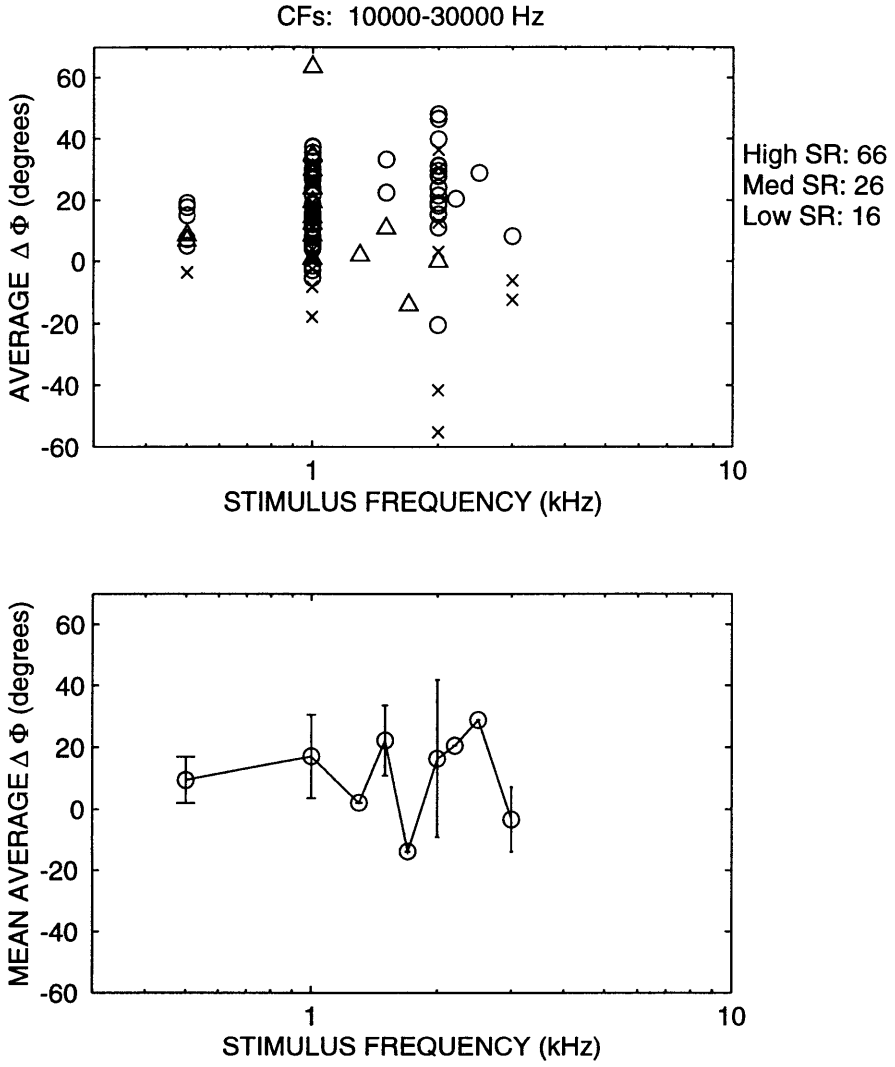

Figure 4-12: Average $\Delta\Phi$ versus stimulus frequency for fibers with CFs between 10–30 kHz. (A) A scatter plot where each point represents one fiber. The legend on the right indicates how many tail-frequency points were plotted for each SR group. Note that the total number of fibers considered (68) is smaller than the total number of points (108) because some fibers were stimulated at multiple tail frequencies. Each point represents $\Delta\Phi$ averaged over all available sound levels up to 85 dB SPL (the exact lower limit depends on synchrony threshold and the exact upper limit depends on availability of the data). (B) The average curve derived from data in (A). Each point is the mean of the average $\Delta\Phi$ at a given frequency; bars indicate standard deviation of the mean. Note that responses from all SR groups were averaged together.

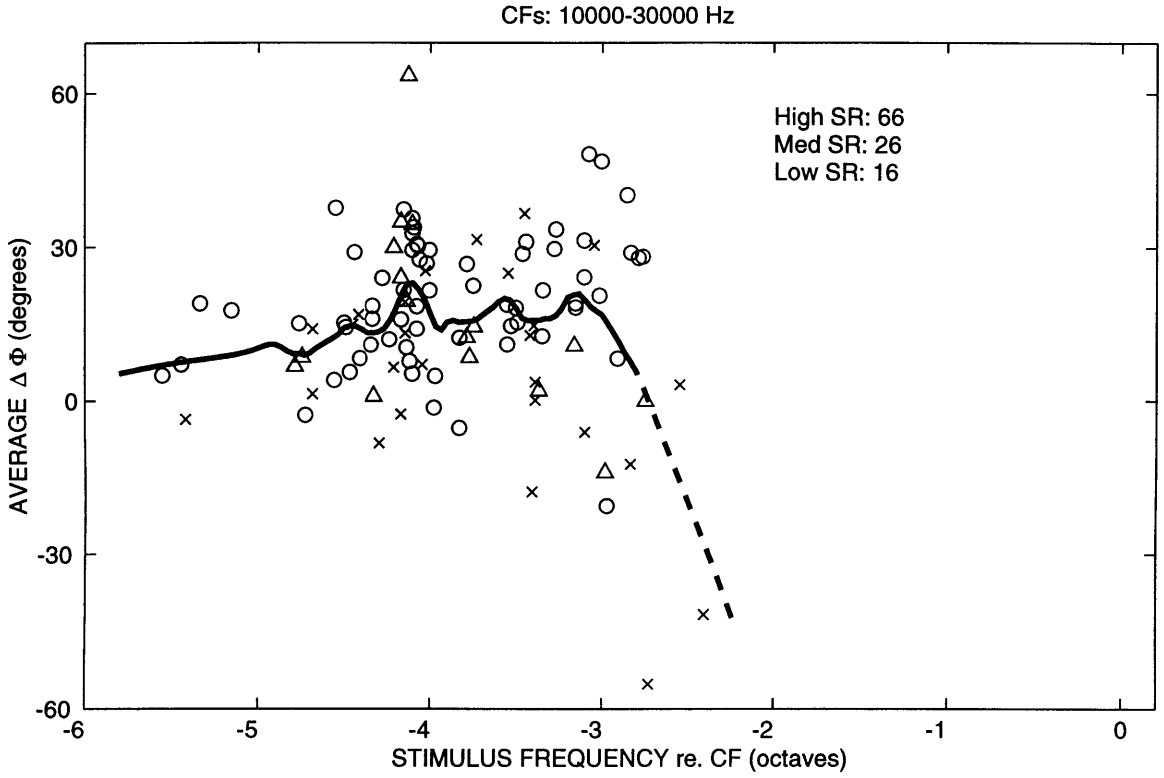

Figure 4-13: Average $\Delta\Phi$ versus the stimulus frequency relative to CF. Each point represents one fiber. Different symbols stand for fibers of different SRs, as explained in the figure.
To guide the eye, a loess fit (smoothing factor=0.2) is shown by the thick line. The dashed part of the line indicates uncertainty in the trend due to paucity of data. Stimulus frequency ranged from 500 Hz to 2.2 kHz.

increases from -6 to -3 octaves below CF, and to decline as stimulus frequency continues to increase. Note, however, that the apparent downward trend is only suggestive because it is determined by a few fibers only.

F. Cochlear microphonic

Cochlear microphonic (CM) potential represents the summed extracellular potential drop from the a.c. components of hair cell receptor currents, and it is generated largely by the outer hair cells (Dallos and Cheatham, 1976). When the CM is recorded at the round window in response to low-frequency tones (i.e., tones whose frequency is well below the CF of the recording location), the CM is thought to be a faithful indicator of the local

outer-hair-cell receptor currents (e.g., Dallos et al., 1974; Patuzzi et al., 1989), and of the basilar-membrane displacement at the cochlear base (Ruggero et al., 1986). In cat, fibers that innervate the cochlear base close to the round window have CFs around 20 kHz. Thus, we used measurements of CM at the round window in response to frequencies lower than 2 kHz as an indirect measure of the efferent effects on outer hair cells and, through them, on the basilar membrane motion. Most frequently, CM was recorded in response to 1 kHz tones.

Measurements of CM magnitude and phase in response to a stimulus frequency of 1 kHz are shown in Fig. 4-14 for two cats. The figure illustrates that efferent stimulation augmented the CM magnitude, but had a very small ($\approx$ few degrees) effect on the CM phase. Similar results on the efferent-induced changes in CM phase were reported for guinea pig by Mountain et al. (1980) using intracochlear electrodes. The lack of a large efferent effect on CM phase is interesting given that response phase of single fibers was often affected to a much greater extent by efferent stimulation. The CM phase is also interesting because it depended on sound level to a much smaller extent than the response phase from single fibers. Differences between the CM phase and single-fiber phase are effectively demonstrated when compared in the same cat. For example, Fig. 4-15 illustrates that both the sound-level dependence, and efferent effects on response phase of a single fiber are much larger than on the CM phase recorded about three hours earlier in the same cat. Note, however, that there is only a partial overlap between sound levels over which CM and the ANF shown in Fig. 4-15 were recorded.

IV. Discussion

A. Is the efferent effect equivalent to an attenuation of sound?

All earlier reports, including our data described in the previous chapter, indicated that efferent activation inhibits the firing rate of ANFs responding to tones in quiet (reviewed by Guinan, 1996). This inhibition is most commonly characterized as an efferent-induced sound-level shift, ΔL, which is also known as "equivalent sound attenuation." In this chapter, we have explored whether the notion that the efferent effect is equivalent to an atten-

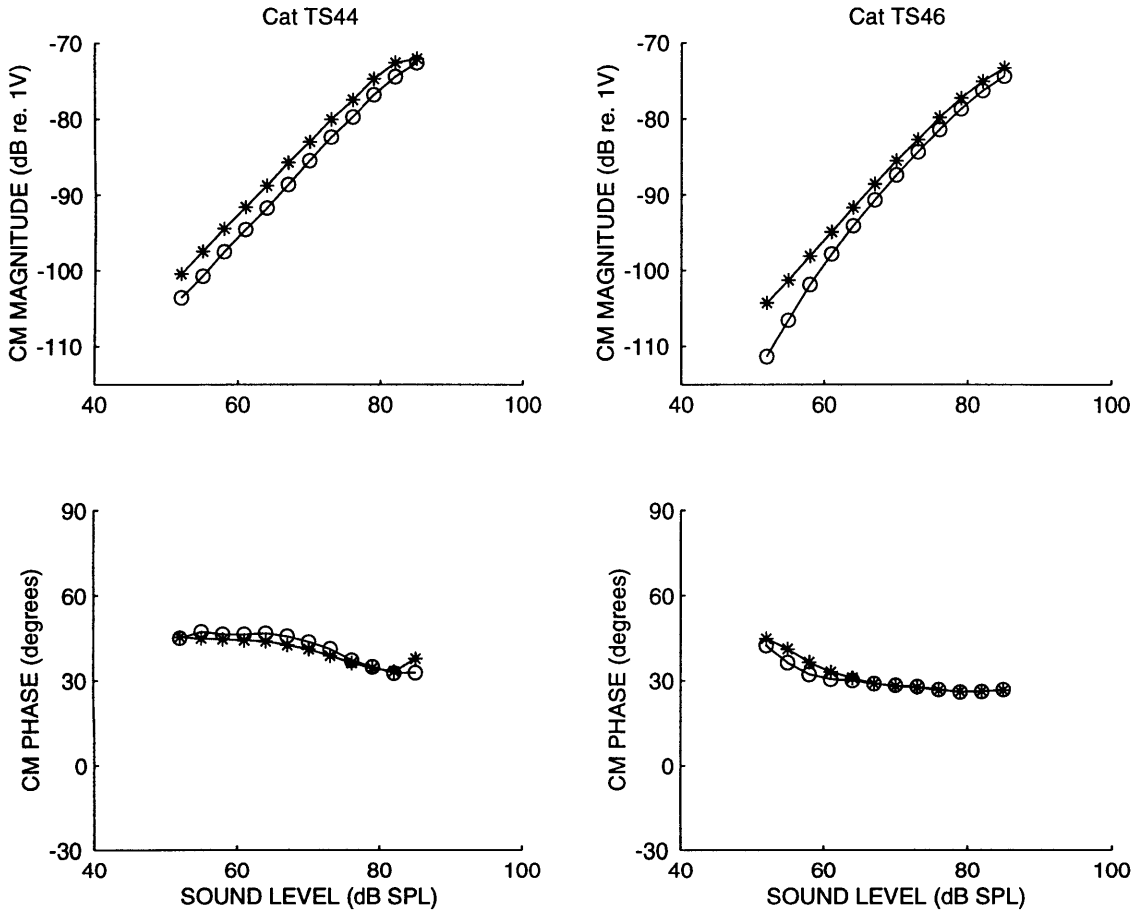

Figure 4-14: Efferent effects on the magnitude (top row) and phase (bottom row) of the cochlear microphonic in response to 1 kHz tone bursts. Data from two cats are shown – cat TS44 in the left column, and cat TS46 in the right column). Circles = no efferent stimulation; Stars = efferent stimulation. Efferent stimulation had a similar effect on the CM in response to 500 Hz and 2 kHz tones (not shown).

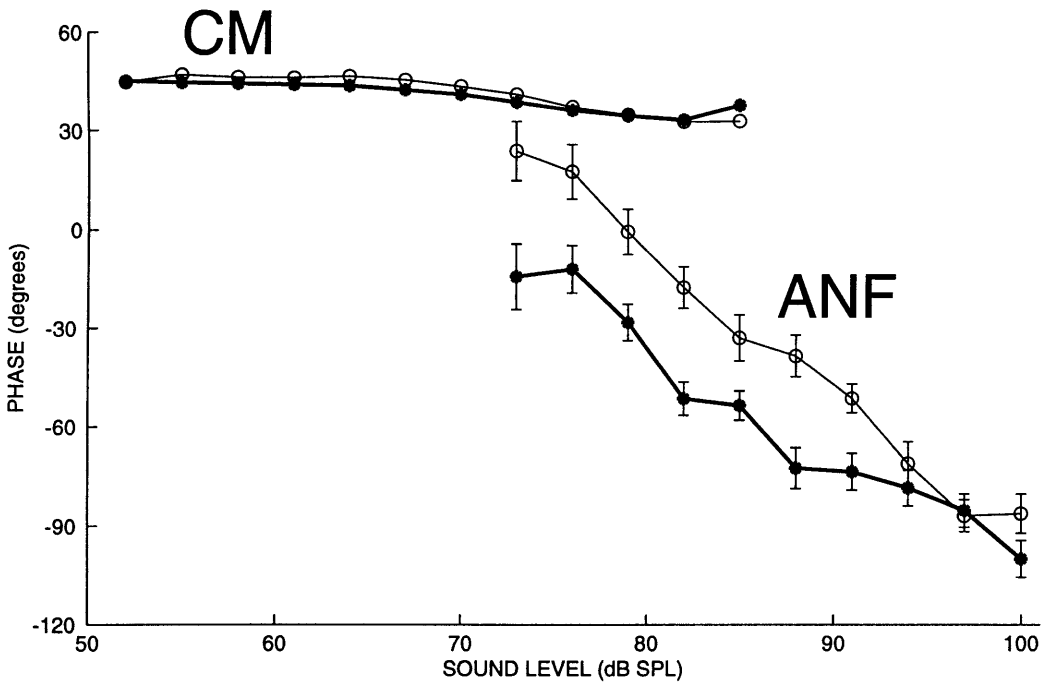

Figure 4-15: A comparison between efferent effects on cochlear-microphonic (CM) phase and auditory-nerve-fiber (ANF) phase. In this example, data are from the same cat (TS44), and the ANF was recorded about three hours after the recording of CM. Note that this figure is a composit of Fig. 4-14(lower left column) and Fig. 4-9(A). Circles = no efferent stimulation; Stars = efferent stimulation.

uation of sound also holds for synchrony and phase measures. The notion appears to hold for synchrony data, but not for phase data, as discussed below.

Although the current data on the efferent-induced level shift for synchrony, ΔL_S, are few (Fig. 4-8, see also Fig. 4-2L and 4-3K), they support the idea that efferents attenuate the drive that produces synchrony, because ΔL_S was usually positive. The data also suggest that ΔL and ΔL_S tend to be of a similar size. In addition, the finding that efferents do not have a statistically significant effect on synchrony at high sound levels is consistent with the view that synchrony is "saturated" at these sound levels, and that saturation is not affected by efferents. This suggests that efferents act at a stage before the afferent synapse, because saturation of synchrony is thought to be determined at the afferent synapse (reviewed by Ruggero, 1992). Thus, both the efferent-induced level shift, ΔL_S, and the lack of a change in synchrony at high sound level, support the idea that efferents exert their effect before the afferent synapse.

In contrast to the efferent effects on synchrony, the effects on phase were usually in the direction opposite to what would be expected if the effect were equivalent to an attenuation of sound (Figs. 4-2, 4-3, 4-5, 4-10, 4-11). Thus, the overall efferent effect at tail frequencies – manifested through changes in phase, synchrony and rate – is not equivalent to an attenuation of sound.

A possible interpretation of this result is that efferent effects on rate and synchrony are due to a single process equivalent to an attenuation of sound, whereas the effect on phase is due to two opposing processes, one of which is equivalent to an attenuation of sound. The second process acting on phase should then be even stronger than the first process so that it can change the negative phase change from the attenuation into the positive phase change actually observed. The second process should also be present concurrently with the the first process across a broad sound level range. These two putative process are unlikely to be the same as "two factors" previously discussed in literature (e.g., Gifford and Guinan, 1983; reviewed by Kiang et al.,1986) in accounting for ANF data, because the "two factors" are usually assumed to be of similar relative strength only over a narrow range of sound level. Overall, the most parsimonious explanation of the current data is that one process controls the efferent-induced changes in rate, synchrony and phase, and that this process is

not equivalent to an attenuation of sound.

The observation that the efferent effect on phase is usually not equivalent to an attenuation of sound, whereas the effect on synchrony appears to be, is consistent with an earlier report by Gifford and Guinan (1983) where a similar conclusion was reached. Gifford and Guinan (1983) studied efferent effects on low-CF fibers stimulated with tip-frequency tones, whereas we studied efferent effects on high-CF fibers stimulated with tail-frequency tones. Although both studies provide evidence that efferent effects on phase are not equivalent to an attenuation of sound, the efferent-evoked changes in phase were different in the two studies. In particular, Gifford and Guinan (1983) saw only small changes in phase, with little difference in the average phase difference (about -5 degrees), and "no systematic relationship" between the efferent-induced phase shift "and anything else." In contrast, in the current study we usually saw efferent-induced phase delays that averaged $\approx$ 20 degrees, and tended to slowly decrease as sound level increased (Figs. 4-10 and 4-11), and slowly increase with frequency up to 3 octaves below CF (Figs. 4-12 and 4-13). Thus, the study of Gifford and Guinan (1983) and the current study are complementary.

B. Dependence of $\Delta\Phi$ on stimulus frequency

The phase data suggest that $\Delta\Phi$ in the tail region depends on frequency (Fig. 4-13). In attempting to understand this frequency dependence, it is useful to compare efferent effects on phase and rate in the same fibers. This comparison is provided in Fig. 4-16 in which $\Delta\Phi$ was used as a measure of the efferent effects on phase, and ΔL as a measure of the effect on rate. To focus on frequency dependence, $\Delta\Phi$ and ΔL were averaged across sound levels. Across a population of fibers (Fig. 4-16), ΔL and $\Delta\Phi$ tended to increase as stimulus frequency increased from -6 to -3 octaves below CF. At higher stimulus frequencies (up to -2.4 octaves below CF), ΔL continued to increase. At still higher frequencies (i.e., -2.4 to -1.3 octaves below CF) ΔL tended to decline, as hinted in Fig. 3-15 where all available ΔL data are considered, not only data from fibers in which both ΔL and $\Delta\Phi$ were measured. Regarding $\Delta\Phi$ for frequencies between -3 and -2.4 octaves below CF, Fig. 4-16 suggests that $\Delta\Phi$ declines with frequency. However, the apparent downward trend is questionable because it it based on a few fibers. Moreover, the downward trend was absent when we

consider ΔL from the few fibers with CFs between 5–10 kHz.

Although across a population of fibers both ΔL and $\Delta\Phi$ appeared to increase with frequency up to -3 octaves below CF, there was little, if any, correlation between ΔL and $\Delta\Phi$ for single fibers. In particular, when $\Delta\Phi$ was plotted versus ΔL, a prominent scatter was a hallmark of the plot (not shown).

The origin of the frequency dependence of the efferent effect at tail frequencies is not known, but it might reflect one or more changes in properties of the various cochlear elements. These changes in properties might themselves be frequency dependent, such as frequency-dependent differences in relative motions of the reticular lamina and the tectorial membrane (Freeman and Weiss, 1990). Alternatively, the changes in properties may be non-frequency dependent – such as an efferent-induced change in stiffness of the cochlear partition – and yet cause a frequency-dependent effect in ANF responses.

C. The mechanisms by which medial efferents might change the response phase of auditory-nerve fibers

Our data suggest that efferents might change cochlear micromechanics because they change the sound-level dependence of phase of ANF discharges – a dependence thought to arise from cochlear micromechanical processes (Ruggero et al., 1996). The basis for attributing the sound-level dependence of ANF phase to micromechanical process (i.e. to signal transformation after the basilar membrane but before changes in the inner-hair-cell receptor potentials) is the discrepancy between the phase of ANFs and of basilar membrane. In particular, at tail frequencies, BM phase appears to be independent of sound level (for the latest measurements see Nuttall and Dolan, 1996 and Ruggero et al., 1997) whereas ANF phase often strongly depends on sound level (e.g., Figs. 4-2, 4-3, 4-9; Ruggero et al., 1996).

The measurements of efferent effects on the cochlear microphonic (Fig. 4-14) suggest that the efferent-induced changes in ANF phase are not produced by efferent effects on the phase of basilar membrane movement. In particular, cochlear microphonic recorded at the round window in response to low frequencies is thought to be a good indicator of basilar membrane (BM) displacement at the cochlear base (Dallos, 1974; Ruggero et al., 1986). Since efferent

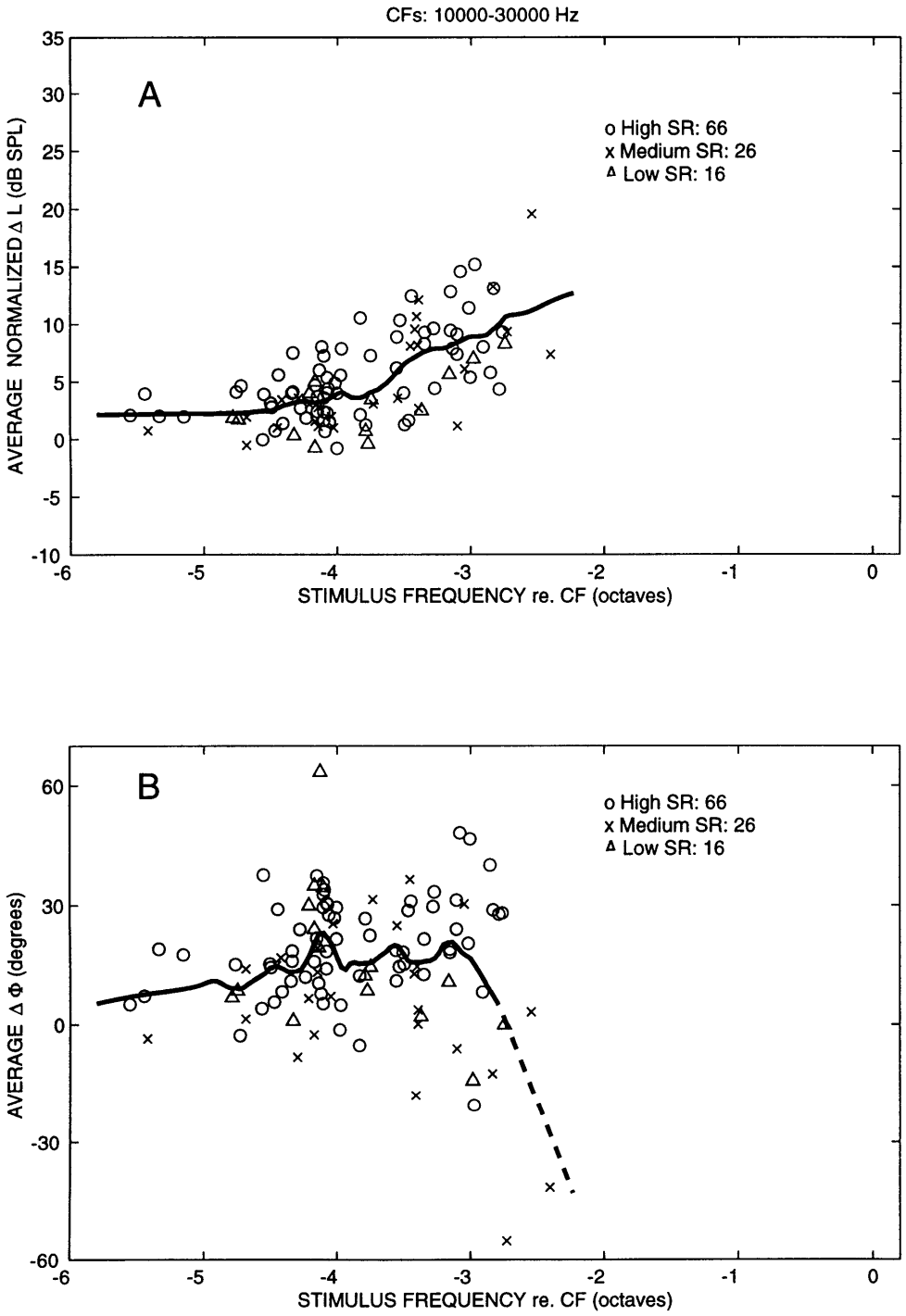

Figure 4-16: A comparison between frequency dependencies of average ΔL and average $\Delta\Phi$ restricted to be from the same fibers. Data in panel (A) are a subset of the data from Fig. 3-15 in the previous chapter. The subset indicates fiber for which phase data existed. (B) A reproduction of Fig. 4-13.

activation only minimally affected ($\approx$ several degrees) CM phase, this suggests that BM phase was also minimally affected by efferent stimulation. In contrast, ANF phase was, on average, shifted by $\approx 20^{o}$ across sound levels (Figs. 4-10, 4-11,4-12, 4-13), suggesting that efferents exerted their effect on ANF phase by modulating signal-transduction steps beyond the basilar membrane. Note, however, that caution is warranted when using CM measurements to interpret BM displacement because, at least theoretically, efferents might change the properties of the system, so that CM would no longer be a direct indicator of the basilar membrane displacement. Nonetheless, both the sound-level dependence of ANF phase – contrasted with the apparent lack of a sound-level dependence of BM phase – and the lack of an efferent-induced change in CM, point to the efferent effect on ANF phase as arising from an efferent effect on cochlear micromechanics.

Conceptually, many mechanisms might play a role in producing the efferent effect at tail frequencies. These mechanisms include (reviewed by Guinan, 1996; see also Dallos, 1996): (1) an increase in basolateral conductance of outer hair cells (2) changes in outer-hair-cell motility, (3) changes in outer-hair-cell longitudinal stiffness, (4) modulation of electrical coupling between inner and outer hair cells, through changes in endocochlear potential, (5) changes in extracellular potentials in the vicinity of auditory-nerve dendrites. Note that pointing to a specific mechanism based on ANF data is complicated by the fact that there is bidirectional mechanical coupling at several stages of signal transduction preceding the excitation of ANFs (e.g., Kiang et al., 1986; Mountain and Cody, 1989; Patuzzi, 1996)

Whatever the mechanisms that produce the efferent effect at tail frequencies might be, they have to meet the constraints imposed by the current data. One constraint is that ANF phase is usually delayed, which is not equivalent to an attenuation of sound. The delay weakly depends on sound level, usually being bigger at low sound levels than at high levels. Another constraint is that CM phase is minimally affected by efferent stimulation, in contrast with ANF phase. An additional constraint is that efferent effects are similar across SR groups. Note, however, that our data were not ideally suited for comparisons across SR groups, so that the issue of whether there are differences across SR groups is not definitively settled. Results of statistical tests presented in Table 4.1 should be interpreted cautiously because: (1) the data were biased toward high-SR fibers, (2) the test were sometimes based

on a few fibers, and (3) fiber grouping into CF bands was somewhat arbitrary.

The main value in exploring how efferent activation affects ANF phase is that the measurements, along with ANF synchrony and rate measurements, provides important constraints for the mechanisms involved. Nonetheless, the data can also be used to speculate on possible functional implications of the efferent-induced phase changes. Phase changes might alter various perceptual tasks. For example, Carney (1994) suggested that phase changes across a population of fibers provide important cues for loudness perception, in addition to cues due to changes in firing rate. If so, an efferent change of phase, as well as the efferent change in rate, could affect loudness perception.

References

Abbas, P. J. and Sachs, M. B. (1976). "Two-tone suppression in auditory-nerve fibers: Extension of stimulus response relationship," *J. Acoust. Soc. Am.* **59**:112–122.

Anderson, D. J., Rose, J. E., Hind, J. E., and Brugge, J. F. (1970). "Temporal position of discharges in single auditory nerve fibers within the cycle of a sine-wave stimulus: frequency and intensity effects," *J. Acoust. Soc. Am.* **49**:1131–1139.

Brown, M. C. and Nuttall, A. L. (1984). "Efferent control of cochlear inner hair cell responses in the guinea pig," *J. Physiol.* **354**:625–646.

Carney, L. H. (1994). "Spatiotemporal encoding of sound level: Models for normal encoding and recruitment of loudness," *Hearing Research* **76**:31–44.

Cheatham, M. A. and Dallos, P. (1992). "Two-tone suppression in inner hair cell responses: Correlates of rate suppression in the auditory nerve," *Hearing Research* **60**:1–12.

Cleveland, W. S. (1993). *Visualizing Data.* AT&T Bell Laboratories, Murray Hill, New Yersey.

Cooper, N. P. and Rhode, W. S. (1992). "Basilar membrane mechanics in the hook region of cat and guinea-pig cochleae: Sharp tuning and nonlinearity in the absence of baseline position shifts," *Hearing Research* **63**:163–190.

Dallos, P. (1992). "The active cochlea.," *J. Neurosci.* **12**:4575–4585.

Dallos, P. and Cheatham, M. A. (1976). "Production of cochlear potentials by inner and outer hair cells," *J. Acoust. Soc. Am.* **60**:510–512.

Dallos, P., Cheatham, M. A., and Ferraro, J. (1974). "Cochlear mechanics, nonlinearities, and cochlear potentials," *J. Acoust. Soc. Am.* **55**:597–605.

Dallos, P., He, D. Z. Z., Lin, X., and Evans, B. N. (1996). "Efferent control of cochlear mechanics: Outer hair cells," in Lewis, E., Long, G., Lyon, R., Narins, P., Steele, C., and Hecht-Poinar, E., editors, *Diversity in Auditory Mechanics*, pages 501–508. World Scientific, Singapore.

de Boer, E. (1990). "Can shape deformations of the organ of corti influence the traveling wave in the cochlea?," *HR* **44**:83–92.

Desmedt, J. E. (1962). "Auditory-evoked potentials from cochlea to cortex as influenced by activation of the efferent olivocochlear bundle," *JASA* **34**:1478–1496.

Dolan, D. F. and Nuttall, A. L. (1994). "Basilar membrane movement evoked by sound iis altered by electrical stimulation of the crossed olivocochlear bundle," *ARO* **17**:89.

Efron, B. and Tibshirani, R. J. (1993). *An introduction to the Bootstrap.* Chapman and Hall, New York.

Evans, B. N., Hallworth, R., and Dallos, P. (1991). "Outer hair cell electromotility: The sensitivity and vulnerability of the dc component," *Hearing Research* **52**:288–304.

Fex, J. (1962). "Auditory activity in centrifugal and centripetal cochlear fibers in cat," *Acta Physiol. Scand.* **55**:2–68.

Fex, J. (1967). "Efferent inhibition in the cochlea related to hair-cell dc activity: Study of postsynaptic activity of the crossed olivocochlear fibers in the cat," *J. Acoust. Soc. Am.* **41**:666–675.

Freeman, D. M. and Weiss, T. F. (1990). "Hydrodynamic forces on hair bundles at low frequencies," *Hearing Research* **48**:17–30.

Galambos, R. (1956). "Suppression of auditory activity by stimulation of efferent fibers to the cochlea," *J. Neurophysiol.* **19**:424–437.

Geisler, C. D. (1974). "Model of crossed olivocochlear bundle effects," *J. Acoust. Soc. Am.* **56**:1910–1912.

Gifford, M. L. and Guinan, Jr., J. J. (1983). "Effects of crossed-olivocochlear-bundle stimulation on cat auditory nerve fiber responses to tones," *J. Acoust. Soc. Am.* **74**:115–123.

Gifford, M. L. and Guinan, Jr., J. J. (1987). "Effects of electrical stimulation of medial olivocochlear neurons on ipsilateral and contralateral cochlear responses," *Hearing Research* **29**:179–194.

Goldberg, J. M. and Brown, P. B. (1969). "Response of binaural neurons of dog superior olivary complex to dischotic stimuli: Some physiological mechanisms of sound localization," *J. Neurophysiol.* **XXXII**:613–636.

Guinan, Jr., J. J. (1986). "Effect of efferent neural activity on cochlear mechanics," *Scand. Audiol. Suppl.* **25**:53–62.

Guinan, Jr., J. J. (1996). "Physiology of olivocochlear efferents," in Dallos, P., Popper, A. N., and Fay, R. R., editors, *The Cochlea*, pages 435–502. Springer, New York.

Guinan, Jr., J. J. and Gifford, M. L. (1988a). "Effects of electrical stimulation of efferent olivocochlear neurons on cat auditory-nerve fibers. I. rate-level functions," *Hearing Research* **33**:97–114.

Guinan, Jr., J. J. and Gifford, M. L. (1988b). "Effects of electrical stimulation of efferent olivocochlear neurons on cat auditory-nerve fibers. II. spontaneous rate," *Hearing Research* **33**:115–128.

Guinan, Jr., J. J. and Gifford, M. L. (1988c). "Effects of electrical stimulation of efferent olivocochlear neurons on cat auditory-nerve fibers. III. tuning curves and thresholds at CF," *Hearing Research* **37**:29–46.

Guinan, Jr., J. J. and Stanković, K. M. (1995). "Medial olivocochlear inhibition of auditory-nerve firing mediated by changes in endocochlear potential," *Asso. Res. Otolaryngol. Abstr.* **18**:686.

Guinan, Jr., J. J. and Stanković, K. M. (1996a). "Medial efferent inhibition is largest at moderate to high sound levels in cat auditory-nerve fibers," *Asso. Res. Otolaryngol. Abstr.* **19**:310.

Guinan, Jr., J. J. and Stanković, K. M. (1996b). "Medial efferent inhibition produces the largest equivalent attenuations at moderate to high sound levels in cat auditory-nerve fibers," *J. Acoust. Soc. Am.* **100**:1680–1690.

Guinan, Jr., J. J., Warr, W. B., and Norris, B. E. (1984). "Topographic organization of the olivocochlear projections from the lateral and medial zones of the superior olivary complex," *J. Comp. Neurol.* **226**:21–27.

Johnson, D. H. (1980). "The relationship between spike rate and synchrony in responses of auditory-nerve fibers to single tones," *J. Acoust. Soc. Am.* **68**:1115–1122.

Kawase, T., Delgutte, B., and Liberman, M. C. (1993). "Antimasking effects of the olivocochlear reflex. II. enhancement of auditory-nerve response to masked tones," *J. Neurophysiol.* **70**:2533–2549.

Kawase, T. and Liberman, M. C. (1993). "Antimasking effects of the olivocochlear reflex. I. enhancement of compound actions potentials to masked tones," *J. Neurophysiol.* **70**:2519–2532.

Kiang, N. Y. S. (1990). "Curious oddments of auditory-nerve studies," *Hearing Research* **49**:1–16.

Kiang, N. Y. S., Liberman, M. C., Sewell, W. F., and Guinan, Jr., J. J. (1986). "Single unit cues to cochlear mechanisms," *Hearing Research* **22**:171–182.

Kiang, N. Y. S. and Moxon, E. C. (1974). "Tails of tuning curves of auditory-nerve fibers," *J. Acoust. Soc. Am.* **55**:620–630.

Kiang, N. Y. S., Moxon, E. C., and Levine, R. A. (1970). "Auditory-nerve activity in cats with normal and abnormal cochleas," in Wolstenholme, G. and Knight, J., editors, *Sensorineural Hearing Loss*, pages 241–273. J. & A. Churchill, London.

Kiang, N. Y. S., Watanabe, T., Thomas, E. C., and Clark., L. F. (1965). *Discharge Patterns of Single Fibers in the Cat's Auditory Nerve.* The M.I.T. Press, Cambridge, MA.

Liberman, M. C. (1978). "Auditory-nerve response from cats raised in a low-noise chamber," *J. Acoust. Soc. Am.* **63**:442–455.

Liberman, M. C. (1980). "Morphological differences among radial afferent fibers in the cat cochlea: An electron-microscopic study of serial sections," *Hearing Research* **3**:45–63.

Liberman, M. C. (1982). "Single-neuron labeling in the cat auditory nerve," *Science* **216**:1239–1241.

Liberman, M. C. (1989). "Rapid assessment of sound-evoked olivocochlear feedback: Suppression of compound action potentials by contralateral sound," *Hearing Research* **38**:47–56.

Liberman, M. C. and Kiang, N. Y. S. (1978). "Acoustic trauma in cats. cochlear pathology and auditory-nerve activity," *Acta Oto.-Laryngol. Suppl.* **358**:1–63.

Liberman, M. C. and Kujawa, S. G. (1997). "Role of the olivocochlear system in conditioning-related protection," *Asso. Res. Otolaryngol. Abstr.* **21**:559.

Mardia, K. V. (1972). *Statistics of directional data.* Academic Press, New York.

Meyer, S. L. (1975). *Data Analysis for Scientists and Engineers.* John Wiley & Sons, Inc., New York.

Moulin, A., Collet, L., and Duclaux, R. (1993). "Contralateral auditory stimulation alters acoustic distortion products in humans," *Hearing Research* **65**:193–210.

Mountain, D. C. (1978). *A comparison of electrical changes in the cochlea caused by stimulation of the crossed olivocochlear bundle and by d.c. polarization.* Ph.D. thesis, Univ. of Wisconsin, Madison.

Mountain, D. C. and Cody, A. R. (1989). "Mechanical coupling between inner and outer hair cells in the mammalian cochlea," in Wilson, J. and Kemp, D., editors, *Cochlear Mechanisms - Structure, Function and Models*, pages 153–160. Plenum Press, New York.

Mountain, D. C., Geisler, C. D., and Hubbard, A. E. (1980). "Stimulation of efferent alters the cochlear microphonic and the sound-induced resistance changes measured in scala media of the guinea pig," *Hearing Research* **3**:231–240.

Murugasu, E. and Russell, I. J. (1996). "The effect of efferent stimulation on basilar membrane displacement in the basal turn of the guinea pig cochlea," *J. Neurosci.* **16**:325–332.

Nuttall, A. L. and Dolan, D. F. (1996). "Steady-state sinusoidal velocity responses of the basilar membrane in guinea pig," *J. Acoust. Soc. Am.* **99**:1556–1565.

Palmer, A. R. and Russell, I. J. (1986). "Phase locking in the cochlear nerve of the guinea pig and its relation to the receptor potential of inner hair cells," *Hearing Research* **24**:1–15.

Patuzzi, R. (1996). "Cochlear micromechanics and macromechanics," in Dallos, P., Popper, A. N., and Fay, R. R., editors, *The Cochlea*, pages 186–257. Springer, New York.

Patuzzi, R. B., Yates, G. K., and Johnstone, B. M. (1989). "The origin of the low-frequency microphonic in the first cochlear turn of guinea-pig," *Hearing Research* **39**:177–188.

Press, W. H., Teukolsky, S. A., Vetterling, W. T., and Flannery, B. P. (1992). *Numerical Recipies in C.* Cambridge University Press, New York, second edition.

Puria, S., Guinan, Jr., J. J., and Liberman, M. C. (1996). "Olivocochlear reflex assays: Effects of contralateral sound on compound action potentials versus ear-canal distortion products," *J. Acoust. Soc. Am.* **99**:500–507.

Rasmussen, G. L. (1946). "The olivary peduncle and other fiber projections of the superior olivary complex," *J. Comp. Neurol.* **84**:141–219.

Rhode, W. S. (1973). "An investigation of postmortem cochlear mechanics using the mössbauer effect," in Moller, A. R., editor, *Basic Mechanisms of Hearing*, pages 49–67. Academic Press, New York.

Rose, J. E., Brugge, J. F., Anderson, D. J., and Hind, J. E. (1967). "Phase-locked response to low-frequency tones in single auditory nerve fibers of the squirrel monkey," *J. Neurophysiol.* **30**:769–793.

Ruggero, M., Rich, N., and Recio, A. (1993). "Alteration of basilar membrane responses to sound by acoustic overstimulation," in Duifhuis, H., Horst, J., van Dijk, P., and van Netten, S., editors, *Biophysics of Hair Cell Sensory Systems*, pages 258–265. World Scientific, Singapore.

Ruggero, M. A. (1992). "Physiology and coding of sound in the auditory nerve," in Popper, A. N. and Fay, R. R., editors, *The Mammalian Auditory Pathway: Neurophysiology*, pages 34–93. Springer-Verlag, New York.

Ruggero, M. A. and Rich, N. C. (1991). "Furosemide alters organ of corti mechanics: Evidence for feedback of outer hair cells upon the basilar membrane," *J. Neurosci.* **11**:1057–1067.

Ruggero, M. A., Rich, N. C., Recio, A., Narayan, S., and Robles, L. (1997). "Basilar-membrane responses to tones at the base of the chinchilla cochlea," *J. Acoust. Soc. Am.* **101**:2151–2163.

Ruggero, M. A., Rich, N. C., Shivapuja, B. G., and Temchin, A. N. (1996). "Auditory-nerve responses to low-frequency tones: Intensity dependence," *Aud. Neurosci.* **2**:159–185.

Ruggero, M. A., Robles, L., and Rich, N. C. (1986). "Basilar membrane mechanics at the base of the chinchilla cochlea. II. responses to low-frequency tones and relationship to microphonics and spike initiation in the VIII nerve," *J. Acoust. Soc. Am.* **80**:1375–1383.

Russell, I. J. and Murugasu, E. (1997a). "Efferent suppression of basilar membrane vibration depends on tone frequency and level: implications for the active control of basilar membrane mechanics," in Palmer, A. R., Rees, A., Summerfield, A. Q., and Meddis, R., editors, *Psychophysical and physiological advances in hearing*, pages 18–24. Whurr Publishers, London.

Russell, I. J. and Murugasu, E. (1997b). "Medial efferent inhibition suppresses basilar membrane responses to near characteristic frequency tones of moderate to high intensities," *J. Acoust. Soc. Am.* **102**:1734–1738.

Sachs, M. B. and Abbas, P. J. (1974). "Rate versus level functions for auditory-nerve fibers in cats: tone burst stimuli," *J. Acoust. Soc. Am.* **56**:1835–1847.

Sellick, P. M., Patuzzi, R., and Johnstone, B. M. (1982). "Measurement of basilar membrane motion in the guinea pig using the mössbauer technique," *J. Acoust. Soc. Am.* **72**:131–141.

Sewell, W. F. (1984). "The effects of furosemide on the endocochlear potential and auditory-nerve fiber tuning curves in cats," *Hearing Research* **14**:305–314.

Siebert, W. M. (1968). "Stimulus transformations in the peripheral auditory system.," in Kolers, P. A. and Eden, M., editors, *Recognizing patterns*, pages 104–133. MIT Press, Cambridge.

Siegel, J. H. and Kim, D. O. (1982). "Efferent neural control of cochlear mechanics? olivocochlear bundle stimulation affects cochlear biomechanical nonlinearity.," *Hearing Research* **6**:171–182.

Siegel, J. H. and Relkin, E. M. (1987). "Antagonistic effects of perilymphatic calcium and magnesium on the activity of single cochlear afferent neurons," *Hearing Research* **28**:131–147.

Sridhar, T. S., Brown, M. C., and Sewell, W. F. (1997). "Unique postsynaptic signaling at the hair cell efferent synapse permits calcium to evoke changes on two time scales," *J. Neurosci.* **17**:428–437.

Sridhar, T. S., Liberman, M. C., Brown, M. C., and Sewell, W. F. (1995). "A novel cholinergic "slow effect" of efferent stimulation on cochlear potentials in the guinea pig," *J. Neurosci.* **15**:3667–3678.

Stanković, K. M. and Guinan, Jr., J. J. (1997). "Efferent effects on auditory-nerve responses to tail-frequency tones: Inhibition without altering basilar-membrane motion?," *Asso. Res. Otolaryngol. Abstr.* **20**:619.

Teas, D. C., Konishi, T., and Nielsen, D. W. (1972). "Electrophysiological studies on the spatial distribution of the crossed olivocochlear bundle along the guinea pig cochlea.," *J. Acoust. Soc. Am.* **51**:1256–1264.

Trahiotis, C. and Elliott, D. N. (1970). "Behavioral investigation of some possible effects of sectioning the crossed olivocochlear bundle," *J. Acoust. Soc. Am.* **47**:592–596.

Viemeister, N. F. (1983). "Auditory intensity discrimination at high frequencies in the presence of noise," *Science* **221**:1206–1208.

Warr, W. B. (1992). "Organization of olivocochlear efferent systems in mammals," in Webster, D. B., Popper, A. N., and Fay, R. R., editors, *The Mammalian Auditory Pathway: Neuroanatomy*, pages 410–448. Springer-Verlag, New York.

Warren, III, E. H. and Liberman, M. C. (1989). "Effects of contralateral sound on auditory-nerve responses. I. contributions of cochlear efferents," *Hearing Research* **37**:89–104.

Wiederhold, M. L. (1970). "Variations in the effects of electric stimulation of the crossed olivocochlear bundle on cat single auditory-nerve-fiber responses to tone bursts," *J. Acoust. Soc. Am.* **48**:966–977.

Wiederhold, M. L. and Kiang, N. Y. S. (1970). "Effects of electric stimulation of the crossed olivocochlear bundle on single auditory-nerve fibers in the cat," *J. Acoust. Soc. Am.* **48**:950–965.

Winslow, R. L. and Sachs, M. B. (1987). "Effect of electrical stimulation of the crossed olivocochlear bundle on auditory nerve response to tones in noise," *J. Neurophysiol.* **57**:1002–1021.

Young, E. D. and Barta, P. E. (1986). "Rate responses of auditory nerve fibers to tones in noise near masked threshold," *J. Acoust. Soc. Am.* **79**:426–442.

Zeng, F. G., Lehmann, K. M., Soli, S. D., and Linthicum, F. H. (1994). "Effects of vestibular neurectomy on intensity discrimination and speech perception in noise," *J. Acoust. Soc. Am.* **95**:2993–2994.

Zheng, X. Y., Henderson, D., Mc.Fadden, S. L., and Hu, B. H. (1997). "The role of the cochlear efferent system in acquired resistance to noise-induced hearing loss," *Hearing Research* **104**:191–203.

Zweig, G. (1976). "Basilar membrane motion.," in *Cold Spring Harbor Symposia on Quantitative Biology, volume XL*, pages 619–633. Cold Spring Harbor Laboratory, Cold Spring Harbor.